

# Introduction to Confocal Microscopy

(from <http://www.microscopyu.com/articles/confocal/>)

Confocal microscopy offers several advantages over conventional optical microscopy, including controllable depth of field, the elimination of image degrading out-of-focus information, and the ability to collect serial optical sections from thick specimens. The key to the confocal approach is the use of spatial filtering to eliminate out-of-focus light or flare in specimens that are thicker than the plane of focus. There has been a tremendous explosion in the popularity of confocal microscopy in recent years, due in part to the relative ease with which extremely high-quality images can be obtained from specimens prepared for conventional optical microscopy, and in its great number of applications in many areas of current research interest.

**Basic Concepts** - Current instruments are highly evolved from the earliest versions, but the principle of confocal imaging advanced by Marvin Minsky, and patented in 1957, is employed in all modern confocal microscopes. In a conventional widefield microscope, the entire specimen is bathed in light from a mercury or xenon source, and the image can be viewed directly by eye or projected onto an image capture device or photographic film. In contrast, the method of image formation in a confocal microscope is fundamentally different. Illumination is achieved by scanning one or more focused beams of light, usually from a laser or arc-discharge source, across the specimen. This point of illumination is brought to focus in the specimen by the objective lens, and laterally scanned using some form of scanning device under computer control. The sequences of points of light from the specimen are detected by a photomultiplier tube (**PMT**) through a pinhole (or in some cases, a slit), and the output from the PMT is built into an image and displayed by the computer. Although unstained specimens can be viewed using light reflected back from the specimen, they usually are labeled with one or more fluorescent probes.

**Laser Systems for Confocal Microscopy** - The lasers commonly employed in laser scanning confocal microscopy are high-intensity monochromatic light sources, which are useful as tools for a variety of techniques including optical trapping, lifetime imaging studies, photobleaching recovery, and total internal reflection fluorescence. In addition, lasers are also the most common light source for scanning confocal fluorescence microscopy, and have been utilized, although less frequently, in conventional widefield fluorescence investigations.

**Imaging Modes** - A number of different imaging modes are used in the application of confocal microscopy to a vast variety of specimen types. They all rely on the ability of the technique to produce high-resolution images, termed **optical sections**, in sequence through relatively thick sections or whole-mount specimens. Based on the optical section as the basic image unit, data can be collected from fixed and stained specimens in single, double, triple, or multiple-wavelength illumination modes, and the images collected with the various illumination and labeling strategies will be in register with each other. Live cell imaging and time-lapse sequences are possible, and digital image processing methods applied to sequences of images allow z-series and three-dimensional representation of specimens, as well as the time-sequence presentation of 3D data as four-dimensional imaging. Reflected light imaging was the mode used in early confocal instruments, but any of the transmitted light imaging modes commonly employed in microscopy can be utilized in the laser scanning confocal microscope.

**Specimen Preparation and Imaging** - The procedures for preparing and imaging specimens in the confocal microscope are largely derived from those that have been developed over many years for use with the conventional wide field microscope. In the biomedical sciences, a major application of confocal microscopy involves imaging either fixed or living cells and tissues that have usually been labeled with one or more fluorescent probes. A large number of fluorescent probes are available that, when incorporated in relatively simple protocols, specifically stain certain cellular organelles and structures. Among the plethora of available probes are dyes that label nuclei, the Golgi apparatus, the endoplasmic reticulum, and mitochondria, and also dyes such as fluorescently labeled phalloidins that target polymerized actin in cells. Regardless of the specimen preparation protocol employed, a primary benefit of the manner in which confocal microscopy is carried out is the flexibility in image display and analysis that results from the simultaneous collection of multiple images, in digital form, into a computer.

**Critical Aspects of Confocal Microscopy** - Quantitative three-dimensional imaging in fluorescence microscopy is often complicated by artifacts due to specimen preparation, controllable and uncontrollable experimental variables, or configuration problems with the microscope. This article, written by Dr. James B.

Pawley, catalogs the most common extraneous factors that often serve to obscure results collected in fluorescence widefield and confocal microscopy. Among the topics discussed are the laser system, optical component alignment, objective magnification, bleaching artifacts, aberrations, immersion oil, cover slip thickness, quantum efficiency, and the specimen embedding medium.

**Aberrations in Multicolor Confocal Microscopy** - Refinements in design have simplified confocal microscopy to the extent that it has become a standard research tool in cell biology. However, as confocal microscopes have become more powerful, they have also become more demanding of their optical components. In fact, optical aberrations that cause subtle defects in image quality in widefield microscopy can have devastating effects in confocal microscopy. Unfortunately, the exacting optical requirements of confocal microscopy are often hidden by the optical system that guarantees a sharp image, even when the microscope is performing poorly. Optics manufacturers provide a wide range of microscope objectives, each designed for specific applications. This report demonstrates how the trade-offs involved in objective design can affect confocal microscopy.

**Three-Color Imaging for Confocal Microscopy** - The laser scanning confocal microscope (**LSCM**) is routinely used to produce digital images of single-, double-, and triple-labeled fluorescent samples. The use of red, green and blue (**RGB**) color is most informative for displaying the distribution of up to three fluorescent probes labeling a cell, where any co-localization is observed as a different additive color when the images are colorized and merged into a single three-color image. In this section we present a simplified version of a previously published method for producing three-color confocal images using the popular image manipulation program, Adobe Photoshop. In addition, several applications of the three-color merging protocol for displaying confocal images are discussed. Note that these digital methods are not confined to images produced using the LSCM and can be applied to digital images imported into Photoshop from many different sources.

**Basics of Confocal Reflection Microscopy** - Confocal reflection microscopy can be utilized to gather additional information from a specimen with relatively little extra effort, since the technique requires minimum specimen preparation and instrument re-configuration. In addition, information from unstained tissues is readily available with confocal reflection microscopy, as is data from tissues labeled with probes that reflect light. The method can also be utilized in combination with more common classical fluorescence techniques. Examples of the latter application are detection of unlabeled cells in a population of fluorescently labeled cells and for imaging the interactions between fluorescently labeled cells growing on opaque, patterned substrata.

**Confocal Microscopy Image Gallery** - The Nikon MicroscopyU Confocal Image Gallery features digital image sequences captured using a Nikon PCM-2000 confocal microscope scanning system coupled to an Eclipse E-600 upright microscope. Successive serial optical sections were recorded along the optical axis of the microscope over a range of specimen planes. These sequences are presented as interactive Java tutorials that allow the visitor to either "play" the series of sections automatically, or to utilize a slider to scroll back and forth through the images.

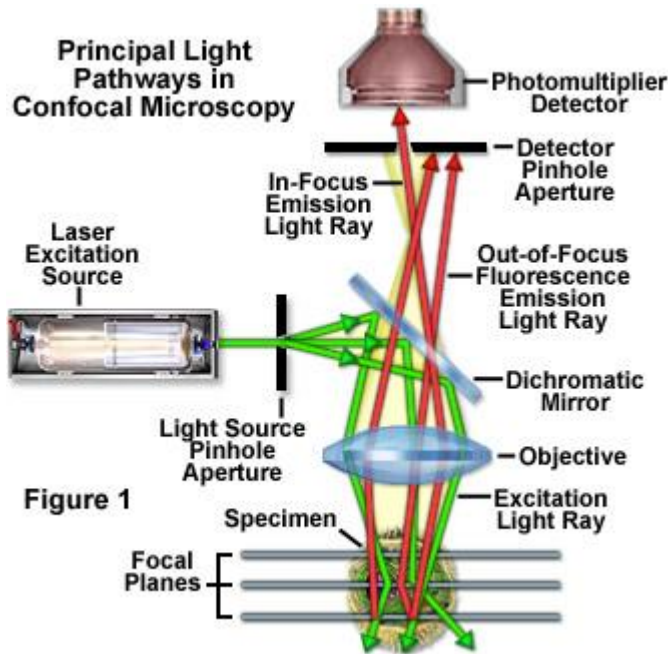
## Interactive Java Tutorials

**Laser Scanning Confocal Microscopy** - (approximately a **30 second download** on 28.8K modems) Several methods have been developed to overcome the poor contrast inherent with imaging thick specimens in a conventional microscope. Specimens having a moderate degree of thickness (5 to 15 microns) will produce dramatically improved images with either with confocal or deconvolution techniques. The thickest specimens (20 microns and above) will suffer from a tremendous amount of extraneous light in out-of-focus regions, and are probably best-imaged using confocal techniques. This tutorial explores imaging specimens through serial z-axis optical sections utilizing a virtual confocal microscope.

**Reflected Confocal Microscopy: Integrated Circuit Inspection** - Examine individual layers on the surface of integrated circuits with this interactive tutorial. Digital images for the tutorial were collected with a Nikon Optiphot C200 reflected light confocal microscope. For each sequence, a series of z-axis optical sections was recorded as the microscope was successively focused (at 1-micrometer steps) deeper within the patchwork of circuitry on the surface of the silicon chips.

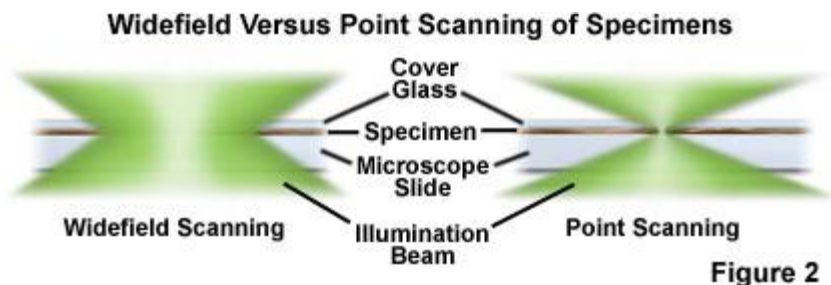
## Basic Concepts

Confocal microscopy offers several advantages over conventional optical microscopy, including shallow depth of field, elimination of out-of-focus glare, and the ability to collect serial optical sections from thick specimens. In the biomedical sciences, a major application of confocal microscopy involves imaging either fixed or living cells and tissues that have usually been labeled with one or more fluorescent probes.



When fluorescent specimens are imaged using a conventional widefield optical microscope, secondary fluorescence emitted by the specimen that appears away from the region of interest often interferes with the resolution of those features that are in focus. This situation is especially problematic for specimens having a thickness greater than about 2 micrometers. The confocal imaging approach provides a marginal improvement in both axial and lateral resolution, but it is the ability of the instrument to exclude from the image the "out-of focus" flare that occurs in thick fluorescently labeled specimens, which has caused the recent explosion in popularity of the technique. Most current confocal microscopes are relatively easy to operate and have become part of the basic instrumentation of many multi-user imaging facilities. Because the resolution possible in the laser scanning confocal microscope (**LSCM**) is somewhat better than in the conventional widefield optical microscope, but still considerably less than that of the transmission electron microscope, it has in some ways bridged the gap between the two more commonly used techniques. Figure 1 illustrates the principal light pathways in a basic confocal microscope configuration.

In a conventional widefield microscope, the entire specimen is bathed in light from a mercury or xenon source, and the image can be viewed directly by eye or projected directly onto an image capture device or photographic film. In contrast, the method of image formation in a confocal microscope is fundamentally different. The illumination is achieved by scanning one or more focused beams of light, usually from a laser, across the specimen (Figure 2). The images produced by scanning the specimen in this way are called optical sections. This terminology refers to the noninvasive method by which the instrument collects images, using focused light rather than physical means to section the specimen.



The confocal approach has facilitated much more useful imaging of living specimens, enabled the automated collection of three-dimensional (z-series) data, and improved the images obtained of specimens using multiple labeling. Figure 3 presents a comparison of a conventional epifluorescence image with a confocal image of similar regions of a whole mount of a butterfly pupal wing epithelium stained with propidium iodide. There is a striking improvement of resolution of nuclei in the LSCM image due to elimination of out-of-focus fluorescence flare.

The laser scanning confocal microscope (LSCM) is currently the most widely used confocal variation for biomedical research applications. Emphasis is placed on the LSCM in this introduction, since it is the design most likely to be encountered by the novice user. Other alternative designs of the instruments are favored in specific niches within the field of biological imaging. Most of the protocols for specimen preparation can be used, with minor modification, for any of the confocal instrument variants, as well as for other methodologies for producing optical sections such as deconvolution techniques and multiple-photon imaging.

### Evolution of Confocal Microscopy

The invention of the confocal microscope is usually attributed to Marvin Minsky, who produced a working microscope in 1955. The development of the confocal approach was largely driven by the desire to image biological events as they occur in living tissue (*in vivo*), and Minsky had the goal of imaging neural networks in unstained preparations of living brains. The principle of confocal imaging advanced by Minsky, and patented in 1957, is employed in all modern confocal microscopes. Figure 1 illustrates the confocal principle, as applied in epifluorescence microscopy, which has become the basic configuration of most modern confocal systems used for fluorescence imaging. Minsky's original configuration used a pinhole placed in front of a zirconium arc source as the point source of light.

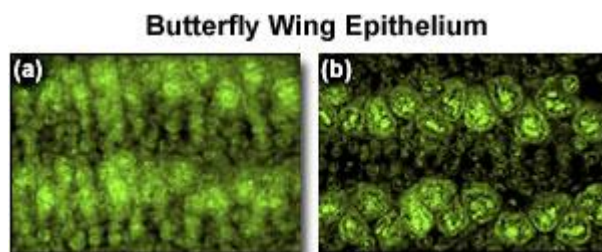


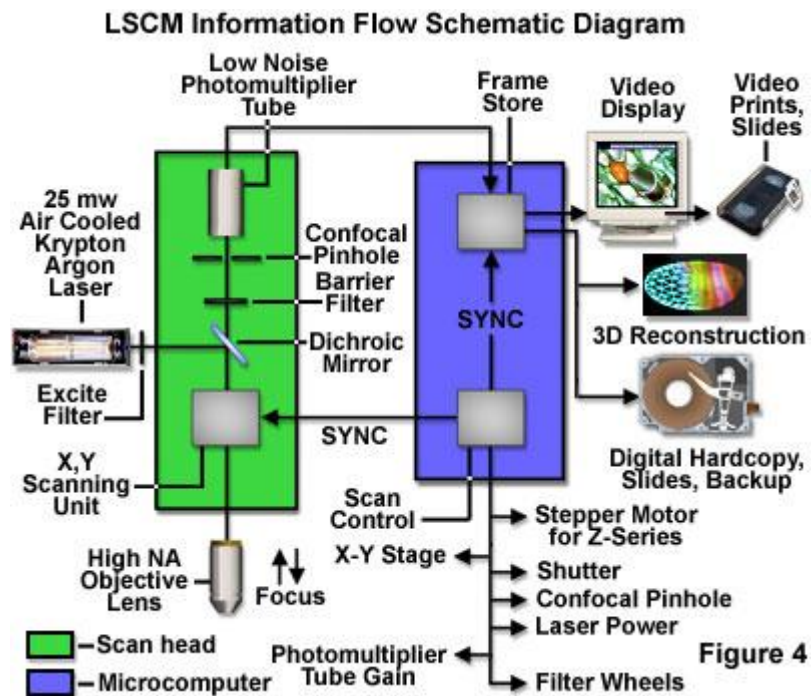
**Figure 3**

The point of light was focused by an objective lens at the desired focal plane in the specimen, and light that passed through it was focused by a second objective lens at a second pinhole having the same focus as the first pinhole (the two were confocal). Any light that passed the second pinhole struck a low-noise photomultiplier, which generated a signal that was related to the brightness of the light from the specimen. The second pinhole prevented light originating from above or below the plane of focus in the specimen from reaching the photomultiplier. The use of spatial filtering to eliminate out-of-focus light or flare, in specimens that are thicker than the plane of focus, is the key to the confocal approach. In Minsky's writings he also described a reflected light version of the microscope that used a single objective lens and a dichromatic mirror arrangement that became the basis for the systems currently in use.

In order to build an image using the confocal principle, the focused spot of light must be scanned across the specimen in some way. In the original instrument built by Minsky the beam was kept stationary and the specimen itself was moved on a vibrating stage. This arrangement has the advantage that the scanning beam is held stationary on the optical axis of the microscope, which can eliminate most lens defects that would affect the image. For biological specimens, however, movement of the specimen can cause wobble and distortion, resulting in a loss of resolution in the image. Furthermore, it is impossible to perform various manipulations on the specimen such as microinjection of fluorescently labeled probes when the stage and specimen are moving.

Regardless of the means by which the illuminating beam is scanned across the specimen, an image of the specimen must be produced. A real image was not formed in Minsky's original design, but instead the output from the photomultiplier was translated into an image on the screen of a military surplus long persistence oscilloscope that had no provision for recording. Following the debut of his invention, Minsky later wrote that the image quality in his microscope was not very impressive because of the quality of the oscilloscope display and not because of poor resolution achieved by the microscope itself. It is now clear that the technology was not available to Minsky in 1955 to fully demonstrate the potential of the confocal approach,

especially for imaging biological structures. He stated that this is possibly a reason that confocal microscopy was not immediately embraced by the biological community, who were, and still are, a highly demanding group concerning the quality of their images. At the time, they had available light microscopes with excellent optics, and could easily view and photograph their brightly stained and colorful histological tissue sections onto high-resolution color film. In today's confocal microscopes, the image is serially built up from the output of a photomultiplier tube or captured using a digital camera incorporating a charge-coupled device, directly processed in a computer imaging system, displayed on a high-resolution video monitor, and output on a hard copy device, with outstanding results. The information flow in a modern laser scanning confocal microscope is diagramed in Figure 4.



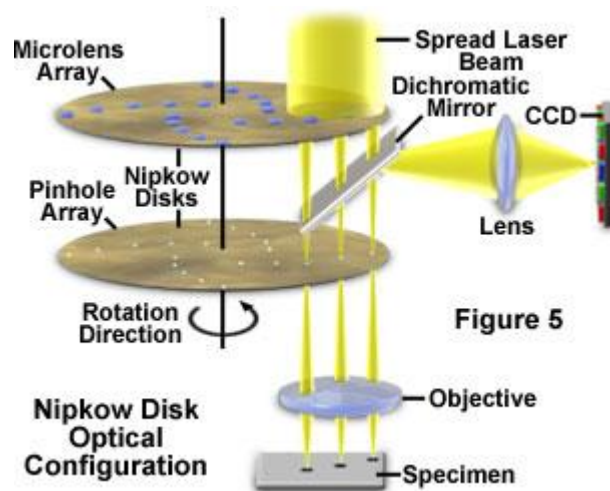
The basic optics of the optical microscope have remained fundamentally unchanged for decades because the final resolution achieved by the instrument is governed by the wavelength of light, the objective lens, and the properties of the specimen itself. The dyes used to add contrast to specimens, and other technology associated with the methods of optical microscopy, have improved significantly over the past 20 years. The growth and refinement of the confocal approach is a direct result of a renaissance in optical microscopy that has been fueled largely by advancements in modern technology. A number of major technological advances that would have been a benefit to Minsky's confocal design have gradually become available (or more affordable) to biologists and other microscopists. Among these are stable multiwavelength lasers for improved point light sources, improved dichromatic mirrors, sensitive low-noise photodetectors, fast microcomputers with image processing capabilities enhanced by availability of affordable large-capacity memory chips, sophisticated image analysis software packages, and high-resolution video displays and digital image printers.

These technologies were developed independently, and since 1955, have been gradually incorporated into confocal imaging systems. As one example, digital image processing techniques were first applied effectively in the early 1980s by researchers at the Woods Hole Oceanographic Institute. Using what they termed "video-enhanced microscopes" they were able to image cellular structures such as microtubules, which are just beyond the theoretical resolution of the optical microscope. The apparent increase in resolution was enabled by digital enhancement of images that were captured using a low light level silicon intensified target (SIT) video camera connected to a digital image processor. The cellular structures were imaged using differential interference contrast (DIC) optics, and the images were further enhanced using digital processing methods.

The classification of confocal microscope designs is usually done on the basis of the method by which the specimens are scanned. The two fundamental means of scanning are to scan either the stage or the illumination beam, and there are at least two fundamentally different methods of beam scanning. The original design by Minsky was a stage scanning system that was driven by a primitive tuning fork device, and it was rather slow in building an image. Current stage scanning confocal designs that have evolved from the

original concept are primarily used in materials science applications such as the microchip industry. Systems based upon this principle have recently become popular in biomedical applications involving screening of DNA on microchips.

A more practical alternative for most imaging of biological systems is to scan the illumination beam across a stationary specimen. This approach is the basis of many of the systems that have evolved into the research microscopes that are in vogue today. The technical details involved in confocal microscopy are not dealt with in this introduction, but basically two fundamentally different methods of beam scanning are used; multiple-beam scanning and single-beam scanning. Single-beam scanning is currently the most popular, and is the method used in the LSCM. Here the scanning of the beam is most commonly achieved by use of computer-controlled mirrors driven by galvanometers at a rate of one frame per second. To achieve faster scanning, at near video frame rates, some systems use an acousto-optical device or oscillating mirrors. The alternative method uses two beams to scan at near real time, and usually relies on using some form of spinning Nipkow disk. Such systems have been derived from the tandem scanning microscope (**TSM**), with improvements to make them more efficient for collecting images from fluorescently labeled specimens. Figure 5 illustrates one such improved system that employs dual Nipkow disks and microlenses to enhance the detection of the low fluorescence levels of real time image collection.

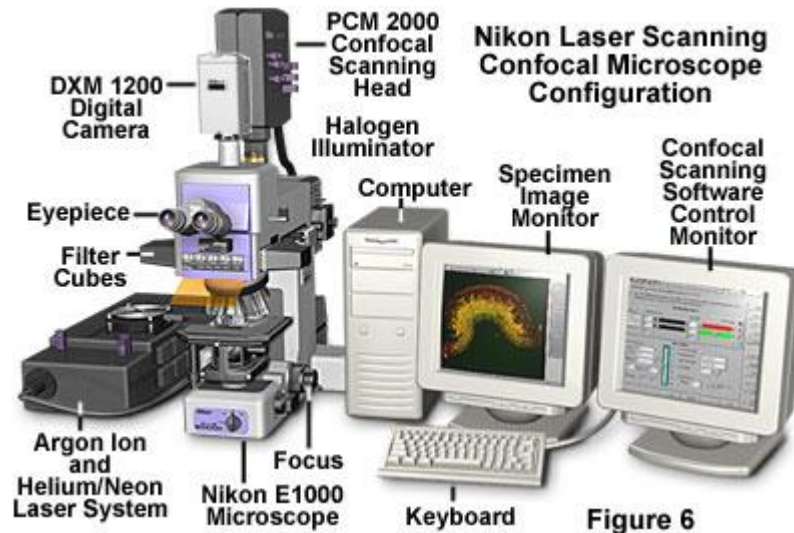


There are currently two alternative methods to confocal microscopy that are in use for producing optical sections: deconvolution and multiphoton imaging. They differ technically, but like confocal methods, are based on the conventional optical microscope. Deconvolution uses computer-based algorithms to calculate and remove out-of-focus information from fluorescence images. Due to more efficient algorithms and much faster mini computers, this technique has become a practical option for imaging. Multiphoton microscopy uses the same scanning system as the LSCM, but does not require the pinhole aperture at the detector. The pinhole is unnecessary because the laser excites the fluorochrome label only at the point of focus, eliminating the out-of-focus emission. An additional benefit in the imaging of living tissues is that photobleaching is reduced in the specimen due to the reduced energy absorbed from the laser beam.

The conventional optical microscope forms the basis around which the LSCM is built. Instead of a tungsten or mercury lamp, a laser is used as a light source, and is combined with a sensitive photomultiplier tube (**PMT**) detector, and a computer to control the scanning mirrors or other scanning devices and to facilitate the collection and display of images. Following acquisition the images are stored on digital media and may be analyzed by any of the numerous image processing software packages available using either the microscope system computer or a second computer.

By design of the LSCM, illumination and detection are confined to a single diffraction-limited point in the specimen. This point of illumination is brought to focus in the specimen by the objective lens, and scanned across it using some sort of scanning device under computer control. The sequences of points of light from the specimen are detected by the photomultiplier through a pinhole (or in some cases, a slit), and the output from the PMT is built into an image and displayed by the computer. Although unstained specimens can be viewed using light reflected back from the specimen, they usually are labeled with one or more fluorescent probes.

One of the more commercially successful LSCMs, reported in the literature about 1990, was designed in response to a perplexing fundamental problem encountered by developmental biologists. Many of the structures and specific macromolecules inside immunofluorescently labeled embryos are impossible to image after the two-cell stage using conventional epifluorescence microscopy because as the cell numbers increase, the overall volume of the embryo remains approximately the same. This means that with more and more closely packed cells, increased fluorescence from cells out of any given focal plane of interest interferes with image resolution.



A group of researchers working on the problem discovered that none of the confocal systems available at the time would satisfy their needs. The technology of the time consisted of stage scanning microscopes that were too slow in producing images, taking about 10 seconds for one image, and the multi-beam scanning instruments, which were not practical for fluorescence imaging at that time in their development. A LSCM was designed that was suitable for conventional epifluorescence microscopy, and along with several others that were developed during the same time period, became a forerunner of the sophisticated instruments that are now available to the biomedical community from several commercial vendors. A typical example of a currently available system (the Nikon E1000) is illustrated in Figure 6.

In the specialized instrument that was developed, the thickness of the optical sections could be varied by adjusting the diameter of the pinhole in front of the photodetector. Compared to some other designs that use a fixed pinhole size, this optical variation is extremely flexible for imaging biological structures. The image can be zoomed with no loss of resolution by decreasing the area of the region scanned in the specimen, and placing the scanned information into the same size of digital array for storage or display (in similar fashion to changing magnification in the scanning electron microscope). The ability to do this imparts a range of magnifications to one objective lens, and can be extremely useful when imaging rare or transient events that may be missed or the location lost if lenses must be changed.

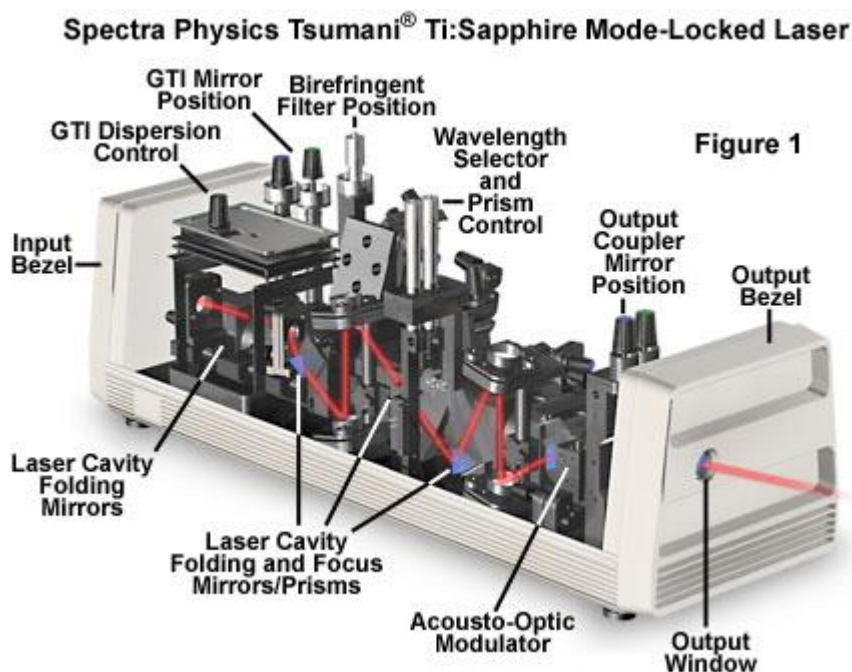
Due to the sophistication and flexibility of the LSCMs available from commercial vendors now, there has been a tremendous explosion in the popularity of confocal microscopy in recent years, with many multi-user laboratories purchasing these instruments in preference to electron microscopes. Confocal microscopy has an advantage in the relative ease with which extremely high-quality images can be obtained from specimens prepared for conventional optical microscopy, and in its great number of applications in many areas of current research interest.

The first-generation LSCMs worked well for fixed specimens, but were extremely wasteful in their use of light energy from the lasers, and tended to kill living specimens unless great care was taken to preserve their viability while they were being imaged. In spite of the limitations, the images of fixed material produced by the microscopes were so good that the confocal approach was fully embraced by the biological imaging specialists. Technological improvements have been made to every aspect of the imaging process in subsequent generations of instruments. In addition, the ergonomics and usability of the newer instruments is much improved so that alignment, changing filter combinations, and adjusting laser power, now usually controlled by software, are all much easier and less time consuming. It is now possible to image up to three fluorochromes simultaneously, and more than that sequentially. The image processing stage is also more

highly developed due to improved, more reliable software, and much faster computers with more disk storage space and more, and less expensive, random access memory.

## Laser Systems for Confocal Microscopy

The lasers commonly employed in laser scanning confocal microscopy are high-intensity monochromatic light sources, which are useful as tools for a variety of techniques including optical trapping, lifetime imaging studies, photobleaching recovery, and total internal reflection fluorescence. In addition, lasers are also the most common light source for scanning confocal fluorescence microscopy, and have been utilized, although less frequently, in conventional widefield fluorescence investigations.



Lasers emit intense packets of monochromatic light that are coherent and highly collimated to form a tight beam with a very low rate of expansion. Compared to other light sources, the extremely pure wavelength ranges emitted by the laser have a bandwidth and phase relationship that is unparalleled by tungsten-halogen or arc-discharge lamps. As a result, laser light beams can travel over long distances and can be expanded to fill apertures or focused to a very small spot with a high level of brightness. Beyond the similarities common to all lasers, which include a gain medium (light source), excitation source (power supply), and resonator, these light sources differ radically in size, cost, output power, beam quality, power consumption, and operating life.

The coherence of monochromatic light produced by most laser systems introduces problems in the application of these light sources for classical widefield microscopy. Light scattering and diffraction patterns are introduced by interference at every surface in the optical path. In addition, the field and aperture diaphragms, as well as dirt, also produce artifacts. These undesirable effects can be minimized or eliminated by a variety of techniques. The most common methods include temporally scrambling laser light by rapidly varying the optical path length between the light source and the microscope, or scanning the specimen point by point as is the case in confocal microscopy systems. In addition, interference and other artifacts can often be eliminated by the aperture scanning technique. If the path length or coherence state of the laser beam fluctuates at a faster interval than the detector integration time (in effect, the video frame rate), the speckle and scattering artifacts disappear from the image.

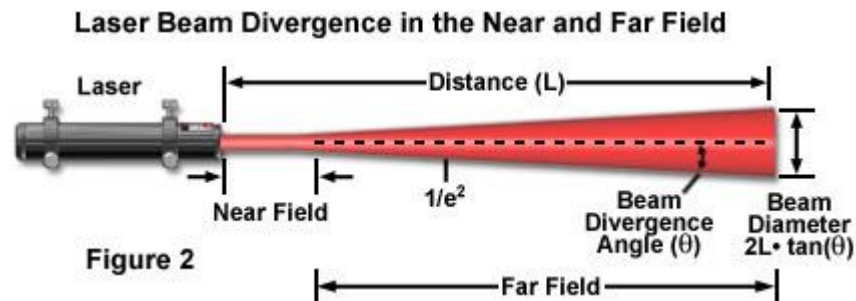
A successful technique employed by some investigators to improve differential interference contrast (**DIC**) images produced with an argon ion laser light source is to position a circular glass wedge, spinning at 2500 revolutions per minute, in the light path. Rapid variations in optical path length are introduced by differences in wedge thickness as the wedge rotates in front of the expanded laser beam. Currently, path length variation is usually accomplished by employing a fiber-optic light pipe to route the light between the light

source and the microscope. Vibrating the fiber produces continual changes in the optical path length, causing the beam to become temporally incoherent at frequencies below that of the vibration level. The vibrations may be generated by a piezoelectric device, a loudspeaker, or the cooling fan utilized in the laser head.

Illustrated in Figure 1 is a self mode-locked Ti:sapphire pulsed laser, which is currently one of the preferred laser excitation sources in a majority of multiphoton fluorescence microscopy investigations. Ti:sapphire mode-locked lasers provide a large wavelength tuning range, from about 690 to over 1050 nanometers, with pulse widths approximately 100 femtoseconds in length. In addition, these lasers have sufficient power (greater than 100 milliwatts throughout the tuning range) for saturation of two-photon excitation in most fluorophores. To ensure proper cooling and humidity control of the laser crystal, nitrogen gas is pumped into the sealed laser head, which is maintained at constant temperature by an external chiller.

The light produced by many laser systems is linearly polarized, with a polarization vector oriented vertically. This property can be exploited in applications requiring a polarized illumination source, such as differential interference contrast, polarized light measurements, or quantitative investigations of fluorescence polarization anisotropy.

The coherence and polarization characteristics of a laser beam are measured by the distribution of light in the beam cross-section, or profile, which changes with increasing distance from the exit mirror of the laser. The following discussion of laser beam characteristics is presented as a general overview of the subject that may prove useful in employing lasers in microscope imaging, laser trapping, and other applications.



When a laser operates in the simplest **transverse electromagnetic mode**, referred to as the **TEM(00)** mode, the emitted beam has a planar wave front and a Gaussian intensity (irradiance) profile. The laser beam diameter is commonly defined as the value at which the intensity has fallen to **e(E-2)** (13.5 percent) of its peak value. The Gaussian profile of the laser beam arises because of diffraction, which prevents the propagation of a perfectly collimated beam and induces transverse spreading of the light waves. Near the laser output aperture (termed the **near field**), the phase fronts of the beam can become disordered. As a consequence, the beam cross-sectional shape, size, and irradiance profile then change rapidly with distance from the laser. At greater distances (the **far field**), the phase fronts stabilize into the resultant Gaussian profile. In some literature references, the near field and far field are referred to by the alternative terms of **Fresnel zone** and **Fraunhofer zone**, respectively. The near field is also sometimes termed the **Rayleigh range**. The far field begins at a distance, **z**, defined by

$$z = A_0^2 / \lambda$$

where **A(0)** is the beam diameter at the exit aperture and **λ** is the wavelength of light emitted by the laser. Applying this equation to an argon laser emitting a 0.6-millimeter-waist-diameter beam at a wavelength of 488 nanometers, the far field begins at approximately 74 centimeters from the exit aperture.

Presented in Figure 2 is a schematic diagram of laser beam geometry and divergence in the near and far fields. As discussed above, the beam can be considered essentially a parallel bundle of wavefronts that undergoes little spreading in the near field. Beyond the near field, the beam divergence angle (**q**), which is measured from the center of the beam to the edge (**e(E-2)**), grows larger and becomes the critical parameter in determining beam diameter (**D**) according to the equation:

$$\text{Beam Diameter (D)} = 2L \cdot \tan(q)$$

where **D** is the variable signifying laser beam diameter and **L** represents the length of the distance from the laser exit aperture to the measurement point on the beam. In practice, several laser beam characteristics, including the irradiance profile, are critical factors in many microscopy applications, and knowledge of the distance to the far field may be necessary in configuring the imaging system. Table 1 presents calculated values of this distance (using the equation given above) for a number of commonly utilized lasers and emission lines, and typical beam waist diameters.

**Distance to the Far Field**

Wavelength (nm)	Beam Diameter (mm)	Far Field Distance (cm)
<b>Argon-Ion</b>		
488	0.6	74
514	1.0	195
<b>Helium-Neon</b>		
543	0.4	30
594	0.7	83
612	0.7	80
632	0.7	78
<b>Nd:YAG</b>		
355	3.0	2535
532	1.0	188
<b>Ti:Sapphire</b>		
790	2.0	506
395	2.0	1012
790	0.8	81

**Table 1**

Whether or not the beam exhibits Gaussian character is important in most laser applications because the beam often has to be focused, shaped, and otherwise modified by lenses and other optical components. A Gaussian beam has certain definable transformation characteristics, and these enable assumptions to be made about how the beam will propagate through an optical system.

The angular radius (or beam divergence angle; see Figure 2), designated by **q** (in radians), of a Gaussian beam in the far field is approximated by the expression:

$$q = l / \rho a_0$$

where **a(0)** is the beam waist radius at the laser exit aperture. The beam waist diameter is a function of laser wavelength, cavity length, and other design parameters of the cavity. As the distance (**z**) from the laser increases, the beam waist radius is given by the equation:

$$a(z) = qz$$

Typically, laser beams are characterized by beam **propagation** parameters such as the square of **M**, or **K** (which is equivalent to the reciprocal of the square of **M**), determined from a combination of near field and far field measurements as follows:

$$M^2 = \rho A_0 q / 4l$$

Smaller values of **M<sup>2</sup>**, which is termed a **propagation constant** or **propagation factor**, are indicative of higher beam quality, particularly in reference to a smaller diameter and divergence. The factor describes the relationship of the real beam to that of an ideal Gaussian beam.

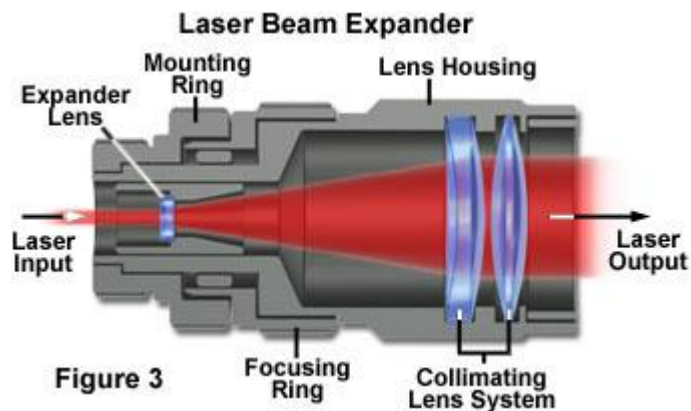
Coherent Gaussian beams have specific properties that cause them to differ from incoherent light beams in their propagation and transformation by lenses and mirrors. In the case of a diffraction-limited beam, the intensity profile of a Gaussian beam is itself Gaussian, provided that the beam is not truncated by the lens aperture. When the Gaussian beam diameter is one-half the aperture diameter of the lens, the intensity profile of the emergent beam remains Gaussian. When the Gaussian beam diameter is equal to the diameter of the lens aperture, the output beam intensity profile is a mixture of the Gaussian function and that of an Airy disk. Finally, a Gaussian beam diameter significantly larger than the diameter of the lens aperture produces the output profile of an Airy disk. In the latter instance, much of the laser power may be lost due to overfilling of the lens entrance aperture.

The overall topic of Gaussian beam optics is thoroughly covered in numerous textbooks, and details not discussed here may be obtained from more comprehensive sources. Two types of manipulation of the Gaussian beam are of particular interest to the microscopist utilizing lasers - **beam concentration** and **beam expansion**.

When a laser beam is focused to a very small spot by an aberration-free microscope objective (beam concentration), the radius of the spot at the focus (at distance  $z$ ) is given by the expressions:

$$a(z) = lf/pa_0$$

where  $f$  is the focal length of the lens. As an example, if a 100x objective having a numerical aperture of 1.3 (producing a focal length of approximately 1.6 millimeters) is employed to concentrate the 488-nanometer beam of an argon laser having a 0.3-millimeter radius, the focused spot radius (determined from the previous equation) is 0.8 micrometer. Increasing the beam waist fivefold through beam expansion (as discussed below) would result in a focused spot radius of approximately 0.16 micrometer.



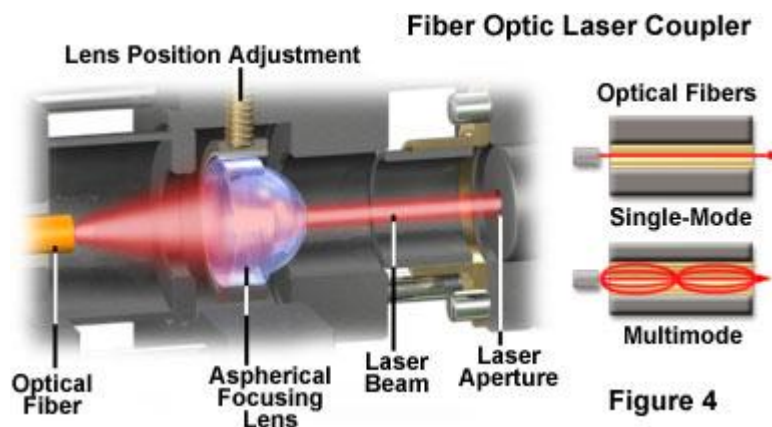
It is important to note that extremely high power densities are achieved at the focal point of a concentrated laser beam. A 10-milliwatt beam focused to a diffraction-limited spot 0.22 micrometers in diameter results in a power density of approximately 30-million watts per square centimeter. Such high energy levels can rapidly degrade or destroy lens and filter coatings, as well as introduce considerable photochemical damage to biological specimens. However, for such a minute spot size, diffusion of thermal energy can be so effective in water that a high-energy, near-infrared beam may do little damage to a biological specimen unless absorption of the energy by the specimen is sufficiently high.

In many applications of lasers in optical microscopy, the laser beam is initially expanded by the use of a **Keplerian** or **Galilean** beam expander, either of which is actually a reversed telescope (typical laser beam expander anatomical features are illustrated in Figure 3). The divergence of a coherent Gaussian beam can be reduced, and the beam optimally collimated over a longer distance, if the laser beam is first expanded. Referring to the previous equations, the angular radius of the beam, designated  $q$ , is inversely proportional to the beam waist radius,  $a(0)$ , at the laser exit aperture. Therefore, expanding the beam waist radius diminishes the divergence proportionally.

It is practical for many applications in microscopy to pipe the laser output directly into the microscope optical path through a flexible optical fiber (as illustrated in Figure 4). This technique is preferable to the alternative method of rigidly aligning the laser and microscope, which requires employing a massive, vibration-free optical table and numerous fixed mirrors and other components.

When a laser beam is focused by a lens onto an optical fiber, the coupling efficiency and characteristics of the beam that emerges from the fiber depend heavily on the fiber geometry. Most of the optical fibers utilized for laser light delivery are constructed with a fused-silica core. These fibers consist of an inner core fabricated with high-refractive-index silica and surrounded by a sleeve, termed the **cladding**, composed of lower-refractive-index material. Light is prevented from escaping the fiber along its length by total internal reflection at the interface of the core and the cladding. The cladding may be composed of silica, glass, a hard fluoropolymer, or a soft silicone.

Optical fibers are classified as **single-mode** or **multimode** according to the diameter of their inner cores. A single-mode fiber allows propagation of only the lowest-order mode at one particular wavelength (Figure 4). The wavelength propagated and polarization preservation of the wave are determined by the fiber diameter. Although other wavelengths may propagate, they do so with reduced efficiency. Typical single-mode fiber diameters range from 3 to 6 micrometers for visible-light wavelengths, and the output irradiance profile of a single-mode fiber is Gaussian.



A multimode optical fiber enables the propagation of more than one mode, and is not restricted to a single wavelength. The inner cores of multimode optical fibers are larger than single-mode fibers, ranging from approximately 100 micrometers to 1.2 millimeters in diameter. The output irradiance profile from a multimode fiber has a flat shape, referred to as a **top-hat profile**, with a numerical aperture that is determined by the core and cladding refractive indices.

The acceptance cone angle,  $q$ , of the fiber core is related to the numerical aperture, **NA**, of the fiber as follows:

$$NA = \sin q / (n_{\text{core}}^2 - n_{\text{cladding}}^2)^{1/2}$$

where  $n$  represents refractive index. Efficient coupling of laser light to the fiber core occurs when the fiber core numerical aperture and that of the beam concentration lens are matched. The efficiency of light transmission through an optical fiber is typically as high as approximately 90 percent, but may be sharply reduced (to only 60 or 70 percent) by bends having very small radii (less than 3 centimeters).

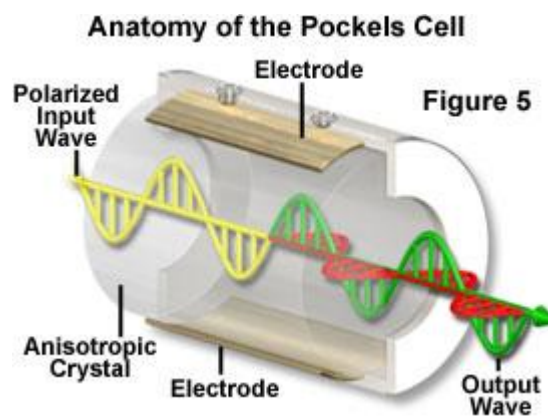
In utilizing any laser, it is crucial not only to prevent any direct or specularly reflected laser light from entering an observer's eyes, but also to avoid reflection of the beam from a component of the optical system back into the laser system. The former is an obvious personal safety precaution, while the latter caution is important to prevent an additional reflector from returning a coherent beam back into the laser, causing possible damage to the system.

Stability of the laser light source is an important aspect in many applications, particularly in quantitative microscopy, where illumination intensity fluctuations can adversely affect experimental results. A number of factors related to stimulated emission and cavity length fluctuations can induce frequency noise in the output beam, but other perturbations causing amplitude fluctuations can create both high-frequency **intensity noise** and slow variations (drift) in optical output power. Some sources of these intensity fluctuations are related to the function of the laser head itself or the power supply. The most common sources of noise in the output beam for various laser categories are listed below:

- **Gas lasers** - Mirror misalignments from resonator vibrations, noise from optical pump sources, plasma oscillations and instabilities of the ion discharge process, fluctuations in power supply current, microphonics from cooling water turbulence, and fan-induced noise in forced-air cooling systems are all potential noise sources.
- **Solid-state lasers** - Noise sources include microphonics, pump source fluctuations for both lamp and diode pumps, cavity alignment errors, and the random frequency-related noise (termed  $1/f$  noise) that is related to thermal fluctuations in the laser medium.
- **Dye lasers** - Both noise (high-frequency) and drift result from density inhomogeneity and air bubbles in the dye solution, and by dye pump and laser pump source instabilities.
- **Semiconductor (diode) lasers** - Noise can result from fluctuations in the drive (bias) current or temperature, and  $1/f$  noise is caused by trapping of carriers in the junction and by other types of carrier (electron-hole) recombination effects.

All lasers are susceptible to noise introduced by their power supplies. **Switching** power supplies, which have become common because of their efficiency and small size, are particularly likely to introduce ripple to the laser system at frequencies ranging into the tens of kilohertz. Such interference, when it affects the light beam in optical microscopy systems, can be especially troublesome to diagnose and remove. The primary difficulty is due to the similarity with noise introduced into the system by other sources, such as electromagnetic fields in the laboratory environment. In order to achieve adequate output stability, semiconductor lasers must be operated with diode current supplies having the highest electrical stability and lowest noise available, and with precise temperature control. Other external noise sources must be controlled, including dust in the laboratory, and vibrations originating from local traffic and building equipment.

The beam intensity of continuous wave (**cw**) lasers can be stabilized by either electronic control of the tube current or through utilization of external components that modulate the light intensity. Two different methods are often employed to control the tube drive current. In the **constant current** mode, tube current is directly controlled by an electronic feedback loop to minimize fluctuations. Because the laser output is also temperature dependent, this type of control circuit is most effective if adequate temperature control is provided. **Constant output power** stabilizing systems operate by controlling the drive current in response to a signal derived from a circuit that samples the output beam using a beamsplitter and photodiode monitor. This physical arrangement is applicable for gas lasers and several other geometries, but smaller diode lasers are commonly assembled in a package that already includes an integral photodiode. The monitor photodiode samples emission from the rear facet of the laser wafer and produces a signal that enables feedback control of the output power.



External components utilized to provide stabilization of laser intensity generally employ a fast feedback system to control an electro-optic modulator that minimizes fluctuations in beam power. The external **Pockels cell** modulator (see Figure 5) is available from a number of manufacturers, and can be used, in principle, to stabilize the output power of any continuous wave laser. Large intensity fluctuations (up to approximately 50 percent) can be corrected by this technique, but with a proportional reduction in total output power. A wide range of correction capability is important with many systems. The helium-cadmium laser, for example, can exhibit variation in output power of around 20 percent, due in part to strong plasma oscillation between certain beam frequencies. Systems exist that are reported to be suitable for regulating **cw** and **mode-locked** lasers to within a few hundredths of a percent of their output power, and over a frequency range from direct current to several hundred megahertz, with noise attenuation of 500:1, or greater.

The basic components of a Pockels cell modulator are presented in Figure 5. External devices for regulating laser output intensity, similar to the design illustrated in Figure 5, are sometimes categorized or marketed under the term **noise eaters**. The fundamental concept behind electro-optic modulators utilizing the Pockels effect is based on a mechanism for varying the polarization properties of the cell at an extremely rapid rate to provide a variable beam attenuator for control of laser intensity. The polarization state of the laser output determines the total attenuation of the modulator, but up to 80 percent transmission is possible. Following emission from the laser head, a portion of the beam is diverted by a beamsplitter to a photodiode, which compares the intensity to a preset (selectable) reference intensity, and amplifies the difference signal so that it can drive the electro-optic Pockels cell modulator. The amplified signal produces a refractive index change in the cell that rotates the plane of polarization, thereby varying the beam attenuation in proportion to the difference voltage that is applied. Among substances that exhibit a change in polarization properties with changes in electric field (Pockels effect) are potassium dihydrogen phosphate and lithium niobate, and crystals of these materials are commonly utilized in the beam modulators.

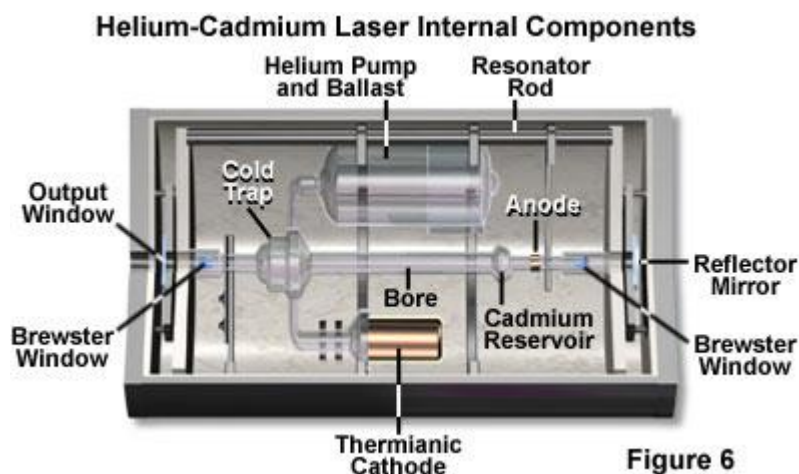
In situations where randomly polarized light is stabilized by a Pockels cell system, the modulator must be positioned between crossed polarizers, and further consideration is necessary to minimize the effects of these additional components on the beam stability. Because dust, vibrations, and other interferences can alter beam stability at any point in the optical path, it is important that external stabilizers are placed as close as possible to the specimen position in optical microscopy systems. This effort will ensure that the most stable beam is delivered to the specimen.

Both the **argon-ion** laser and **krypton-ion** laser produce multiple emission lines from rare-gas transitions that differ substantially in power levels, and only a few of the lines are suited for microscopy applications. The air-cooled argon-ion laser is widely employed as a light source for confocal microscopy because of its brightness level, small size, excellent beam geometry, and the suitability of its spectral lines for fluorescein and (less efficiently) rhodamine excitation. Most argon-ion lasers utilized in widefield or confocal fluorescence microscopy emit only two usable lines, 488 and 514.5 nanometers, which represent approximately 75 percent of the total laser power. Higher-power (greater than 5 watts) argon-ion lasers equipped with special mirrors can emit ultraviolet lines at 334, 351, and 364 nanometers, and additional lines at visible wavelengths extending from 458 to 529 nanometers.

Krypton-ion lasers have found fewer applications in microscopy than argon lasers due to their somewhat longer wavelength output. In addition, krypton produces only 10 to 30 percent as much power as argon when used in the same tube, and often requires water-cooling to generate the equivalent power output of an air-cooled argon system. A major drawback of air-cooled ion lasers is their lack of efficiency, which results in large power requirements and excessive heat generation that must be removed from the system by forced air with exhaust fans. The lifespan of ion lasers is reduced due to gas consumption, with trapped gas being buried within the walls of the discharge tube as a result of the high current densities necessary for laser operation.

Air-cooled lasers using argon-krypton mixtures have become popular in confocal microscopy when several illumination wavelengths are required for dual or multiple-fluorophore studies. Such **mixed-gas** lasers are only capable of producing stable output on major lines that are well separated in the wavelength spectrum. Of the three laser lines typically utilized for confocal microscopy, the 488-nanometer and 568-nanometer lines have approximately equal power (10 to 15 milliwatts), while the 647-nanometer line has about 50 percent more (15 to 25 milliwatts). All ion lasers exhibit excellent beam quality and can be purchased from a variety of manufacturers in single-line, multi-line, and tunable configurations.

The emission at 633 nanometers (termed the **He-Ne line**) of the common **helium-neon** laser has been supplemented by development of variants having emissions in the green (543 nanometers), yellow (594 nanometers), orange (612 nanometers), and near infrared (1523 nanometers) spectral ranges. Although most of these lasers are single-line emitters and relatively low in power (less than 10 milliwatts), the helium-cadmium laser is an exception, emitting at 325 or 442 nanometers with greater than 50 milliwatts of power.

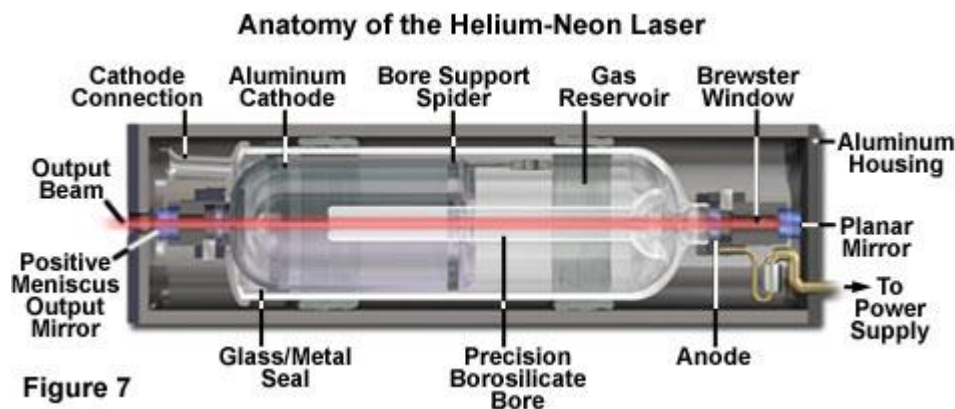


**Helium-cadmium** lasers (illustrated in Figure 6) are considered to be a member of the helium-neon family, and represent an economical source for continuous-wave output in the ultraviolet (325 nanometers at 75 milliwatts and 353 at 20 milliwatts) and violet (442 nanometers at 200 milliwatts) spectral regions. These lasers rely on cadmium vapor as a lasing medium, which is distributed uniformly throughout the bore from the heated cadmium reservoir (at approximately 250 degrees Celsius) by gas-phase electrophoresis. The helium pump maintains a constant helium pressure, which is about a thousand times higher than that of the cadmium vapor. Helium-cadmium lasers display more beam noise than their helium-neon counterparts, primarily because of localized fluctuations in metallic cadmium vapor concentrations in the bore. They also have a shorter lifespan, typically around 5,000 operating hours.

One group of investigators has described the use of a ratio-imaging confocal microscope coupled to both an argon laser operating at 488 nanometers and a helium-cadmium laser emitting at 442 nanometers. This system allowed the group to measure the intensity ratio from the pH-sensitive dye **BCECF** [having an **IUPAC** name of 2',7'-bis-(2-carboxyethyl)-5-(and-6-)-carboxyfluorescein] in isolated renal tubules. Similar measurements have been made utilizing the 458-nanometer line of the argon laser in both widefield and confocal microscopy systems. Another researcher reported using the 325-nanometer output of a helium-cadmium laser to excite two dyes simultaneously and perform emission ratio imaging.

Helium-neon lasers are the most widely utilized laser systems for a broad range of biomedical and industrial applications, and display the most superior Gaussian beam quality of any laser. These lasers are readily available at relatively low cost, have compact size dimensions, and exhibit a long operating life (often reaching 40,000 to 50,000 hours). The low power requirements, superior beam quality (virtually a pure Gaussian profile), and simple cooling requirements (convection) make helium-neon lasers the choice system for many confocal microscopes.

Presented in Figure 7 is a cut-away diagram of a typical helium-neon laser system, which is constructed of glass with a large oxidized-aluminum **cold cathode** as the electron emitter. Operating in the **abnormal glow** current density gas discharge region, helium-neon lasers are generally high-voltage and low current systems, with discharge currents being limited to a few milliamperes and potentials ranging from several hundred to a thousand volts. Progressive deterioration of the oxide coating on the cathode, which ultimately leads to sputtering of aluminum, is the limiting factor in helium-neon laser operating life. Large-diameter discharge tubes typically have longer life spans than smaller tubes (40,000 hours versus about 10,000 hours, respectively).



The **nitrogen** laser has been in use for a number of years as a pulsed light source for both spectroscopy and microscopy. The output is confined to a single line, having a 337.1-nanometer wavelength, with pulse durations ranging from picoseconds to nanoseconds. The pulse repetition rate can be as high as 200 pulses per second. Nitrogen lasers can also be employed to pump dye molecules for longer-wavelength emission. In addition, these lasers have been utilized as a light source for high-speed calcium ratio imaging using the ultraviolet-excitable dye **Fura-2**. In this application, two lasers are used; one serves as a direct source of 337-nanometer light, and the other is dye-pumped to produce emission at 380 nanometers. Pulsing each laser at a repetition rate of 15 per second, in synchrony with the video rate, produces a ratio image every 66 milliseconds.

**Diode lasers**, semiconductor devices that have been under development for decades, are now available with sufficient output power to be of interest to microscopists. The most common of these devices operates in the near infrared, but diode lasers operating in the red and blue regions (and recently, other wavelengths), with substantial output power, have been developed. In addition, those diode lasers now available exhibit improved beam shape and stability, allowing them to replace helium-neon lasers in many applications. Diode lasers typically have a lifespan ranging between 10,000 and 50,000 hours, but are extremely sensitive to electrostatic shock, so they must be handled carefully.

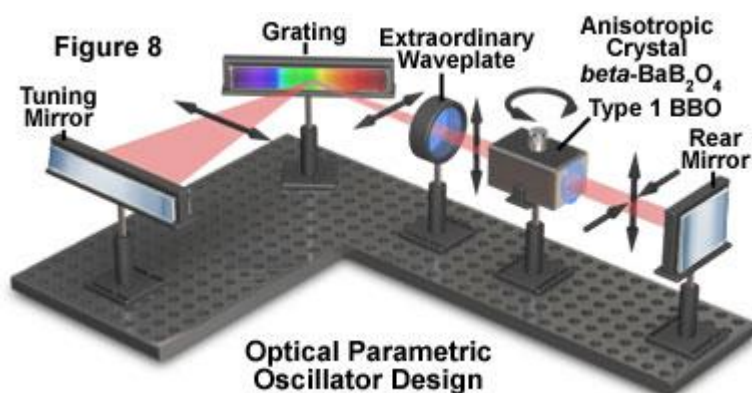
Of great interest to optical microscopists is the development of tunable diode lasers, which can now compete in terms of power and versatility with tunable dye lasers and Ti:sapphire lasers (discussed below and illustrated in Figure 1). Tunable dye lasers have a wavelength range of 600 to 1800 nanometers and can deliver 5 to 25 milliwatts of power. They have the advantages of relatively low cost, compact size, long lifetime, and low heat production, eliminating the requirement for external cooling systems.

Diode-pumped solid-state lasers (**DPSS**) utilize a diode laser instead of noble gases, arc lamps, or flashlamps to pump the solid-state lasing material. The power output, beam quality, and stability exhibited by diode-pumped lasers approaches that of a gas (helium-neon) laser, but the efficiency and size are more comparable with diode lasers. Typical operating and maintenance costs of diode-pumped lasers is less than that of gas lasers, and most systems are cooled either by convection or forced air.

Diode-pumped neodymium-yttrium aluminum garnet (**Nd:YAG**) lasers generate 1064-nanometer light in the milliwatt power range. Frequency doubling leads to a compact device with a continuous-wave output at 532 nanometers, and frequency tripling can also be employed to generate a pulsed output at 355 nanometers. The tightly folded resonator (**TFR**) was developed for pumping a crystal of neodymium-yttrium lithium fluoride (**Nd:YLF**) with high power and efficiency using an array of diode lasers to generate several watts of power at 1047 nanometers. Frequency doubling, tripling, and quadrupling in this type of laser results in power outputs up to hundreds of milliwatts of coherent light at 523, 349, and 262 nanometers (second, third, and fourth harmonics). Other advantages of diode lasers as pump sources include an extended lifetime (typically more than 5000 hours, compared to a few hundred hours for lamps), a collimated and easily focused output that matches the small lasing volume of the solid-state laser, and greatly reduced thermal loading of the laser rod, which usually requires water cooling when halogen arc lamps are used as pumps.

Development of diode-pumped solid-state lasers has been driven by industrial and commercial applications requiring high power (generally several watts) in the green (532 or 523 nanometers) and ultraviolet (355 or 349 nanometers, and the fourth harmonic at 266 nanometers) wavelength ranges. Output in the ultraviolet spectral region is pulsed, with energies ranging from 100 microjoules to 10 millijoules, pulse durations in the nanosecond range, and repetition rates as high as 10 kHz. These lasers are very useful in microscopy for

triggering the release of caged compounds. The pulse repetition rates, however, are still too slow for use as an illumination source for most confocal microscopy applications.



Further development has led to the combination of diode-pumped solid-state lasers with **optical parametric oscillators (OPOs)**; see Figure 8) to produce a tunable, pulsed output that is continuously variable from 205 nanometers to 2000 nanometers. Although the initially-available systems have been expensive and complex in operation, scaled-down versions more suitable for use in microscopy are being introduced.

**Titanium-doped sapphire** lasers (commonly known as **Ti:sapphire** lasers, see Figure 1) provide the advantages of tunability for pulsed and continuous light delivery, as well as solid-state dependability. These lasers can deliver very short light pulses (approximately 80 to 100 femtoseconds) at high repetition rates (100MHz). The range of tunable wavelengths extends from the far red to the near-infrared spectral regions (700 to 1000 nanometers). Most of these lasers are operated with optical pumping by high-power argon lasers, as well as requiring water cooling. As a result of the expense and complexity involved with operating and maintaining Ti:sapphire lasers, their use has been limited primarily to multiphoton microscopy in relatively few laboratories.

Recently, a diode-pumped **Cr:LiSAF** (chromium-doped lithium strontium aluminum fluoride) laser has been developed that delivers high-frequency 90 femtosecond pulses at a wavelength of 860 nanometers, and an average output power of 88 milliwatts. The small size and low power requirements of the Cr:LiSAF laser make it an attractive light source for multiphoton fluorescence microscopy in place of the Ti:sapphire laser.

## Conclusions

Among the major differences between multiphoton and confocal laser fluorescence microscopy is the type of laser utilized in these often complementary techniques. Lasers for multiphoton microscopy are considerably more expensive and difficult to operate than the small air-cooled lasers employed in confocal microscopy.

Development of user-friendly turnkey laser sources for multiphoton microscopy is a necessity if the technique is destined to enjoy widespread acceptance. To date, the scope of multiphoton investigations is limited by the restricted choice of excitation wavelengths provided by suitable laser illumination sources. In order to alleviate complex laser daily maintenance schedules and expand the spectrum of useful excitation wavelengths, new developments in femtosecond-duration optical pulse lasers are essential. Specifically, new laser sources must be engineered that are wavelength-tunable throughout the upper visible (500+ nanometers) and near-infrared portions of the spectrum.

During the past ten years, many new short-pulse laser system variations were made possible by the discovery of Kerr-lens mode locking in titanium-doped sapphire crystal lasers. Other new systems, such as diode-pumped solid-state and single-mode fiber femtosecond lasers are being investigated for their potential as excitation sources for multiphoton microscopy. In the future, frequency doubling of femtosecond pulsed lasers by optical parametric oscillators (**OPOs**) may provide a universal solution to cover the useful wavelength range.

Present applications of lasers in microscopy are expanding rapidly in the areas of confocal microscopy, optical trapping, and the release of caged compounds and fluorophores. The development of compact solid-state lasers with emission lines in the blue-green and ultraviolet regions of the spectrum should serve to further increase the utilization of these devices in microscopy.

## Imaging Modes

The major application of the confocal microscope is in the improved imaging of thicker sections of a wide variety of specimen types. The advantage of the confocal approach results from the capability to image individual optical sections at high resolution in sequence through the specimen. A number of different imaging modes are used; all rely on the optical section as their basic image unit.

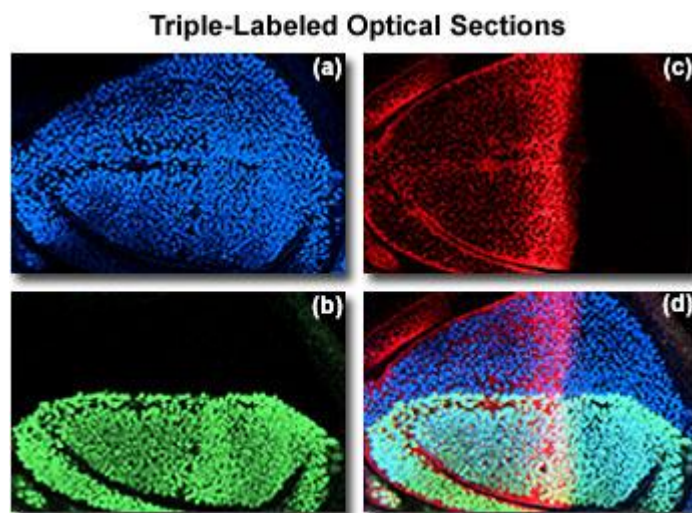


**Figure 1**

### Single Optical Sections

The optical section is the basic image unit in confocal microscopy methods. Data can be collected from fixed and stained specimens in single, double, triple-, or multiple-wavelength illumination modes, and the images collected from multiple-labeled specimens will be in register with each other (if an objective lens with adequate correction for chromatic aberration is used). Minor registration errors can usually be corrected using digital image processing methods. Most laser scanning confocal microscopes (**LSCMs**) take approximately 1 second to acquire a single optical section, although several acquisitions are usually averaged by the software to improve signal-to-noise ratio. The time of image collection will of course vary with the size of the image in pixels and the speed of the system computer. When saved, a typical 8-bit image of 768 x 512 pixels in size will require about 0.3 Mb of storage space.

Presented in Figure 1 are optical sections collected simultaneously at three different excitation wavelengths (488, 568, and 647 nanometers) using a single krypton/argon laser. The specimen is a fruit fly third instar wing imaginal disk labeled for three genes involved with patterning the wing. The three genes imaged and their respective fluorochrome labels are (a) vestigial (fluorescein - 496 nanometers); (b) apterous (lissamine rhodamine - 572 nanometers); and (c) CiD (cyanine 5 - 649 nanometers). The merged composite of the three spatial expression domains of the wing patterning genes is shown in the lower right (image (d)).

### Time-Lapse and Live Cell Imaging

Time-lapse studies of living cells are enhanced by the improved resolution of imaging with the LSCM. Early studies of cell locomotion were carried out using 16 mm movie film with a clockwork intervalometer coupled to the camera, and more recently using a time-lapse video cassette recorder, optical memory disk recorder, or video capture card. Now the LSCM can be used to collect single optical sections at preset time intervals.

Imaging living tissues with the LSCM is substantially more difficult than imaging fixed specimens, and is not always a practical option because the specimen may not tolerate the conditions involved. Table 1 lists some of the factors to be considered in imaging live and fixed cells with the LSCM. Some specimens simply will not physically fit on the stage of the microscope, or they cannot be kept alive on the stage during observation. The phenomenon or structures of interest may not be accessible to the objective lens field of view. For example, the wing imaginal disks of the fruit fly develop too deeply in the larva to be imaged, and when dissected out, they cannot be grown in culture. Therefore, the only method currently available to image gene

expression in this type of tissue is to dissect, fix, and stain imaginal disks taken from different specimens at various stages of development.

### Imaging Fixed and Living Cells with the LSCM

	Fixed Cells	Living Cells
Limits of illumination	Fading of fluorophore	Phototoxicity and fading of dye
Antifade reagent	Phenylenediamine, etc.	NO!
Mountant	Glycerol ( $n = 1.51$ )	Water ( $n = 1.33$ )
Highest NA lens	1.4	1.2
Time per image	Unlimited	Limited by speed of phenomenon; light sensitivity of specimen
Signal averaging	Yes	No
Resolution	Wave optics	Photon statistics

Table 1

Successful imaging of live cells requires extreme care to be taken throughout the imaging process to maintain tolerable conditions on the microscope stage. Photo damage from the illuminating laser beam can be cumulative over multiple scans so the exposure to the beam should be kept to the minimum necessary to acquire the image. Antioxidants such as ascorbic acid are commonly added to the culture medium to reduce oxygen, which can be released in the excitation of fluorescent molecules, causing free radicals to form and kill the cells. It is usually necessary to carry out extensive preliminary control experiments to assess the effects of light exposure on the fluorescently labeled cells, keeping detailed notes on all the imaging parameters, whether they are thought to be relevant or not. Following the imaging tests, the continued viability of the living specimens should be evaluated. Embryos, for example, should continue their normal development following the imaging process, and any abnormalities caused by the imaging or the fluorochromes used should be determined. Time-lapse imaging of a living fruit fly embryo injected with calcium green is presented in Figure 2. The series of images shows the change in distribution of the fluorescent probe over time.

Specific requirements for life have to be met for each cell type that is to be imaged. Some cells such as insect cells can usually be maintained at room temperature in a large enough volume of the appropriate medium. Most cell types, however, require a stage heating device and possibly a perfusion chamber in which the proper carbon dioxide balance can be maintained during the time they are on the microscope stage. Choosing a cell type that is more amenable to the conditions of imaging in the LSCM can avoid many experimental problems. Potential problems have been reduced significantly by improvements in modern confocal instruments. Their increased photon efficiency, higher numerical aperture (brighter) objective lenses, and less phototoxic dyes for labeling has made live cell confocal analysis a practical option. The best approach is to use the least amount of laser power that allows imaging and to collect the images as quickly as possible. If the pinhole aperture is opened wider than for non-living fixed specimens to speed up the image acquisition, post-imaging deconvolution can sometimes be relied upon to restore lost image quality.

#### Time-Lapse Imaging

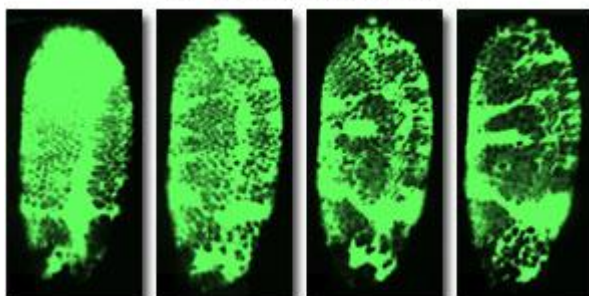


Figure 2

Many physiological processes and events take place faster than they can be captured by most LSCMs, which have image acquisition rates typically on the order of one frame per second. LSCMs using acousto-optical devices and a slit for scanning are faster than the galvanometer-driven point scanning systems, and are more practical for physiological studies. These faster designs combine good spatial resolution with good temporal resolution, which may be 30 frames per second at full screen resolution, or near video rate. The slower point scanning microscope systems can achieve the best temporal resolution only by scanning a much reduced area on the specimen. If full spatial resolution is required, the frames must be collected less frequently, losing some temporal resolution. The confocal systems using disk scanning or oscillating mirror scanning methods are also capable of imaging fast physiological or other transient events.

### Z-Series and Three-Dimensional Imaging

A z-series is a sequence of optical sections collected at different levels perpendicular to the optical axis (the z-axis) within a specimen. Z-series are collected by coordinating step-by-step changes in the fine focus of the microscope with sequential image acquisition at each step. The steps in focus are usually accomplished by a computer-controlled stepping motor that changes focus by predetermined increments. A macro program in the computer can be used to acquire and save an image, change the focus by the programmed distance in the specimen, acquire and save a second image, change the focus again, and so on until the programmed number of images have been collected.

Several images may be extracted from a z-series taken through a region of interest, and merged in an image processing program to highlight the cells of interest. The z-series can also be displayed as a montage of images, such as those shown in Figure 3. This type of image combination and display, and many other image operations, are standard features of most current commercial image acquisition and processing software packages. The images chosen for the figure (Figure 3) are representatives of a larger series showing even smaller increments along the z-axis. The green-emitting stain localizes the peripheral nervous system of a fruit fly embryo that was labeled with the antibody designated 22C10.

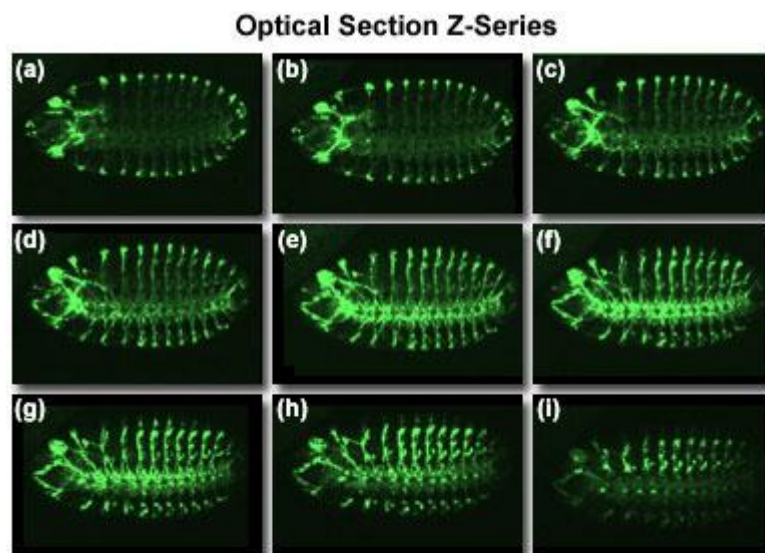


**Figure 3**

It can be conceptually difficult to visualize complex interconnected structures from a series of several hundred optical sections taken through the volume of a specimen with a LSCM. Once collected, however, a z-series is ideal for further processing into a three-dimensional representation of the specimen using volume visualization techniques. This approach is now commonly used to elucidate the relationships between the structure and function of tissues in biological and medical studies. It is important that the images are collected at an appropriate z-step size of the motor that changes focus, so that the actual depth of the specimen is reflected in the image. As long as the specimen itself does not move during the acquisition of the images, the z-series produced in the LSCM will be in perfect register, and saved in digital format, they are relatively easily processed into a three-dimensional representation of the specimen. Figure 4 presents a comparison of a single optical section (a) with a z-series projection (b), and illustrates the value of this technique in visualizing the fruit fly peripheral nervous system stained with the antibody 22C10.

The step size taken by the stepper motor, and set up by the microscope operator, is related to the optical section thickness, but they may not have the same value. The optical section thickness refers to the thickness of the section of sample imaged by the microscope, and depends upon the objective lens and the diameter of the pinhole used. In some cases the focus step size and the optical section thickness do have the same value, however, and this may be a source of confusion.

Following acquisition of a z-series file it is usually exported into a computer three-dimensional reconstruction program designed specifically for processing confocal images. Such software programs run at extremely high speeds on graphics workstations, or, with current faster processors and large amounts of RAM, can be run quite effectively on personal computers or the workstation of the confocal microscope. The three-dimensional software packages can be used to produce either a single three-dimensional representation of the specimen or a movie sequence compiled from different views of the specimen that can produce the effect of rotating or other spatial transformation that enhances the appreciation of the specimen's three-dimensional character. The software allows various length, depth, and volume measurements to be made, and specific parameters of the image such as opacity can be interactively changed to reveal structures of interest at different levels in the specimen.

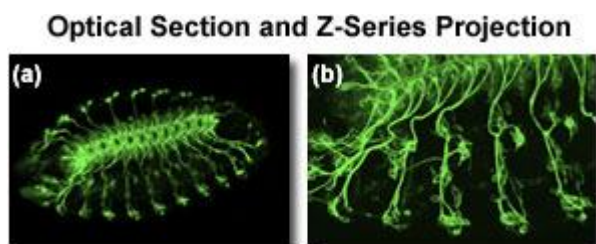


**Figure 4**

Another way in which a series of optical sections from a time-lapse sequence might be utilized is to process the data into a three-dimensional representation so that time is the z-axis. This is a useful approach for visualizing physiological changes during organism development. An example in which this method has been used is in the elucidation of calcium dynamics in developing sea urchin embryos. Color-coding optical sections taken at different depths is a simple method of displaying three-dimensional information. In practice a color (usually red, green, or blue) is assigned to each optical section obtained at a different depth in the specimen, then the colored images are merged and the colors manipulated to achieve the desired effect using an image processing program.

### **Four-Dimensional Imaging**

Living tissue preparations or other specimens exhibiting dynamic phenomena present the possibility of using the LSCM to collect time-lapse sequences of three-dimensional data to be presented with time as the fourth dimension. Z-series data collected at time intervals will produce 4-dimensional data sets, three spatial dimensions (**x**, **y**, and **z**) with time as the fourth dimension, which can be viewed using a 4D viewer program. Such programs allow stereo pairs taken at each time point to be constructed and played back as a movie, or, alternatively three-dimensional reconstructions for each time point can be processed and displayed as a movie or a montage.

### **X-Z Imaging**

If a profile view is needed of a specimen, such as a vertical slice of an epithelial layer, an **x-z** section can be produced in one of two ways. The profile can be constructed by scanning a single line across the specimen (the **x**-axis) at different **z**-axis depths by stepper motor control of focus changes, then displaying the series as a merged image. Another method is to use a **cut plane** option in a three-dimensional reconstruction program to extract the profile from an existing z-series of optical sections. In construction of the images of butterfly wing epithelium in Figure 5, the laser was scanned across a single line (horizontal black line in the left-hand image) at different **z**-axis positions, or depths, progressing into the specimen. The **x-z** image presented in Figure 5 was built up and displayed by the confocal imaging system. The wing epithelium is

made up of two epithelial layers, but as fluorescence intensity drops off at greater depths in the specimen, only the upper layer is clearly visualized.

### Reflected Light Imaging

Reflected, or backscattered, light imaging was the imaging mode used in all of the early confocal microscopes. Many specimens can be viewed in the LSCM in an unstained state using reflected light, or the specimen can be labeled with a probe that is highly reflective, such as immunogold or silver grains. An advantage of the reflected light method, especially for living tissue samples, is that photobleaching is not a problem. Some types of probes may attenuate the laser beam, and another potential problem is that in some microscopes, internal reflections can occur from optical elements in the light path. The reflection problem is not present in the slit or multi-beam versions of LSCM, and in instruments where it is troublesome, use of polarizers or imaging away from the artifact and off the optical axis can alleviate it.

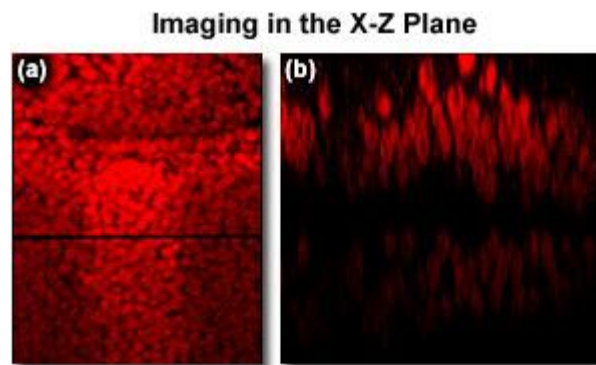


**Figure 5**

### Transmitted Light Imaging

Any of the transmitted light imaging modes commonly employed in microscopy can be used in the LSCM, including phase contrast, differential interference contrast (DIC), dark field, or polarized light. A transmitted light detector is used to collect light passing through the specimen, and a fiber optic light guide transmits the signal to one of the photomultiplier tubes in the microscope system's scan head. The transmitted light images and confocal epifluorescence images can be acquired simultaneously using the same illumination beam, ensuring that all of the images are in registration. When the images are combined or merged using image processing software, the precise location of labeled cells within the tissues can be mapped. An informative approach in some studies is to combine a transmitted light, nonconfocal image of a specimen with one or more confocal fluorescence images of labeled cells in the same specimen. Use of this approach would allow, for example, determining the spatial and temporal aspects of the migration of a subset of labeled cells within a population of unlabeled cells for a period of hours or even years.

A color transmitted light detector has now been introduced that collects the signal transmitted in the red, green, and blue (**RGB**) color channels to create a real color image in a way that is similar to some digital color cameras. Such a detector is especially useful to pathologists, who are accustomed to viewing true colors in tissues in transmitted light and overlaying these images with fluorescence data.

## **Specimen Preparation and Imaging**

The procedures for preparing and imaging specimens in the confocal microscope are largely derived from those that have been developed over many years for use with the conventional wide field microscope. The best approach in developing a new protocol for a specimen to be imaged with the confocal microscope is to begin with one known to be appropriate for conventional microscopy, and to modify it as necessary.

### Merged Three-Channel Image

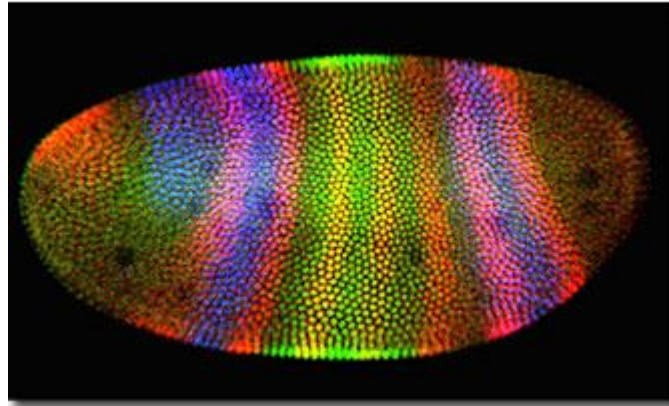


Figure 1

Regardless of the specimen preparation protocol employed, a primary benefit of the manner in which confocal microscopy is carried out is the flexibility in image display and analysis that results from the simultaneous collection of multiple images, in digital form, into a computer. This is discussed in more detail below, but one elegant example of the image display possibilities is presented in Figure 1, a triple-labeled *Drosophila* embryo at the cellular blastoderm stage. The specimen was immunofluorescently labeled with antibodies to three different proteins. After three corresponding images were collected in the red, green, and blue channels of the confocal system, the images could be rearranged by copying them to different channels. By evaluating the image resulting from merging the three, the most effective color-to-channel assignment for illustrating the various protein domains was chosen. Figure 1 presents the merged three-channel image (combined red, green, and blue channels).

Most of the methods that have proven successful in preparing specimens for the conventional wide field optical microscope are specifically aimed at reducing the amount of out-of-focus fluorescence, since this produces flare in the image that greatly reduces the resolution of the features of interest. Due to the optical sectioning achieved by the confocal approach, the confocal microscope undersamples the fluorescence in a thick specimen as compared to the conventional epifluorescence microscope. The result is that samples may require increased staining times or stain concentrations for confocal analysis, and if evaluated in the conventional microscope, may appear to be over stained.

Although the illumination in the typical laser scanning confocal system appears to be extremely bright, the average illumination at any given point on the specimen is relatively moderate, due to the fact that many points are scanned per second. At a typical scan speed of one point per 1.6 microseconds, the actual illumination at any given point is generally less than in a conventional wide field epifluorescence microscope. It is usually advisable to use the lowest laser power that is practical for imaging in order to protect the fluorophore. Although many protocols include an antibleaching agent to prevent fading of the fluorescent species, such additives may not be required with many of the more modern confocal instruments.

The primary advantage and application of the confocal microscope is in improved imaging ability of thicker specimens, although the success can be limited by the specific properties of the specimen. Certain minimum physical requirements for the specimen apply; it must fit on the microscope stage, and the area of interest must be able to be placed within the working distance range of the objective lens. In some cases resolution may have to be compromised in order to accommodate a specimen, and to avoid damage to it or the objective lens. For example, a high resolution lens such as a 60x having a numerical aperture of 1.4 may have a working distance of 170 micrometers, whereas a 20x (having a typical numerical aperture of 0.75) might offer a relatively large 660 micrometer working distance, with the ability to access more restricted areas of a specimen without physical interference.

Specimens that have three-dimensional structure that is to be studied with the confocal microscope, have to be mounted in such a way as to preserve the structure. Some sort of spacer, such as fishing line or a piece of cover slip, is commonly placed between the slide and the cover slip to avoid deforming the specimen. When living samples are to be studied, it is usually necessary to mount them in a chamber that provides all of the necessary requirements for life, and that will also allow sufficient access by the objective lens to image the desired area.

### Objective Lens Parameters and Optical Section Thickness

Objective		Pinhole	
Magnification	NA	Closed (1 mm)	Open (7 mm)
60x	1.40	0.4	1.9
40x	1.30	0.6	3.3
40x	0.55	1.4	4.3
25x	0.80	1.4	7.8
4x	0.20	20.0	100.0

**Table 1**

Specimen properties that affect light transmission, such as opacity and turbidity, can greatly influence the depth of penetration of the laser beam into the specimen, and consequently the structures that can be imaged. Unfixed and unstained corneal epithelium of the eye, for example, is relatively transparent and a laser beam will penetrate it to a depth of about 200 micrometers. In contrast, unfixed skin is relatively opaque and scatters more light, limiting the laser penetration to about 10 micrometers. Many fixation protocols include some form of clearing agent intended to increase the transparency of the tissue.

If sufficient laser penetration cannot be achieved with a whole mount specimen, thick sections can be cut using a microtome. Fixed tissue is usually used for sectioning, but tissue (such as living brain) has been cut by vibratome and successfully imaged. To gain access to deeper parts of a section mount, it is possible to remove the specimen from the slide, invert it, and remount it, but this is usually not very successful. Images from a somewhat deeper part of a specimen can be obtained by using dyes that are excited at longer wavelengths (such as cyanine 5), as opposed to those that require shorter wavelength excitation. The use of longer wavelength illumination will, however, slightly reduce the maximum resolution that can be achieved in comparison to images acquired at shorter wavelengths. For similar reasons, multiple-photon imaging techniques allow images to be collected from deeper levels within a specimen (due to the use of red light for excitation).

### The Objective Lens

For confocal microscope studies, the choice of the objective lens used is extremely important, as the light-collecting ability of the lens, measured as its numerical aperture, is a determinant of both resolution and optical section thickness. Holding other microscope variables constant, the higher the objective numerical aperture is, the thinner the optical section will be. As examples for one particular instrument, the optical section thickness using a 60x (numerical aperture of 1.4) objective with the pinhole diameter set at 1mm is approximately 0.4 micrometer, and with a 16x (numerical aperture of 0.5) lens, with the same 1-millimeter pinhole, the section thickness is on the order of 1.8 millimeters. By opening the pinhole to a larger diameter, the optical section thickness can be increased. Table 1 gives optical section thickness values (in micrometers) for various objective lenses at two different pinhole diameters for one model of **LSCM**. The image resolution is always poorer vertically than it is horizontally. For example, using the 60x, 1.4 numerical aperture, objective lens the horizontal resolution is approximately 0.2 micrometer, and the vertical resolution about 0.5 micrometer. Flatness of field and chromatic aberration are additional lens characteristics to be considered when choosing an objective lens. The degree of chromatic aberration correction is particularly important when imaging multilabeled specimens at different wavelengths.

Objective lenses that are capable of the highest resolution generally are those with the highest magnification and the highest numerical aperture. They are also the most expensive, so a compromise is often made between the area of the specimen that is scanned and the maximum resolution that can be achieved for that area. If imaging insect embryos and imaginal disks, for example, a 4x lens might be used to locate the specimen on the slide, a 16x (numerical aperture of 0.5) lens for imaging whole embryos, and a 40x (numerical aperture of 1.2) or 60x (numerical aperture of 1.4) lens for resolving individual cell nuclei within embryos or imaginal disks. For imaging larger tissues, such as butterfly imaginal disks, the 4x lens would be useful for whole wing disks, and the 40x or 60x for resolution of individual cells. Figure 2(a) illustrates use of a 4x objective to obtain an overall view of an entire butterfly fifth instar wing imaginal disk, and the additional nuclear detail provided by a 16x lens (Figure 2(b)). One way in which high resolution and large image fields of view can be combined is to acquire many images from adjoining areas and to combine them digitally into montages. Some microscopes have automated x-y stages that can be set up to move around the specimen and collect multiple images into a large-area montage.

## Objective Lens Zooming

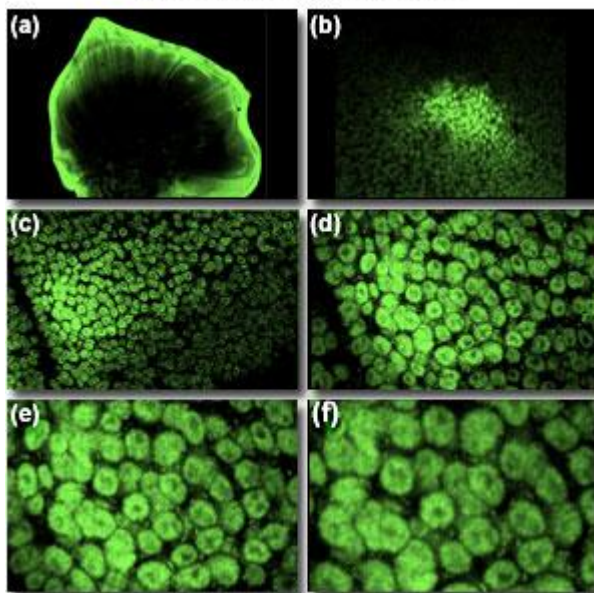


Figure 2

One of the more useful features that is characteristic of most LSCMs is the ability to zoom an image using the same objective lens, with no loss of resolution. This capability is achieved simply by decreasing the area of the specimen scanned by the laser, by control of the scanning mirrors, while maintaining the same image display size or memory storage array size, effectively increasing the magnification. In this way several magnifications are achieved with a single lens without disturbing the specimen or losing track of reference points in the field of view. Whenever possible, however, a lens of higher numerical aperture should be used to maximize resolution, rather than zooming using a lens of lower numerical aperture. The capability of zooming with a single lens (40x) is illustrated in Figure 2(c-f). Panel (c) of the figure shows the additional nuclear detail provided by the 40x objective (compared to the 16x view of panel (b)). Panels (d) through (f) are images obtained by zooming the same 40x lens by progressive increments, accomplished by reducing the area scanned on the specimen.

A number of confocal instrument designs have an adjustable pinhole that limits the out-of-focus light that reaches the detector. Opening the pinhole to a larger diameter produces a thicker optical section and reduced resolution, but is often necessary to include more specimen detail or to increase the light striking the detector. As the pinhole is closed (diameter reduced) the optical section thickness and brightness decrease. Resolution increases until a certain minimum pinhole diameter is reached, beyond which resolution does not increase but brightness continues to decrease. The pinhole diameter at which this condition is reached is different for each objective lens.

### Probes for Confocal Imaging

The development of confocal instrumentation continues to both influence and be influenced by the synthesis of novel fluorescent probes that improve immunofluorescence localization. Fluorochromes are being introduced that have excitation and emission spectra more closely matched to the wavelengths produced by the lasers supplied with most commercial LSCMs. Improved probes that can be conjugated to antibodies of current research interest are continually developed. As one example group of dyes, the cyanines have developed as alternatives to other long-established dyes, with cyanine 3 as a brighter alternative to rhodamine, and cyanine 5 finding increased use in triple-label strategies.

Fluorescence *in-situ* hybridization (**FISH**) has advantages in resolution and sensitivity of probe detection that are further enhanced when coupled with the LSCM, and is a valuable approach for imaging the distribution of fluorescently labeled DNA and RNA sequences in cells. In addition, brighter fluorescent probes are currently available for LSCM imaging of total DNA in both nuclei and isolated chromosomes.

A large number of fluorescent probes are available that, when incorporated in relatively simple protocols, specifically stain certain cellular organelles and structures. Among the plethora of available probes are dyes that label nuclei, the Golgi apparatus, the endoplasmic reticulum, and mitochondria, and also dyes such as fluorescently labeled phalloidins that target polymerized actin in cells. Such dyes are very useful in multiple

labeling approaches to locate antigens of interest having specific compartments in the cell. For example, Figure 3 presents the employment of a combination of phalloidin and a nuclear dye (**ToPro**) with the appropriate antigen in a triple labeling scheme applied to whole mounts of butterfly pupal wing imaginal disks. As illustrated in Figure 3(a), phalloidin can be used to accentuate cell outlines in developing tissues, with the peripheral actin meshwork being labeled as bright fluorescent rings. Panel (b) of the figure illustrates the dramatic specificity of the nuclear dye in labeling just that one cellular component. In addition to this cellular compartment labeling strategy, antibodies to proteins of known distribution or function in cells (such as antitubulin) can be usefully included in multilabel studies.

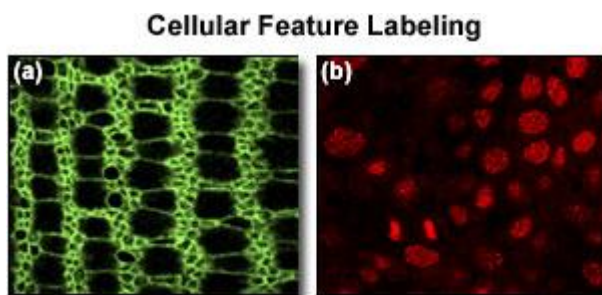


**Figure 3**

If living cells are being imaged, it is critical to be aware of the effects of adding fluorochromes to the system. These probes can be toxic to living cells, especially when they are excited with the laser. Toxic affects are reduced in some preparation protocols by the addition of ascorbic acid to the cell medium. The particular cellular component that is labeled can affect the viability of the cells during imaging. For example, stains for the cellular nucleus tend to have more deleterious effects than do cytoplasmic stains. Probes are available that distinguish between living and dead cells (among these are acridine orange), and that can be used in assays of cell viability during imaging. Most such assays are based upon the premise that the membranes of dead cells are permeable to many materials, such as the dyes, that cannot penetrate them in the living state.

Fluo-3 and rhod-2 are examples of dyes that have been synthesized to change their fluorescence characteristics in the presence of certain ions such as calcium. New probes have been developed for imaging gene expression, including for example, the jellyfish green fluorescent protein (**GFP**), which enables gene expression and protein localization to be observed *in vivo*. The use of GFP has enabled the monitoring of gene expression in a number of different cell types including living *Drosophila* oocytes, mammalian cells, and plants (using the 488nm line of the excitation laser of the LSCM). Mutants of GFP with spectral variations are available for use in multilabeling experiments, and these have also found use for avoiding interference from autofluorescence in living tissues.

### **Autofluorescence**

Autofluorescence of tissues occurs naturally in many cell types, and can be a major source of background interference during imaging. For example, chlorophyll in yeast and plant cells fluoresces in the red part of the spectrum. Certain reagents, such as glutaraldehyde fixative, are sources of autofluorescence, which can be reduced by treatment with borohydride. Autofluorescence can sometimes be avoided by using fluorophores that can be excited at wavelengths that are out of the range of natural autofluorescence. Cyanine 5 is often chosen since it is excited at a longer wavelength that avoids the shorter-wavelength autofluorescence.

Although it is most often considered a problem, tissue autofluorescence can be utilized for imaging overall cell morphology as a part of multilabeling studies. The contribution from autofluorescence to the total fluorescence can be assessed by viewing an unstained specimen at different wavelengths and noting the laser power and PMT settings of black level and gain. Autofluorescence can often be bleached out by brief exposure to the laser at high power, or by flooding the specimen with light from a mercury lamp. More sophisticated approaches to dealing with autofluorescence include using time resolved imaging, or removal using digital image processing techniques such as image subtraction.

### **Collecting Images**

Beginning users of confocal microscopes can gain experience in several ways. The microscope manual provided by the manufacturer usually includes a series of simple procedures necessary for getting started. In most multi-user facilities, the person primarily responsible for operating the instrument may provide

orientation sessions, or the facility manager may require a short training session and demonstration of a certain competence level before solo use of the instrument is allowed. Particular attention should be paid to the house rules of the facility. Information and training can also be gotten from training courses conducted by the microscope companies, from workshops on microscopy, and from a variety of publications.

Before work is done with experimental specimens, it is essential to be familiar with the basic operation of the imaging system. It is usually beneficial for the novice to begin trial imaging with a relatively easy specimen rather than a more difficult experimental one. Some better test samples include paper soaked in one or more fluorescent dyes or a preparation of fluorescent beads. Both types of specimen are brightly fluorescent and relatively easy to image with a confocal system. Another excellent sample is a slide of mixed pollen grains that exhibit autofluorescence at many different wavelengths. These can be easily prepared from pollen collected from garden plants, or can be obtained from commercial suppliers of biological specimens. The pollen grain images in Figure 4 were collected simultaneously with the same PMT black level and gain, and pinhole diameter settings, but reveal three types of pollen that each fluoresce at different excitation wavelengths. These specimens are valuable as test subjects because they not only have some interesting surface details, but also maintain their properties relatively well when exposed to the laser beam. For trials with living tissue, specimens prepared from onion epithelium or the water plant *Elodea* sp. are reliable, using either autofluorescence or staining with DiOC6.

Before attempting imaging, the confocal instrument should be set up to give the best possible performance. This requires optimal alignment, especially when one of the older confocal microscopes is being used. The alignment routine used is highly specific to the particular instrument, and is usually best done by the person who has overall responsibility for maintaining it. In no case should alignment be attempted without proper training and permission from the owner of the microscope. Improper procedures used to attempt alignment can result in complete loss of the beam and can, in the case of some instruments, require a service visit to rectify.

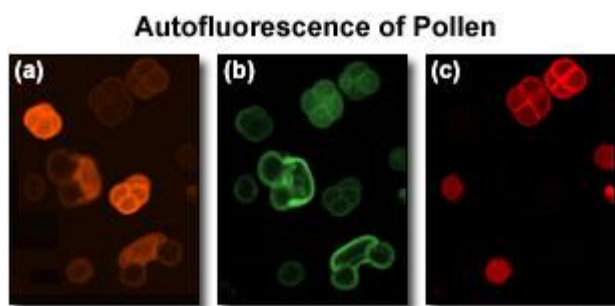


**Figure 4**

The confocal system is based on a conventional optical instrument, and the fundamental procedures and practices of optical microscopy should be followed at all times. It is extremely important that all glass surfaces in the optical path be clean because dust, oil, or grease on slides, cover slips, and objective lenses is a primary cause of poor images. The refractive index between the objective lens and the specimen must be appropriate to the lens in use. For example, the correct immersion oil must be used for a given objective numerical aperture, and the specimen must be mounted to be within the working distance of the lens. Cover slip thickness must be correct for the lenses used, especially for the higher power objectives, which require a No. 1 or No. 1.5 cover slip instead of a No. 2. The cover slip must be sealed to the slide using an appropriate medium, and mounted flat. Nail polish can be used for fixed specimens if care is taken to ensure that it is dry before imaging. A mixture of petroleum jelly, beeswax, and lanolin, or some other nontoxic sealing material must be used with living specimens. Following strict basic cleanliness procedures at the specimen preparation stage can save much time and effort later.

In preparation for confocal mode imaging, a region of interest is located using either brightfield or conventional epifluorescence microscopy. It is preferable to do this survey using the microscope of the confocal system, but it can be extremely difficult for the novice to find the correct focal plane using the confocal imaging mode alone. If conventional imaging modes are not available on the confocal system, then structures of interest can be located using a separate fluorescence microscope, and their positions marked using a diamond marker on the microscope, a marking pen, or by recording the position coordinates from the microscope stage. It is especially useful to be able to preview specimens with the actual microscope of the confocal system when attempting to image a rare phenomenon such as a gene expressed at a particular stage of development in a specimen containing perhaps hundreds of embryos of different ages. A great deal of time can be saved in this way, over having to scan many specimens using the confocal mode. Confocal

instruments commonly have a low-resolution rapid scanning mode that makes the preliminary scanning more efficient. The best approach when searching for rarely occurring events, however, is to scan the slides using a conventional microscopy mode and then to immediately switch to confocal mode on the same microscope to collect the images.

Successful confocal imaging relies on the "secret" of mastering the interplay between objective lens numerical aperture, pinhole size, and image brightness, and using the lowest laser power possible to achieve the best image. The novice user should experiment with varying these parameters using test specimens and several objective lenses of different magnifications and numerical apertures to gain a sense of the capabilities of the microscope before attempting imaging on experimental specimens. A comparison should be made of images acquired using the zoom function of the confocal system with those obtained using objectives having higher numerical aperture. The particular specimen and features being imaged will determine which lenses and methods are most appropriate. Two examples of the many objectives suitable for confocal microscopy are illustrated in Figure 5. The figure includes a 60x planapochromat oil-immersion lens, and a 20x planfluorite. The latter objective has an adjustment collar that allows it to be utilized with oil, glycerin, or water as an immersion medium.

Specific microscope settings appropriate to the specimen should be set up away from the primary region of interest to avoid photobleaching of the fluorescent species in valuable regions of the specimen. Usually this requires setting the gain and black levels of the photomultiplier detectors together with the pinhole size to obtain the best balance between acceptable resolution and adequate contrast, using the lowest laser power possible to minimize photobleaching. Many instruments utilize color lookup tables designed to aid in setting the correct dynamic range for the image. Such tables are designed so that the darkest pixels, having brightness values around zero, are arbitrarily displayed as green (for example), and the brightest pixels, with brightness values near 255 in an 8-bit system, are displayed as red. The microscope parameters such as gain and black level, and the pinhole diameter, are adjusted so that there are only a few green and red pixels in the image, ensuring that the full dynamic range from 0 to 255 is utilized, but with little cutoff at either end of the brightness range. Although these adjustments can be made by eye, the use of pseudocolor at the extremes of the dynamic range of the imaging system makes the adjustment much less subjective. In some cases images must be collected at less than the full dynamic range of the system because less than optimum laser power must be used or the specimen has uneven fluorescence, causing a bright region to obscure a dimmer region that is of interest in the frame.



During scanning of the specimen an image averaging routine is usually employed to reduce random noise from the detection system and to enhance the constant (nonrandom) features in the image. An image equalization algorithm can be applied after collection of images to scale them to the full dynamic range of the display. Care should be taken not to apply this type of routine if measurements of fluorescence intensity are to be made unless a control image is included in the same frame as the experimental images before the equalization routine is applied. In using any type of image processing routine, it is a good strategy to save raw unprocessed images in addition to any processed ones.

The usual strategy in image collection is to save images onto the hard disk of the confocal system's computer, and later to back them up onto another mass storage device. In general it is always advisable to collect as many images as possible during a microscope session, and to discard unneeded ones during later review. Many images that seem unnecessary at first consideration become highly valuable at a later date after further review (especially with one's peers). If it seems wasteful to take seemingly superfluous images,

consider that it much harder to prepare another specimen, and harder still to reproduce the exact conditions of an experiment or even to exactly duplicate the specimen preparation protocol.

A strategy for labeling image files in an informative way should be developed before imaging is begun. During imaging many notes should be taken or added to the image file along with the image if this capability is available on the system used. Tests should be done to ensure that any saved information is accessible after saving the images, keeping in mind that text and other information related to an image may be lost when it is subsequently transferred to image editing programs such as NIH Image or Adobe Photoshop on other computers. A well-organized notebook or laptop computer file may be preferable over other means of recording imaging session details, and should include filenames, comments, and details of the objective and any zoom factor used to allow calculating scale bars at a later date. Most confocal systems do not automatically record the objective lens used, and this information is important for calculating field widths and scale bars for later publication. Many modern systems utilize an image database that organizes file names and locations of the files, and that usually will display thumbnail files of the images. Care must be taken to follow image naming restrictions imposed by the system, such as the number of characters allowed in a file name and whether characters such as periods or spaces might be misinterpreted by the software.

## **Troubleshooting**

In any experimental discipline, a protocol that has produced good results will sometimes inexplicably cease to work. When this occurs with confocal imaging experiments, there may be an initial reflex to blame the instrument rather than the specimen, but tests should be conducted to confirm that the specimen is not at fault before any troubleshooting is begun on the instrument. A good first test is to view the specimen on a conventional epifluorescence microscope. If some fluorescence is visible by eye, the signal should be very bright on a properly functioning confocal system. Having confirmed that fluorescence is present in the specimen, some tests of the confocal system should then be done using a known test specimen rather than the experimental one. For reference purposes, the confocal system should have a digital file of an image of the test specimen accessible to users of the microscope, including all parameters of its collection, such as laser power, pinhole diameter, objective lens and zoom value, and gain and black level of the detector.

If initial tests do not provide a clear solution, it is advisable to seek help from an expert who may have experienced the problem before. As a rule, if a user is not sure of something, it is best that they step back and ask for help before attempting any remedies. All of the companies that supply confocal microscopes have telephone help lines and websites that may be accessed for additional help.

Problems that are traced to the preparation protocols are usually caused by degradation of reagents, and this should be checked by performing a series of diagnostic tests. It is usually advisable for the person doing the experiments to make up their own reagents, or at least to obtain them from trusted co-workers. Antibodies should be allocated from frozen stock in small batches, then stored under refrigeration, and should not be reused unless absolutely necessary. Sometimes this is unavoidable with rare or expensive reagents, and often does not present a problem.

In experiments with multilabeled specimens, bleed-through from one channel into another can occur as the result of properties of the specimen itself, or due to problems with the microscope. Published reviews in the literature should be consulted for the details of causes of bleed-through and possible remedies. A good test of the instrument itself involves imaging of a test specimen with known bleed-through properties, using both multiple-label and single-label settings. Images of the test specimen should be stored along with records of all pertinent microscope settings, so that when problems do occur the test specimen can be re-imaged with the same instrument conditions and the images compared with the stored ones recorded when the instrument was known to be operating optimally.

Other tests that may be done when problems arise include a visual inspection of the color of the laser illumination and a check of the anode voltage of the laser. If, for example, the beam from a krypton/argon laser appears blue instead of white when scanning on a multiple-label setting then this may indicate that the red line is weak. In this case, the anode voltage will probably be too high, and can usually be reduced to an acceptable level by adjusting the mirrors of the laser. Such adjustments should be done by, or supervised by, the person responsible for maintaining the confocal system. If the voltage cannot be brought into an acceptable range, a replacement for the laser may be required.

Another problem that may be encountered is that antibody probes may have degraded or need to be repurified or otherwise cleaned. Specimens that have been prepared for some time may develop increased

background fluorescence and bleed-through caused by the fluorochrome separating from the secondary antibody and diffusing into the surrounding tissue. If at all possible, imaging should be carried out on freshly prepared specimens. Sometimes changing the concentration and/or the distribution of the fluorochromes will help alleviate problems. As one example, fluorescein may bleed into the rhodamine channel, and can be switched so that rhodamine is on the stronger channel. The rationale for this is that the fluorescein excitation spectrum has a tail that overlaps with and is excited in the rhodamine wavelength range. In subsequent experiments, the concentration of the secondaries can be reduced.

### **Image Processing and Publication**

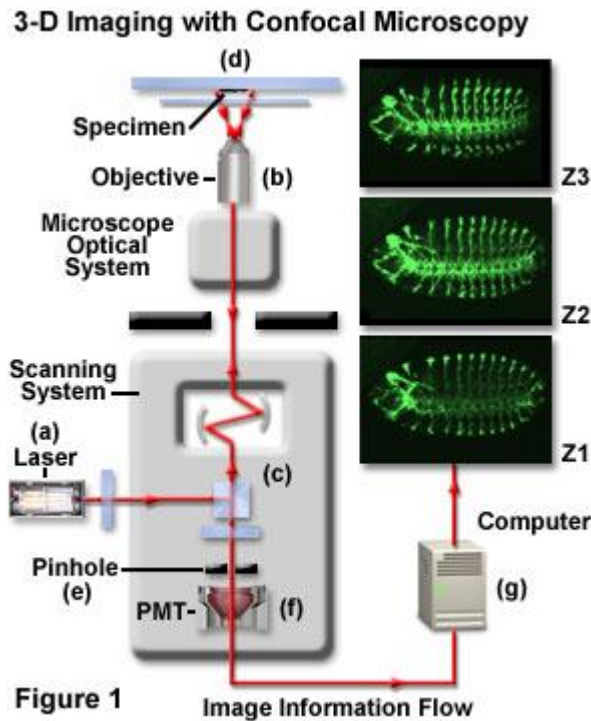
Images acquired with the confocal microscope are usually saved as digital computer files in a format that allows them to be easily manipulated using the proprietary software provided as part of the confocal system. One of the most dramatically improved capabilities of current LSCMs is their display of confocal images. This is of great importance because the improvements in imaging using the confocal microscope are of little value if there is no means to effectively display the images or reproduce them as hard copy.

As recently as 5 or so years ago most laboratories were still using traditional photographic darkrooms and chemical processing of film and paper for their final hard copy of images. There was particular difficulty in reproducing color images, because they were usually printed by independent printers who often had little idea of what constituted correct color balance in a micrograph, and the cost of quality prints was high. To obtain hard copy of images now, the image files can be exported to a slide printer, a color laser printer, or to a dye sublimation printer for publication quality prints, with direct control of the image characteristics being maintained by the person who acquired the images. Photographs for prints or slides can be taken directly from the video monitor screen, and movie sequences can be published on the Web.

Most journals are now able to accept digital image files for publication, and this has resulted in a dramatic improvement in the quality of published images. The image quality achieved by the confocal imaging system can now be more faithfully reproduced in published articles. In some cases journals also make their articles available on CD ROM, which means that readers can have access to published images exactly as they appeared when collected on the confocal systems of those doing the research. Not surprisingly the technological advances in image acquisition, display, and publication are especially beneficial in the case of color images in that journals can now accurately reproduce images with their original resolution and color balance, and theoretically, at much lower cost to the author.

## **Critical Aspects of Fluorescence Confocal Microscopy**

We all know that fluorescent micrographs reveal the location of the labeled molecules in a tissue, right? Well, maybe not. In fact, all you can be really sure of measuring with most laser-scanning confocal microscopes in the fluorescence mode is some feature of the number of photons collected at a particular time. We can hope this is an accurate measure of one or two interesting parameters—the local analyte concentration or the local ion concentration. In fact, many factors affect the numerical values actually stored in the computer memory at any given moment.



A flow diagram of a generic laser scanning confocal microscope showing the locations of a number of the "39" features mentioned in the text is shown in Figure 1. The system illustrated is based on an inverted optical microscope configured for live cell imaging. Individual components referred to in the following text are labeled in the figure with the letters (a) through (g). The illustration includes three optical sections, taken at different levels along the z-axis through an antibody-labeled fruit fly embryo, and designated **Z1**, **Z2**, and **Z3**.

Over the years, students taking The Three-Dimensional Microscopy of Living Cells course held each June at the University of British Columbia, compiled a list of these extraneous factors. In the first year, the list grew to 39 entries, and so we borrowed the name of the Alfred Hitchcock film for our list. Since then, the list has continued to grow! (More information on the course can be found on the Web at the [3-D Microscopy Course Bulletin Board](#)).

Although this article can't fully describe each term, brief and useful explanations are included. The terms appear in bold lettering and many interact with other terms in bold lettering. Note that many of these variables are usually thought of in terms of their effect on spatial resolution. They are listed here because reduced resolution translates into "putting the same number of exciting photons into a larger spot". This lowers the excitation intensity—the number of photons produced by a given molecule—and the fraction of these that are detected. It is often forgotten that normal signal levels in fluorescence confocal microscopy correspond to only 10–20 photons/pixel in the brightest areas. Under such conditions, statistical noise is a more important limitation on spatial resolution than that defined by the Abbe equation:

$$d_{\min} = \lambda_0 / (NA_{\text{obj}} + NA_{\text{cond}})$$

In the equation, **d(min)** represents the minimum spacing in a periodic grating that can just be resolved, and is expressed as lateral distance in the specimen space; **λ(0)** is the wavelength of light in vacuum; and **NA(obj)** and **NA(cond)** are the numerical apertures of the objective and condenser lenses, respectively. The equation establishes the role of the objective and condenser numerical apertures in determining image resolution for a given wavelength of light.

**The laser unit** (Figure 1(a)) is the illumination source, and in general, the fluorescence measured is proportional to the laser power level. Although total **laser output power** is usually regulated, the amount of power in each line of a multiline laser may not be, and may vary widely with time. The **wavelength** affects optical performance, and through the absorption spectrum of the dye, it determines the amount of fluorescence produced.

**Power output instability** is usually noise; its instability is usually less than 1 percent, but lasers can become increasingly unstable as they age. Because dust, misalignment, or mechanical instability can cause random changes of 10-30 percent, **the efficiency of the optical coupling** to the connecting fiber (if used) is critical.

The **alignment and reflection characteristics** of laser mirrors can be the source of long-term drift in laser output. Since the source of the laser light is determined by the laser mirrors, **beam-pointing error/alignment** is important. Instability here will show up as changes in brightness because changes in the apparent source position will alter the efficiency of the optics coupling the laser light into the single-mode optical fiber used in most instruments.

The **numerical aperture** of the **objective lens** (Figure 1(b)) affects the fraction of the light emitted by the specimen that can be collected. This is also true for light from the laser.

**Objective magnification** is inversely related to the diameter of the objective lens entrance pupil. The objective will only function properly if the entire entrance pupil is filled with exciting laser light. Underfilling will reduce spatial resolution and the peak intensity. Overfilling will cause some laser light to strike the metal mounting of the objective and be lost, also reducing the intensity of the spot.

**Cleanliness** is important, and dirty optics produce much larger and dimmer spots. **Transmission** (the fraction of light incident on the objective that can be focused into a spot on the other side of it) varies with wavelength. Beware of using some relatively new, multicoated optics in the infrared range. **Chromatic and spherical aberration** both make the spot bigger, and vary with wavelength. In addition, spherical aberration varies strongly with the cover slip thickness and the refractive index of the immersion and embedding media.

**Diffraction** is the unavoidable limit to optical resolution. It effectively enlarges the image of objects smaller than the diffraction limit, making them appear dimmer than they should be.

**The scanning system** (Figure 1(c)), and especially the **zoom magnification** control, determines the size of a pixel at the specimen. For Nyquist sampling, the pixel should be at least two times smaller than the smallest features that you expect to see in your specimen. Assuming a Rayleigh Criterion resolution of 200 nanometers, the pixels should be smaller than 100 nanometers. Larger ones produce undersampling, reducing the recorded brightness of small features.

The **effects of the bleaching rate** are proportional to the square of the zoom magnification. As for **scan speed**, the longer the dwell time on a particular pixel, the more signal will be detected and the less it will be distorted by Poisson Noise. At high scan speeds (less than 100 nanoseconds/pixel), signals from dyes with fluorescent decay constants that are longer than this dwell time can be reduced.

**Raster size**—Together with the zoom magnification, the number of pixels along the edges of your raster will determine the pixel size. More pixels (1024 x 1024 versus 512 x 512) make undersampling less likely, but mean that one must either spend less time on each pixel by reducing the number of photons collected and increasing Poisson Noise, or take more time to scan the larger image and possibly cause more bleaching. The optics or the scanning mirrors can introduce **geometrical distortion** that can result in discordance between the shape of the object and the image. The **environment** is important: vibration and stray electromagnetic fields can be caused by various pieces of equipment, for example, cooling fans. These can cause improper mirror deflections that result in distortions that may vary with time.

**Other optics** include **transmission**, which describes a measure of the absence of absorption and reflectance losses in optical components, particularly neutral density or bandpass filters, beamsplitters and objectives. **Reflections from air/glass interfaces** usually represent lost signal but may appear as bright spots unrelated to specimen structure. **Mirror reflectivity** can be a strong function of wavelength in the infrared and ultraviolet, and degrades with exposure to humidity and dust.

The **cover slip thickness** is the least expensive optical component and the most likely to be carelessly chosen. It should be  $170 \pm 5$  micrometers in thickness. As for **immersion oil**, its refractive index must be exactly matched to the objective used. This may only occur over a small temperature range, and alternatively, it can be custom-mixed. The **focus-plane position** is important because a feature slightly above or below the plane of focus will appear dimmer than a feature in the plane of focus. When collecting three-dimensional data, Nyquist sampling must also be practiced in the spacing of z-planes. Finally, the **mechanical drift of the stage** can cause the plane of the object actually imaged to change with time.

The concentration of **the dye** of interest is probably what you are trying to measure. **Penetration** into (or steric exclusion from) the specimen is often a function of ionic strength and pH. The **absorption cross-section** is a measurement of the fraction of the exciting photon flux that will be absorbed by a dye molecule. It is affected by the method of conjugation to the probe, pH, specific ion concentration, and ionic strength.

**Quantum efficiency** describes the chance that energy absorbed from an exciting photon will be re-radiated as a fluorescent photon. It is a strong function of wavelength, and is also affected by pH, specific ion concentration, ionic strength, and dye-protein interactions. **Singlet state saturation** occurs when greater than one milliwatt of laser power is used with a high numerical-aperture objective. Then, the light is intense enough to put most of the dye molecules near the crossover into an excited state, reducing the effective dye quantum efficiency.

**Loading** refers to the amount of dye you put into your cell. Important variables include the number of dye molecules/antibody, or other protein marker, and the fixation/permeabilization protocol used. **Quenching** is the absorption of the fluorescence emitted from one dye molecule by others nearby. **Unloading** refers to dye that was in the cell but has now been pumped out or otherwise inactivated.

The **substrate-reaction rate** applies to dyes with fluorescent properties that are related to their interaction with ions or other molecules in the cell. The pixel-dwell is on the order of microseconds, and so there may not be enough time to reach equilibrium. **Prebleaching** refers to bleaching of the dye before the present measurement was made.

**Compartmentalization** is the redistribution of the dye by intracellular processes. **Dye/dye interactions** refer not only to the quenching just mentioned, but also to fluorescence resonance energy transfer (**FRET**). This occurs when the emission spectrum of one dye overlaps with the absorption spectrum of a second dye molecule, a few nanometers away. **FRET** can result in the emission of light only at the emission wavelength of the second dye. If the second molecule isn't fluorescent, as usually happens, the fluorescent light is lost or quenched. The effects of dye on the specimen may affect many environmental variables, including the deterioration of viability of the specimen.

The refractive index of **the specimen** (Figure 1(d)) and its **embedding medium** will determine the severity of the spherical aberration present. Even for viewing aqueous biological specimens using a water objective, the match is unlikely to be perfect, or even close. Spherical aberration of this type is the major cause of signal loss with increasing penetration depth.

It is essential to use an **immersion oil** with the correct refractive index and dispersion (change of refractive index with wavelength). Also, be sure there are no air bubbles that will act as a lens in the middle of the immersion medium. Check by focusing up and down with the Bertrand lens used for aligning your phase rings.

The **vital state of the specimen** can affect the results of an experiment, because, for example, dying cells have different shapes, sizes and ionic environments than living ones. **Autofluorescence** refers to the presence of endogenous fluorescent compounds. The efficiency of these molecules may vary with pH, ionic concentration, and metabolic state. Additional autofluorescence can be produced by improper fixation, particularly when using glutaraldehyde.

**Refractile structures** or organelles between the objective and the plane of focus, for example, spherical globules of lipid, may refocus the beam to a totally unknown location. Smaller features may have lesser effects but any refractile features that scatter light out of the beam will reduce the intensity of the excited spot and hence, of the detected signal. Their cumulative effect also adds up to cells having a refractive index much higher than that of water.

The **presence or absence of highly stained structures** above or below the focus plane refer to the z-resolution that is finite. Large structures also may absorb substantial exciting light if highly stained.

The signal that passes through **the pinhole** (Figure 1(e)) is proportional to the square of the diameter of the pinhole (or its **size**), which is usually set to be equal to the diameter of the Airy Disk at the plane of the pinhole. **Alignment** is important and the image of the laser that is focused onto the specimen and then refocused back through the optical system should coincide with the center of the pinhole.

**The detector** (Figure 1(f)) is usually a photomultiplier tube (**PMT**). The detected signal is directly proportional to the **quantum efficiency**. The effective quantum efficiency of the photomultiplier tubes used in most confocal instruments drops from about 15 percent in the blue end to approximately 4 percent in the red end of the spectrum. As for **response time**: most fluorescent signals can be amplified rapidly, but detectors for others, such as transmembrane currents, respond slowly, making slow scanning speeds necessary.

The **PMT voltage** determines the amplification of the PMT. An increase of 50 volts corresponds to a factor of about two more in gain. Beware that **PMT black level** or (brightness) control permits the addition or subtraction of an arbitrary amount from the signal presented to the digitizer. The black level should be set so that the signal level in the darkest parts of the image is 5–10 digital units.

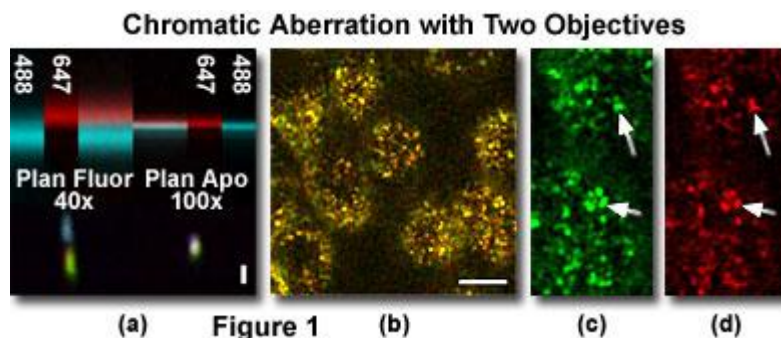
There are many possible sources of **noise** and all will distort the recorded value. Usually, PMTs produce dark current noise that is small compared to the signal level. However, this is less true for red-sensitive PMTs that are allowed to become warm or when viewing poorly stained specimens. Apart from any stray light that may inadvertently reach the PMT, the main remaining noise source is Poisson or statistical noise. This is equal to the square root of the number of photons recorded in a given pixel. The result is it becomes larger at higher signal levels, even though the ratio of signal to noise improves.

**Digitization**, usually using a computer (Figure 1(g)) should be linear. The electronic signals presented to the digitizer of “8-bit” microscopes must be of a size to be recorded between 1 and 255. Because of statistical noise, a value between 10 and 220 is safer. The **digital conversion factor** refers to the ratio between the number of photons detected and the number stored. This depends on the PMT voltage and other electronic gain, but is usually about 30 for normal specimens recorded on 8-bit instruments.

Remember, to measure one of these factors accurately, one must hold the other 38 constant.

### Optical Aberrations and Objective Choice in Multicolor Confocal Microscopy

Refinements in design have simplified confocal microscopy to the extent that it has become a standard research tool in cell biology. However, as confocal microscopes have become more powerful, they have also become more demanding of their optical components. In fact, optical aberrations that cause subtle defects in image quality in widefield microscopy can have devastating effects in confocal microscopy. Unfortunately, the exacting optical requirements of confocal microscopy are often hidden by the optical system that guarantees a sharp image, even when the microscope is performing poorly. Optics manufacturers provide a wide range of microscope objectives, each designed for specific applications. This report demonstrates how the trade-offs involved in objective design can affect confocal microscopy.



Over the past ten years, confocal microscopy has developed from a technique limited to specialists in microscopy into a standard research tool. Its proliferation of applications results as much from the rapid technological developments in confocal microscopy as from the maturing user interface of commercial confocal microscope systems. The latest systems are nearly turnkey systems with which even novice microscopists can rapidly collect high-quality images. Ironically, the same technical developments that have stimulated the spread of confocal microscopy in experimental biology have also pushed the limits of the optics of confocal microscopes in a way that makes understanding the optical properties of a confocal microscope more important than ever.

The most common application of confocal microscopy is to compare the distributions or behaviors of multiple probes in the same cells. Such studies have been made possible by the development of confocal microscopes that are capable of efficiently collecting multiple colors of fluorescence and developing new dyes that have extended the useful spectrum of fluorescence microscopy. Depending on the configuration of the microscope, such studies may require optics that use wavelengths of light ranging from the ultraviolet through the infrared. The requirements for accurate color imaging have been further increased by the development of colorimetric methods of quantitative microscopy, such as fluorescence ratio measurements of ion concentrations.

Freedom from chromatic aberration is only part of the equation of optical design, which also considers monochromatic aberrations and parameters such as high photon efficiency, field size, field flatness, working distance, and the ability to image deep into aqueous biological tissues. Since the design of microscope optics reflects a compromise of these various parameters, manufacturers typically design a variety of different microscope objectives, with each representing a particular set of design trade-offs and each suited to a particular application. The studies discussed here demonstrate that the choice of microscope objective can have profound effects on the results of confocal microscopy experiments. They emphasize the importance of carefully choosing a microscope objective that is appropriate for the experimental application.

An ideal lens would focus all colors of light to the same point. In reality, all lenses have chromatic aberration, a property in which different colors of light are focused to different points. When observing a sample through the microscope eyepiece, this defect makes objects appear to have colored edges. When imaging a sample in color confocal microscopy, this defect results in different colors of excitation illumination being focused to different points in the sample and different colors of emission being collected from different points in the sample. Horizontal displacements in the image plane, termed lateral chromatic aberration, result in different magnification of different colors. This problem can be minimized by restricting the analysis to the center of the microscope field. However, vertical color displacements along the focal axis, referred to as axial chromatic aberration, are present throughout the microscope field. This is clearly a problem for any researcher trying to use color confocal microscopy to determine the relative distribution of multiple probes. The images presented in Figures 1 through 3 show how the results of color confocal imaging critically depend on the nature of the microscope objective.

The figures provide a comparison of the performance of a plan fluor 40x objective, which is designed for maximum UV light transmission, with that of a plan apochromat 100x objective, designed with minimal chromatic aberration. For one aspect of the comparison, a vertical series of images of the reflection from the face of a glass cover slip was collected, using either 488 or 647-nanometer light. As the different colors of light are reflected by a single surface, a lens free of chromatic aberration would focus the different colors to the same focal plane. When reproduced as a vertical cross-section, images collected with an ideal lens would show a single horizontal line in which the two colors overlap completely. The images in the top half of Figure 1(a) illustrate  $xz$ -sections of the glass reflection, with the focal ( $z$ ) axis oriented vertically, and demonstrate that the plan apochromat 100x objective does a credible job of approaching this ideal, resolving the two colors of light to a depth within 0.1 micrometer of one another. In contrast, the minimally corrected 40x plan fluor objective detects the reflection of 647-nanometer light approximately 1.2 micrometers above the 488-nanometer light. In the images of the glass reflection, 647-nanometer light is shown in red, and 488-nanometer light is shown in blue. The scale bar indicates a distance of 1 micrometer.

### Correction of Axial Chromatic Aberration

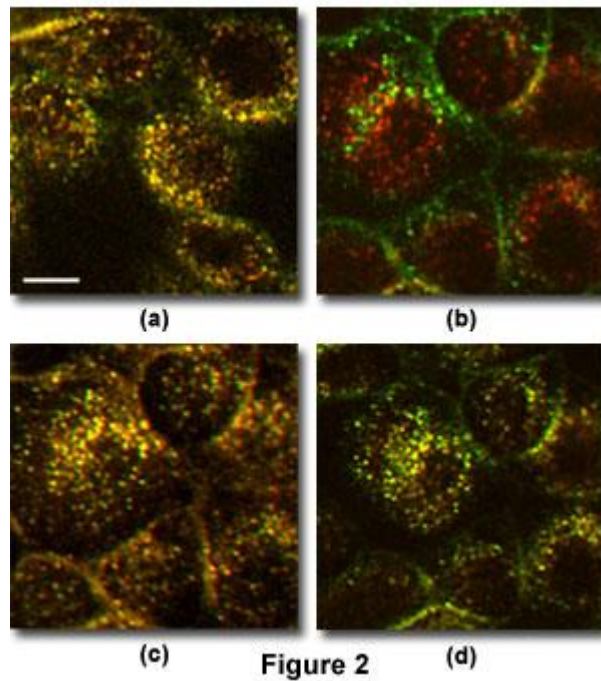


Figure 2

The effect of this vertical discrepancy is apparent in fluorescence. The bottom half of this panel (Figure 1(a)) shows vertical cross-sections of image volumes of beads labeled with three fluorophores. When imaged with the 100x plan apochromat objective, the three colors are coincident, resulting in a white, reasonably round image. In contrast, the 40x objective generates an image in which the far-red fluorescence (680-nanometer emissions, depicted in blue) is distinctly vertically displaced from that of either the red (600 nanometer) or the green (520 nanometer) fluorescence. In addition, a slight horizontal displacement of the far-red fluorescence reflects lateral chromatic aberration.

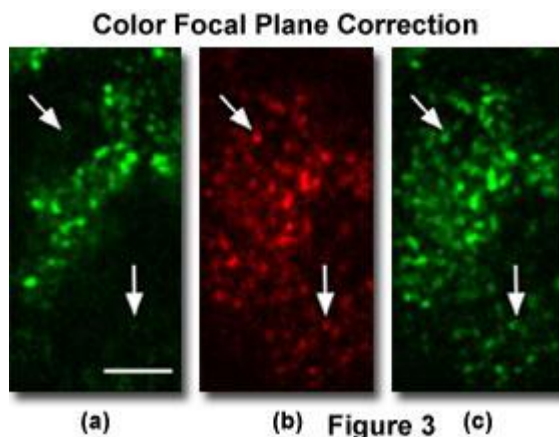
To provide a biological test specimen, advantage was taken of the fact that endosomes can be labeled by incubating cells with fluorescently tagged endocytic ligands. The large number of molecules included in each endosome ensures that each will contain the same ratio of fluorescent probes. Thus, endosomes provide an excellent test of color confocal imaging as they present subresolution objects in biological samples with color that will reflect the relative fluorescent contributions of each fluorophore. Figure 1(b) shows a color image of cells in which the endosomes have been labeled with both fluorescein-transferrin (F-Tf, which fluoresces green) and Cy5-transferrin (Cy5-Tf, which fluoresces far-red), collected using the 100x plan apochromat objective. The co-localization of the two probes is apparent in the constant yellow-orange colors of the individual endosomes and is more apparent in comparisons of the high magnification images of F-Tf (Figure 1(c)) and Cy5-Tf (Figure 1(d)). In these images (Figure 1(b) through Figure 1(d)), the scale bar represents a length of 10 micrometers.

When switching to the 40x plan fluor objective, however, slight differences in the focal plane are apparent even between the red and green fluorescence, as shown in cells labeled with Tf conjugated to both fluorescein and rhodamine (Figure 2(a)). The differences in focal planes between far-red and green fluorescence result in startling differences in the apparent distributions of F-Tf and Cy5-Tf, which now appear to be completely distinct (Figure 2(b)).

For a cell biologist who is assessing the relative distributions of various probes, these displacements would have disastrous consequences. The discrepancy in focal plane can be circumvented by summing the entire vertical series of the image volume into a single projection, which removes the effect of differences in the focal plane of the two colors (Figure 2(c)). The consistent yellow color of every endosome in the projection demonstrates the constant ratio of the two probes in each endosome. However, as this procedure discards all vertical information, it is seldom an appropriate way of presenting confocal images. The effects of axial chromatic aberration can also be minimized by measuring the axial offset of different colors and combining the images collected from the focal planes appropriate for each color. An example of this procedure is shown in Figure 2(d), which shows the combined green and far-red images collected 1.2 micrometers apart with the 40x plan fluor objective. The scale bar in the images of Figure 2 represents a 10-micrometer length. The correction achieved by combining images from different focal planes is apparent when comparing the images of the individual probes, shown in Figure 3. Whereas Figure 3(a) and Figure 3(b) show poor agreement in

distribution between F-Tf and Cy5-Tf in images collected at the same focal plane, a comparison of Figure 3(b) and Figure 3(c) shows that the far-red image can be superimposed with the green fluorescence image collected 1.2 micrometers deeper. In these images (Figure 3(a) through Figure 3(c)), the scale bar corresponds to a length of 5 micrometers.

While chromatic aberration results in different colors of light being focused to different points in the image volume, spherical aberration can profoundly decrease the signal in a confocal microscope. A spherically aberrated lens focuses axial and peripheral rays to different points, thus blurring the image of a point source of light. In the same way that the confocal pinhole so effectively improves image contrast by rejecting out-of-focus light, it effectively eliminates much of the fluorescence of an object imaged with spherical aberration.



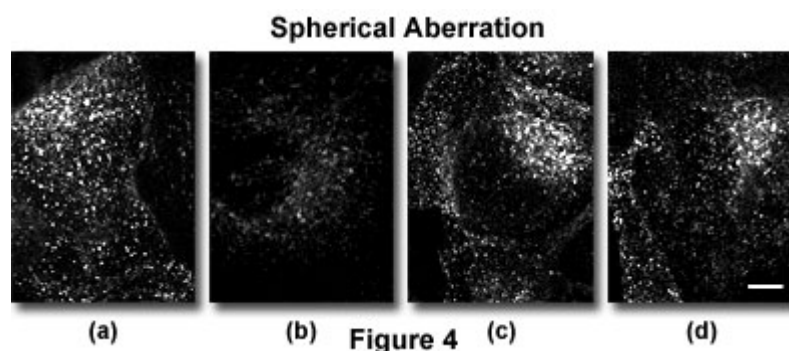
For many samples, the primary source of spherical aberration derives from the difference between the refractive index of the immersion medium and the mounting medium. Until recently, the highest-resolution, best-corrected microscope objectives were designed for use with oil as an immersion fluid. For these objectives, spherical aberration is minimized only when the entire light path has the refractive index of immersion oil (which is the same as that of glass) and accumulates with distance into a medium with a different refractive index. Since most samples - particularly living samples — are mounted in media with a refractive index that is significantly lower than immersion oil, spherical aberration has thus limited the depth of image volumes using oil immersion objectives.

Figure 4 shows the effects of spherical aberration in confocal microscopy, where the oil immersion 100x plan apochromat objective was used to collect an image of cells labeled with F-Tf and mounted at a depth of either 0 micrometers (the surface of the cover slip) (Figure 4(a)) or 35 micrometers into an aqueous medium (Figure 4(b)). In both cases, the endosomes appear sharply defined, but the accumulated spherical aberration of a light path 35 micrometers into an aqueous medium has profoundly compromised the fluorescent signal in Figure 4(b). The scale bar represents a length of 10 micrometers in each of the images presented in Figure 4.

Recently, optical manufacturers have addressed this problem by designing objectives that use water as the objective immersion medium. For aqueous samples, the matched refractive index of immersion and sample media makes spherical aberration independent of imaging depth. This enables these objectives to collect images as deeply as the working distance permits, frequently hundreds of micrometers into a sample. The success of this design is shown in Figure 4 ((c) and (d)), which shows images of cells labeled with F-Tf, collected either zero (Figure 4(c)) or 66 micrometers into an aqueous medium (Figure 4(d)) using a water immersion 60x plan apochromat objective. Here, the fluorescent signal is unaffected by the light path through the aqueous sample medium. This new generation of high numerical aperture, plan apochromat water immersion objectives has significantly helped confocal microscopy realize its potential in three-dimensional biological imaging.

The color performance of this water immersion objective falls between that of the oil immersion plan fluor and the plan apochromat objectives discussed previously. The cross-sectional images of the reflection of a glass surface in the top half of Figure 5(a) show that 647-nanometer light is focused approximately 0.6 micrometer above 488-nanometer light. Similar patterns for volumes collected either 0 or 63 micrometers into an aqueous medium show that this discrepancy is independent of imaging depth.

The bottom-left image of those in Figure 5(a) shows that this color discrepancy results in the far-red image of a triple-labeled bead being displaced from that of either the red or green fluorescence images. In the fluorescent bead images, 520-nanometer emissions are shown in green, 600-nanometer emissions in red, and 680-nanometer (far-red) emissions in blue. The bottom-right portion of this panel demonstrates the critical importance of cover slip thickness correction in minimizing spherical aberration in this kind of objective. Since the correction for spherical aberration depends on the length of the optical path through the cover slip, it is adjustable by a collar that is set according to the thickness of the cover slip. While the bead cross-section on the left was collected with the collar set to the measured cover slip thickness (174 micrometers), the image on the right was collected with the collar misadjusted to 150 micrometers. The spherical aberration that results from an improper collar setting severely attenuates the fluorescence signal and compromises vertical resolution. Although this misadjustment was chosen to dramatize the point, we emphasize that such an error is easily encountered in practice because the actual thickness of cover slips can vary by more than 40 micrometers around their nominal value. Proper collar setting can only be ensured through measurements of individual cover slips. In all images in Figure 5(a), the focal axis is oriented vertically, and the scale bar indicates a distance of 1 micrometer.

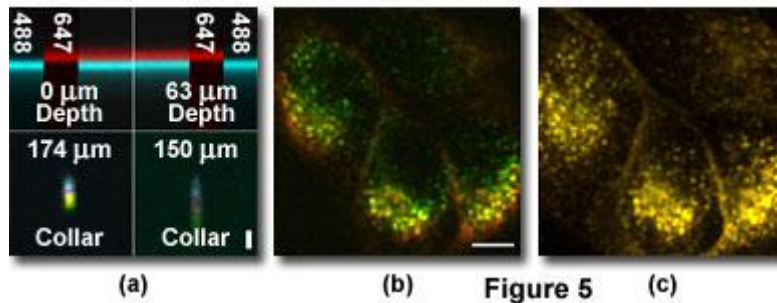


The images shown in Figure 5(b) and Figure 5(c) are of a field of cells labeled with both F-Tf and Cy5-Tf, and were collected at a depth of 63 micrometers into an aqueous buffer. The scale bar represents 10 micrometers in these two images. Although the images appear sharp, the axial chromatic aberration of this objective has the effect of making the distributions of F-Tf and Cy5-Tf appear discrete (Figure 5(b)). Nonetheless, the projection of the vertical series of images of these cells (Figure 5(c)) shows that the two probes equally label all endosomes. In agreement with the reflection images shown in Figure 5(a), axial chromatic aberration is similarly apparent in images of endosomes collected at a depth of zero micrometers (at the cover slip surface). Little difference is observed in the focal plane of red and green fluorescence in images of endosomes labeled with Tf conjugated to both fluorescein and rhodamine (Figure 6(a)), but F-Tf and Cy5-Tf again appear to label discrete populations of endosomes (Figure 6(b)).

The distribution of the two probes can be better compared when allowing for the difference in focal plane and combining the Cy5-Tf image with a fluorescein image collected 0.6 micrometer deeper. The co-localization of the two probes is now apparent in the constant yellow color of the endosomes shown in Figure 6(c). Apparent differences in the distribution of the two probes shown in images collected at a single focal plane (Figure 6(d) and Figure 6(e)) disappear when the Cy5-Tf image is compared with the F-Tf image collected 0.6 micrometer deeper (Figure 6(f)). The scale bar represents 10 micrometers length in Figure 6(a) through Figure 6(c), and corresponds to 5 micrometers in Figure 6(d) through Figure 6(f).

The effects of chromatic aberration can also be quantified by measuring fluorescence ratios in images of endosomes labeled with multiple probes. Semi-logarithmic plots of ratio histograms are presented in Figure 7(a) for cells labeled with F-R-Tf, with images collected using the 100x plan apochromat (red curve), the 40x plan fluor (blue curve), and the 60x plan apochromat water immersion objective (green curve). Figure 7(b) displays ratio histograms of cells labeled with F-Tf and Cy5-Tf using the same three objectives. Figure 7(a) shows that the ratio of rhodamine to fluorescein (red to green) emissions is reasonably constant for all three objectives. In contrast, Figure 7(b) shows that while the 100x plan apochromat still shows minimal variation in the ratio of Cy5 to fluorescein (far-red to green), the water immersion 60x plan apochromat shows more variation, and the 40x plan fluor shows even more. The effects of chromatic aberration in the 60x plan apochromat and 40x plan fluor are more apparent when the distributions for a single focal plane are compared to those measured in the projections of the vertical image series for each objective (Figure 7(c) and Figure 7(d), respectively). In each case, the narrow distribution of fluorescence ratios in the projected images reports the nearly constant ratio of the two probes in the endosomes, which is misrepresented in any single focal plane image.

### Chromatic and Spherical Aberration in Water Immersion

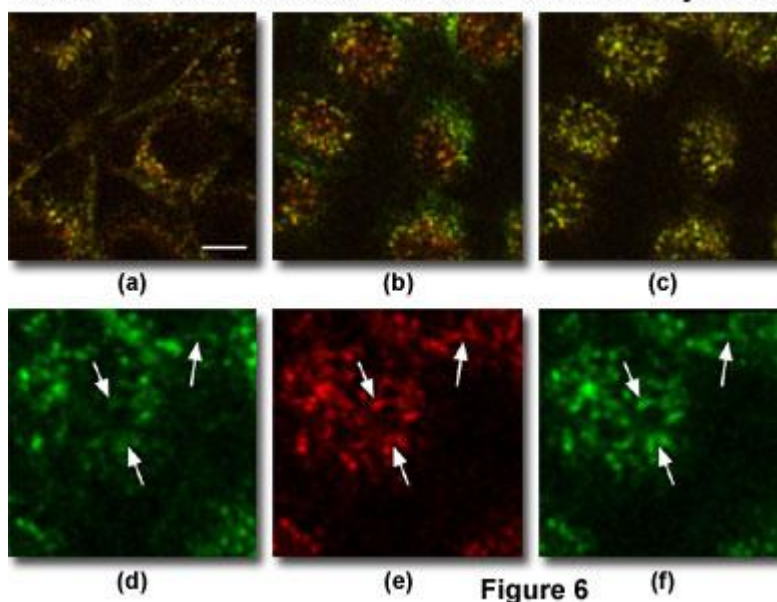


The studies presented here demonstrate vividly how chromatic and spherical aberrations compromise the performance of confocal imaging. At the same time, they emphasize the critical importance of objective choice in confocal microscopy. Poor color correction will lead to erroneous interpretations of the relative distributions of multiple probes, one of the major applications of confocal microscopy. The ratio quantifications also demonstrate how chromatic aberrations compromise microscope quantitation. Spherical aberration resulting from mismatched immersion and sample media worsens vertical resolution and can obliterate fluorescence detection altogether. Although particularly apparent in the high-contrast images provided by confocal microscopy, these errors also compromise images collected by conventional epifluorescence and transillumination techniques.

Chromatic aberration has been characterized primarily with respect to UV fluorophores. Other results demonstrate significant axial chromatic aberration in the far-red as well, a range increasingly used by microscopists with the development of new far-red fluorescent probes and lasers capable of exciting them. Although the studies presented here involve characterization of point sources, these samples readily display problems that would be manifest (but not necessarily obvious) with more extensive probes. Such probes include the cytosolic dyes that are frequently used in fluorescence ratio measurements of ionic concentrations.

For example, fluorescence of the cytosolic pH indicator SNARF-1 is excited by 488-nanometer light, and pH is measured from the ratio of fluorescence at 580 nanometers to that at 640 nanometers. For measurements of the cytosolic pH of thin cells, it is easy to imagine how the fluorescence ratio can be influenced by the position of the cell relative to the separate focal planes of the green excitation light, the red emissions and the far-red emissions. Although these errors will frequently simply add variation to measurements (doubling or tripling standard deviations in the presented quantifications), they can also systematically affect ratio measurements, for example, when comparing ratios in different parts of cells of varying thickness.

### Axial Chromatic Aberration in Water Immersion Objectives



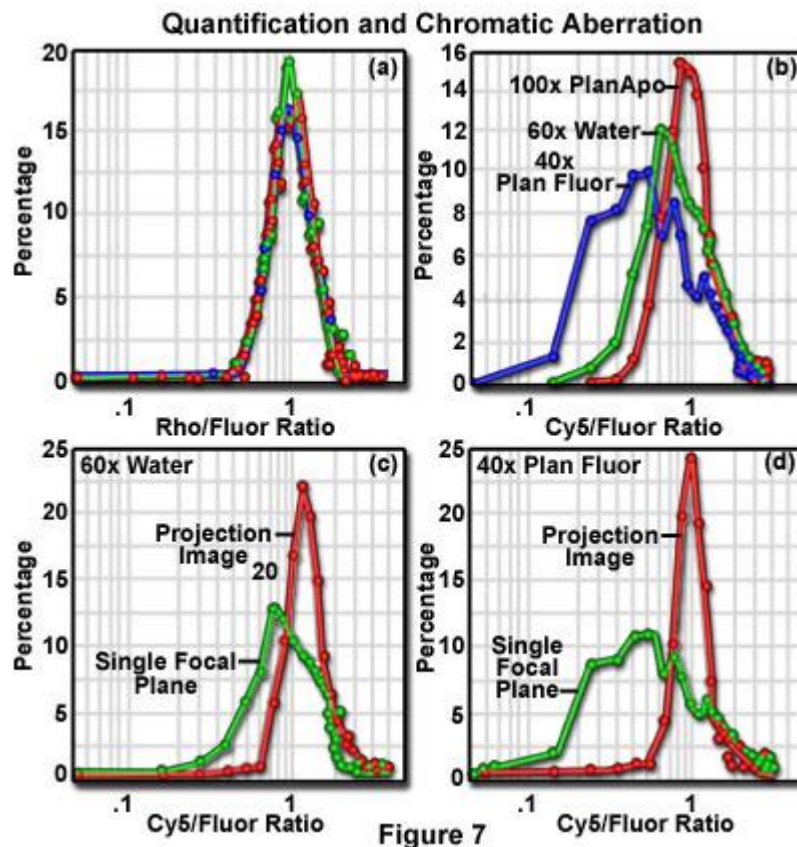
A final consequence of chromatic aberration, although not discussed here, is how it affects fluorescence detection. In a confocal system with chromatic aberration, the difference between the excitation and

emission wavelengths results in the excitation of one volume and imaging of a different volume, attenuating the fluorescence signal. For beam-scanning systems (most confocal microscopes), this loss of signal worsens with distance off axis as the imaged spot is focused farther and farther from the confocal pinhole.

It must be emphasized that these observations are not unique to the particular objectives used in the data presented, or to a particular manufacturer. The characterizations of the color correction were identically reproduced in three examples of the 60x water immersion objective and two examples of the 100x oil immersion objective on both Quantum and Diaphot microscope stands. Significant axial chromatic aberration has been identified in objectives from every major manufacturer. Indeed, the ubiquity of chromatic aberration has led to the development of alternative microscope designs that address chromatic aberration either by imposing special auxiliary correcting lenses or avoiding refraction altogether and turning to reflecting objectives. Nonetheless, microscope optics is likely to continue to evolve, and preliminary experience with the new generation of CFI60 optics from Nikon, Inc. indicates that axial chromatic correction is much improved.

Superficially, it may appear that some objectives are simply better than others. However, as discussed previously, objective design represents a compromise of design parameters. As such, each objective reflects a different set of design compromises according to its intended application. Nonetheless, it is possible that researchers will require more than what is currently available in optical design, forcing them to design experiments that do not stretch the limits of objective design.

If an oil immersion objective must be used to image a sample in an aqueous medium—for example, in studies of living cells—spherical aberration can be minimized either by minimizing the optical path through the aqueous medium or by using an oil with a refractive index tailored to the spherical aberration induced by the aqueous optical path.

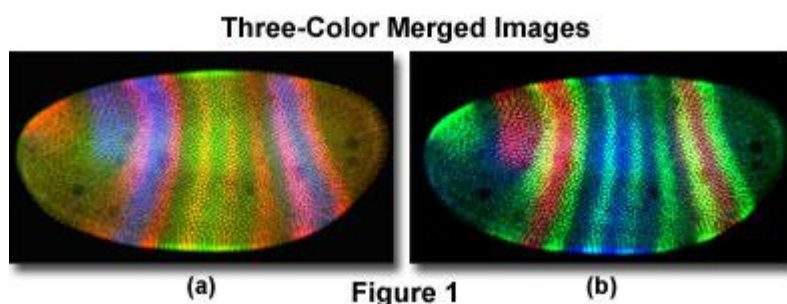


The problem of chromatic aberration can be minimized in several ways. If a particular experiment requires the use of an objective with significant chromatic aberration, the most obvious solution is to simply avoid the use of far-red fluorescing dyes such as Cy5 altogether. The results discussed in this review demonstrate satisfactory agreement between green and red fluorescence with all the tested objectives. In general, it is best to use dyes with maximum excitation and emission near the specific wavelengths for which a particular objective has been corrected. A second solution, discussed above, is to collect images of each fluorophore in a vertical series of focal planes and combine the different color images according to the difference in focal

plane between the two. This is a simple solution, but one that will not be appropriate when rapid image acquisition is necessary, as with live cells. Analyses not shown here also indicate that this solution does not have sufficient accuracy to correct images intended for ratio quantification. A more expensive (or less widely accessible) solution is to use two-photon microscopy, which is inherently unaffected by chromatic aberration as long as no detector pinhole is used. However, its multicolor capability is only now being explored.

## Methods and Applications of Three-Color Imaging for Laser Scanning Confocal Microscopy

The laser scanning confocal microscope (**LSCM**) is routinely used to produce digital images of single-, double-, and triple-labeled fluorescent samples. The use of red, green and blue (**RGB**) color is most informative for displaying the distribution of up to three fluorescent probes labeling a cell, where any co-localization is observed as a different additive color when the images are colorized and merged into a single three-color image.



In this section we present a simplified version of a previously published method for producing three-color confocal images using the popular image manipulation program, Adobe Photoshop. In addition, several applications of the three-color merging protocol for displaying confocal images are discussed. Note that these digital methods are not confined to images produced using the LSCM and can be applied to digital images imported into Photoshop from many different sources.

Images of fluorescently labeled specimens were collected using a Bio-Rad Model MRC-600 Confocal Laser Scanning System, and employing methods previously described in the literature. Selected images were transferred from the host microcomputer of the confocal microscope to a second computer as binary files. Images were imported directly into Adobe Photoshop, either as plain binary files (**RAW**) or as tag image file format (**TIFF**) files. In the case of RAW files, the actual dimensions of the confocal image must be entered; for example, a typical image size is 768 x 512 pixels with a 76-byte header. The header is specific to the Bio-Rad proprietary **PIC** file format and may vary with imaging systems from different companies. This information on the image files should be freely available from each confocal company. In contrast, TIFF files are opened directly into Photoshop. If necessary, confocal image files can be converted to TIFF files using commercially available programs designed for manipulation of confocal files, or other software, such as **NIH Image**, which is available for download on the Internet. A number of programs exist that are useful for further manipulation of confocal images.

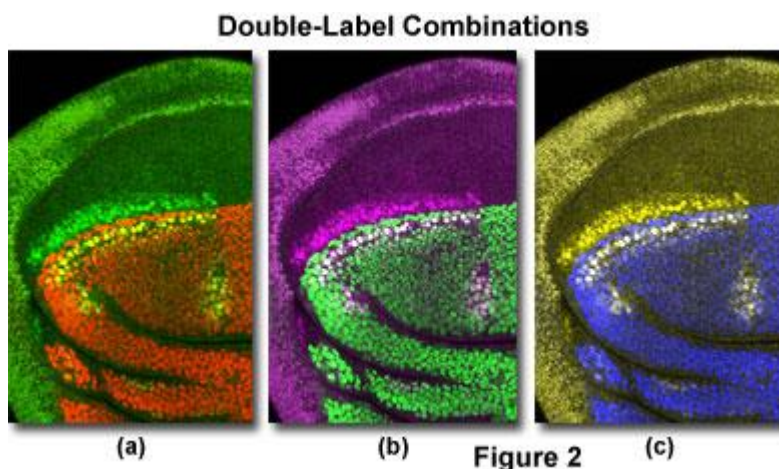
Three-color images are produced in Photoshop by pasting each of the grayscale images from the confocal microscope into the red, the green, and the blue channels of an RGB color image. In the following description of the process, the location of various commands within the Photoshop program is included (in italics) after each operation. Different versions of Photoshop may utilize slightly different command structure, or menu location of specific commands, to carry out the same operation. More-detailed information on specific operations in a particular version is available in the Photoshop User Guide.

Once the three grayscale images have been opened in Photoshop, a blank RGB image is constructed (**File, New**). The image must be the same size and pixel resolution as the three original grayscale images from the confocal microscope; in this example, 768 x 512 pixels and 72 pixels/inch. The size and resolution of an image can be determined and adjusted (**Image, Image Size**). This new RGB image should be black since the background in fluorescence images is usually very close to or at black (black = 0, white = 255). Another color can be chosen for the background for cosmetic purposes, but a black mask for the actual region

delineated by the image should be constructed so the new background color does not interfere with the information in the actual image.

If not already open, the **Channels** palette should be opened at this time (**Window, Show Channels**). The three grayscale images are now ready to be pasted into the newly created RGB image. This is achieved by selecting the first of the grayscale images (**Select, All**) and copying it into the required red, green or blue channel of the new RGB image (**Edit, Copy**) by clicking on the newly created RGB image with the mouse and then on the required channel in the **Channels** palette column. For example, for the red channel, click on the red window in the column. Finally, the grayscale image is pasted into the RGB image (**Edit, Paste**). The image will now appear in the **Channels** palette column in both the red and the RGB channel. The second and third grayscale images are now selected, copied and pasted into the green and blue channels, respectively, of the RGB image using the same routine. The result of these manipulations is a single three-color merged image (Figure 1, (a) and (b)), which is displayed by double-clicking on the RGB image in the **Channels** palette column. There is no loss of bit-depth information from the three original source images since three 8-bit images are merged into a single 24-bit image. The images of a *Drosophila* embryo displayed in Figure 1 were each created from the same three images collected at three different excitation and emission wavelengths, which were then assigned to different color channels using Photoshop to produce two versions of the three-color merged image.

The color levels in the resulting merged image can be changed using **Levels (Image, Adjust, Levels)** to independently adjust the red, green and the blue values of the image. Finally, for presentation purposes, the brightness and contrast (**Image, Adjust, Brightness/ Contrast**) of the image is fine-tuned. Subtle changes to the image can be viewed and selected using **Variations (Image/Adjust/Variations)**. Many additional operations can be achieved at this time using the image manipulation features nested within Photoshop. Especially useful features allow addition of graphics and compilation of the images into multi-panel figures. Graphics are subsequently more easily edited if they are pasted into a separate layer in the image rather than permanently replacing pixels in the actual image itself.



Images are saved to the hard disk of the computer by selecting **Save As (File, Save As)**. Images are usually saved in the TIFF format and compressed using the Lempel-Ziv-Welch (**LZW**) scheme, which is entirely lossless. Other compression methods such as Joint Photographic Experts Group (**JPEG**) compression can introduce artifacts that may be compounded each time a file is resaved. Images are eventually archived to CD-ROM or DVD-ROM.

Color hard copies of the images can be produced directly from Photoshop using a high-resolution digital color slide maker or digital dye-sublimation or other color printer. These devices are controlled directly from Photoshop as plug-ins, which avoids the need to transfer the images to yet another program. Detailed aspects of mass storage and the preparation of hard copies have been reviewed extensively in recent literature. Single-color images often lack contrast when printed on a dye-sublimation printer. The problem can be overcome, somewhat, by producing a single RGB image, as before, and adjusting the relative levels of the three channels so that there is information in all channels for printing (**Image, Adjust, Levels**).

For merging two images using this method, the third channel is left vacant. Early versions of Photoshop required the use of an empty or black, blank background image for the third channel and placing the red image in the red channel, the green image in the green channel, and the blank image in the blue channel of

an RGB image to produce a red/green double-label image. Using Version 3.0.5 of Photoshop (and later versions), two grayscale images can be pasted into a newly created black RGB image. For example, to produce a red/green image, separate images are pasted into the red and the green channels (Figure 2(a)).

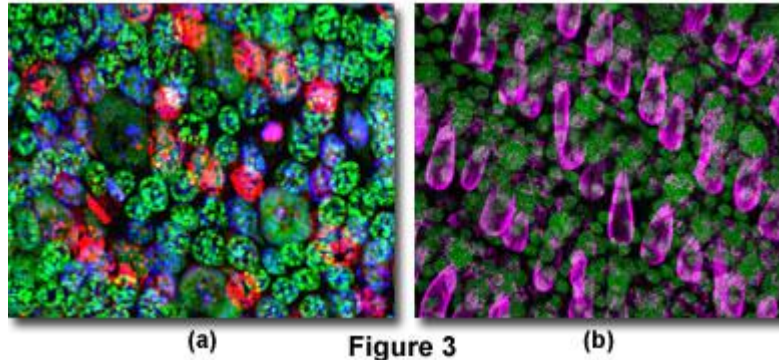
The combination of colors within a three-color merged image is important for clearly conveying the biological information collected by the confocal microscope. The true emission colors of two of the most commonly used fluorophores, rhodamine and fluorescein, are conveniently red and green, respectively, and overlapping domains of expression are yellow. These are the colors observed by eye in a conventional epifluorescence microscope equipped with the appropriate filter sets for simultaneous double-label imaging, which is now available from most of the microscope manufacturers. Note that the third channel in a triple-label sample prepared for confocal analysis usually emits in the far red, for example Cyanine-5 (Cy5), which is conveniently shown as blue in digital images, whereas the real Cy5 emission is often extremely difficult to visualize by eye and not so easily depicted in a digital image.

Using Photoshop, it is a relatively simple task to experiment with various color combinations by rearranging the images into different channels. The two versions of the three-color merged image presented in Figure 1 serve as examples. The specimen is a *Drosophila* embryo at the cellular blastoderm stage, triple-labeled for three segmentation proteins: *hairy* in green (Figure 1(a)) or red (Figure 1(b)), *Krüppel* in blue (Figure 1(a)) or green (Figure 1(b)), and *giant* in red (Figure 1(a)) or blue (Figure 1(b)). The different versions are achieved by rearranging the component grayscale images of the three-color RGB image into different channels using **Split Channels (Window, Show Channels, Channels Palette Dropdown Menu, Split Channels)** and recombining the images using **Merge Channels (Channels Palette Dropdown Menu, Merge Channels, RGB Color Mode)**. Using the **Specify Channels** input boxes, the component grayscale images may be assigned to different channels of the RGB image. The colors therefore do not always correspond to the actual colors of the specimen.

Extra colors can be included in double-label images by placing two versions of the same image into two of the three channels, with the second image of the merge in the third channel. For example, a purple and green image is produced by pasting the same image into the red and the blue channels to give purple, and the second image is placed into the green channel (Figure 2(b)). Additional color combinations are red and light blue, where light blue comprises the blue and green channels; or blue and yellow, where yellow comprises the red and the green channels (Figure 2(c)). Here, overlaps of expression invariably appear white in the image since all three channels now contribute to the overlapping signals (Figure 2, (b) and (c)). The different color combinations demonstrated here utilize a *Drosophila* third instar wing imaginal disk specimen double-labeled for *apterous* in red, green, or blue (Figure 2 (a) through Figure 2(c), respectively), and *achaete* in green, purple, or yellow (Figure 2 (a) through Figure 2(c), respectively). These additional color combinations can be useful when making a multi-panel figure of several double-label images where the expression patterns of more than three proteins are displayed in separate panels so that different colors are assigned to each protein. Note that the nuclei that coexpress *apterous* and *achaete* appear as yellow in Figure 2(a) and white in Figure 2(b) and Figure 2(c).

This method of merging confocal images is used extensively for mapping the distribution of macromolecules in double- and triple-labeled specimens. Because of the exquisite specificity of immunofluorescence, many of the images are rather abstract when viewed as single grayscale images and, in many instances, can only be interpreted when a second or third image of a known landmark within the tissue is displayed at the same time. This is typical of nuclei labeled by fluorescence in-situ hybridization (**FISH**). These images are often made up of relatively few bright pixels on a mostly black background, and the images can only be interpreted when a second, counterstained image of the entire nucleus or chromosome spread is collected and merged with the brightly stained centers of hybridization. The dimeric nucleic acid stains such as YOYO-1 (excitation maximum 491 nanometers) or TOTO-3 (excitation maximum 642 nanometers) are excellent counterstains for these purposes. Recently, more than three probes have been localized on the same chromosome using combinatorial labeling strategies. Here, more sophisticated computer methods of image merging and measurement have been developed to display the biological information in the images.

### Color Coding to Depth



Multi-label confocal imaging is a perfect tool for developmental biologists studying cell lineages and analyzing clones where the distribution of one, or sometimes two, proteins can be used as landmarks to map a third protein of interest within a developing tissue. Furthermore, fluorescently labeled phalloidin is a convenient probe to include in a triple-labeling strategy for imaging cell outlines. Specific combinations of dyes, for example rhodamine phalloidin to label cell outlines, TOTO-3 to label nuclei (on the Cy5 channel), and an antibody to the protein-of-interest (on the fluorescein channel) can be used in a triple-labeling strategy for mapping the location of a protein to the nucleus, to the cytoplasm, or to the extracellular matrix.

In addition to displaying the relative distribution of up to three different macromolecules within cells, this method of combining three images can be used as an alternative to three-dimensional (**3-D**) reconstruction for displaying depth information within a specimen. Using the LSCM, a series of images from different focal planes within the specimen is collected into a single file or z-series. These images maintain the x, y, and z registration from the specimen and are the same size and pixel resolution. Three images are chosen from such a z-series, exported as single-image files into Photoshop and then merged as before, so that the colors red, green and blue are assigned to structures at different depths within the specimen (Figure 3, (a) and (b)). In a similar way, single images of three different time points can be extracted from a time-lapse movie sequence file collected from the confocal microscope and combined into a three-color merged image. These files are similar to z-series files except that time has replaced the z-dimension. Here, color differences are used to summarize changes in the positions of structures over time in a single image.

The image shown in Figure 3(a) is the result of merging three images from a z-series projection that are colorized so that color is coded to depth in the specimen. Epithelial nuclei are shown in green with the nuclei of the scale-forming cells shown in blue and red (at different levels in the epithelium). The specimen is a whole mount butterfly pupal wing epithelium stained with propidium iodide. In Figure 3(b), different structures are mapped to depth in a double-label image in a whole mount of a butterfly wing epithelium at a slightly later stage of development than that of Figure 3(a). Here nuclei are labeled with TOTO-3, and the emerging wing scales at a more dorsal position in the epithelium to the nucleus are labeled with Texas Red phalloidin.

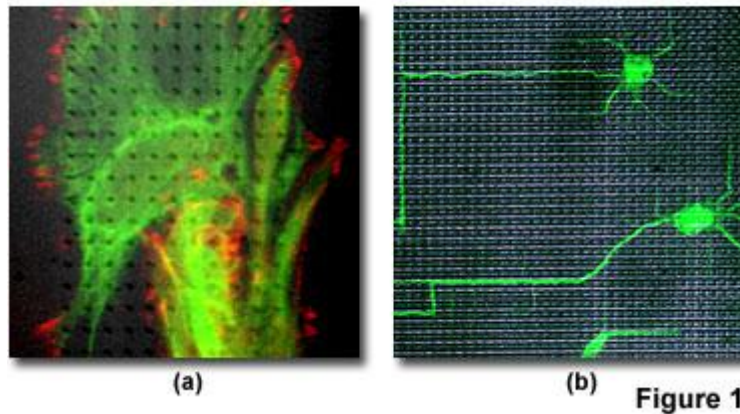
Photoshop can also provide a bridge to further manipulation of images since the files are compatible with many other programs. For example, sequences of confocal images of development have been manipulated using Photoshop and subsequently transferred to a commercially available morphing program and processed into short animated sequences of development. These sequences can be further edited and compiled using Adobe Premiere and viewed as a digital movie using Apple QuickTime software directly on the computer (other applicable software could be used as well), or exported to video tape for presentation purposes.

Photoshop is available for many different computer platforms and can be run on the host computers of most confocal microscopes. Some of the more sophisticated confocal imaging systems are able to collect, merge, and colorize three images simultaneously using a three-detector system, which may obviate the use of Photoshop. However, it is often necessary to use additional laboratory microcomputers to manipulate confocal images in order to liberate the confocal workstation for its primary purpose of collecting images. Moreover, for compiling final figures, it may be necessary to combine confocal images with images from other sources in the final plates, and in this situation, the versatility of a single image manipulation program that can be used on many different laboratory computers is invaluable.

## Basics of Confocal Reflection Microscopy

When many biomedical research think "confocal microscopy", they usually have fluorescence imaging in mind. This is a very good reason for this seemingly obvious connection. A majority of the common biomedical applications of the confocal microscope have utilized its optical sectioning power, combined with the exquisite specificity of immunofluorescence or fluorescence *in-situ* hybridization (**FISH**) to produce improved images of multiply-labeled cells and tissues.

### Confocal Reflected Microscopy of Cells on Substrata



Confocal reflection microscopy can be utilized to gather additional information from a specimen with relatively little extra effort, since the technique requires minimum specimen preparation and instrument re-configuration. In addition, information from unstained tissues is readily available with confocal reflection microscopy, as is data from tissues labeled with probes that reflect light. The method can also be utilized in combination with more common classical fluorescence techniques. Examples of the latter application are detection of unlabeled cells in a population of fluorescently labeled cells and for imaging the interactions between fluorescently labeled cells growing on opaque, patterned substrata, as illustrated in Figure 1.

The digital image presented in Figure 1(a) illustrates a glial cell growing on a silicon substratum that is patterned with small 1-micrometer high pillars and imaged using confocal reflection microscopy. The cell is immunofluorescently labeled for vinculin (red) and glial fibrillary acidic protein (**GFAP**, green). Figure 1(b) depicts neurons growing on a similar silicon substratum and labeled with an antibody to microtubule associated protein 2 (**MAP-2**) and a fluorescein-labeled secondary antibody. Again, the surface of the silicon substratum was imaged with confocal reflection microscopy.

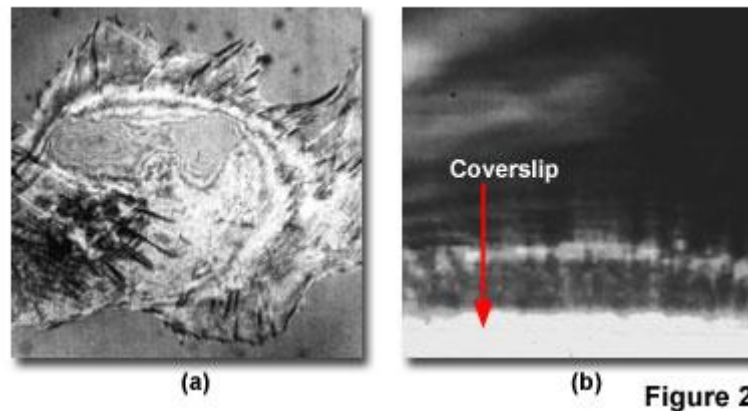
A major attraction of confocal reflection microscopy for biomedical imaging is the ability to image unlabeled living tissue. In fact, the technique has been utilized to image a variety of different tissues, including brain, skin, bone, teeth, and eye tissue. Confocal reflection microscopy works especially well for imaging the cornea and lens of the eye because they are transparent. For example, optical sections have been collected from as deep as 400 micrometers into the living cornea and lens using long working distance water immersion objectives.

Imaging unstained specimens with confocal reflection microscopy was very common for designers of early confocal instruments prior to the emergence of epifluorescence techniques. Both the laser scanning confocal microscope (**LSCM**) and the Nipkow spinning disk microscope can be utilized in confocal reflection mode. The spinning disk microscope has the advantage that images can be collected in real time, viewed in real color, and lack a reflection artifact that is sometimes present in the LSCM. This artifact appears as a bright spot in the image and is caused by reflection from one or more of the optical elements in the microscope. There are several remedies for the reflection artifact. It can be avoided by scanning the specimen in a region away from the optical axis of the microscope and zooming the bright spot out of the frame. Alternatively, the reflection can be removed from the image by digitally subtracting a background image of the spot or by flat-field correction. Another method for removing the troublesome artifact is to apply polarizing filters to the instrument in order to eliminate the reflection from optical elements.

A traditional biological application of widefield reflected light imaging is for observing the interactions between cells growing in tissue culture on glass cover slips using a technique termed interference reflection microscopy. Here, the adhesions between the cell and its substratum are visible at the interface of the glass

cover slip and the underside of the cell. These regions of cellular adhesion continue to be a research area of great interest. The proteins associated with the focal contacts are analyzed utilizing immunofluorescence, and the contacts themselves can be viewed using interference reflection microscopy.

### Interference Reflection in Confocal Reflection Microscopy



Cell-substratum adhesions are viewed in a similar manner using confocal reflection microscopy, as illustrated in Figure 2. Again, the interface between the cover slip and the cell is imaged. This surface can be difficult to locate in the confocal microscope, but the highly reflective cover slip can be employed as an aid in focusing. The cell-substratum interface can be located by focusing in fast scan mode, and the adhesions appear just after the bright flash of the cover slip when penetrating the cell layers. Care should be taken not to overload the photomultiplier tubes from the very bright cover slip surface when focusing in this manner.

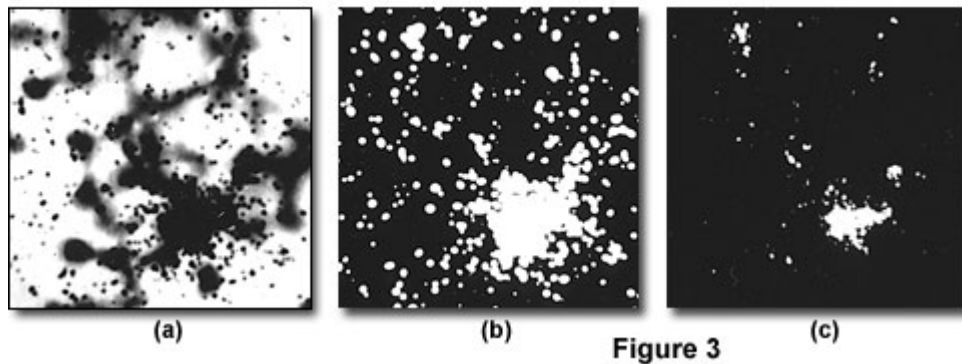
Presented in Figure 2 are interference reflection digital images captured with confocal reflection microscopy techniques. Figure 2(a) illustrates a single optical section of a chicken heart fibroblast cell imaged at the cell-substratum interface. The dark streaks at the periphery of the cell are focal contacts. An  $x-z$  section of a cell similar to the one shown in Figure 2(a) is depicted in Figure 2(b). Note that the cover slip in Figure 2(b) is extremely bright. This appears as a flash when focusing the microscope (red arrow), and the cell-substratum interface is imaged directly after the flash.

Recently, using a related technique, improved images of filopodia were collected from PC12 cells (rat pheochromocytoma) by growing the cells on a more reflecting substrate. The technique, termed **backscatter-enhanced reflection confocal microscopy**, produces images that resemble those collected using traditional differential interference contrast (**DIC**) microscopy. Using this method, unstained cells can be observed growing on opaque substrata, such as silicon chips, a technique that is impossible with conventional transmitted light DIC imaging.

One advantage of using reflected light, rather than fluorescence, for live-cell imaging is the absence of photobleaching artifacts in the reflected light mode. Attention should still be paid to the threat of photodamage to the living specimen, however, and all of the precautions for imaging live cells should be taken. Confocal reflection microscopy has been successfully utilized to follow cell migration through a collagen matrix and collagen fibrillogenesis *in vitro*, using time-lapse imaging of z-series and subsequent three-dimensional reconstruction (termed **4-D** imaging). These methods take advantage of the high reflectance or albedo of the collagen biopolymer.

A drawback of confocal reflection microscopy (when compared with confocal fluorescence imaging) is the lack of specific probes that differentially reflect light for multiple label experiments. It is difficult to improve upon the multiple-wavelength probes that are available for immunofluorescence and live-cell imaging. Probes that can be used in reflected light mode for single label experiments include gold particles, peroxidase labels, and silver grains.

### Confocal Reflection Microscopy of Silver Grains

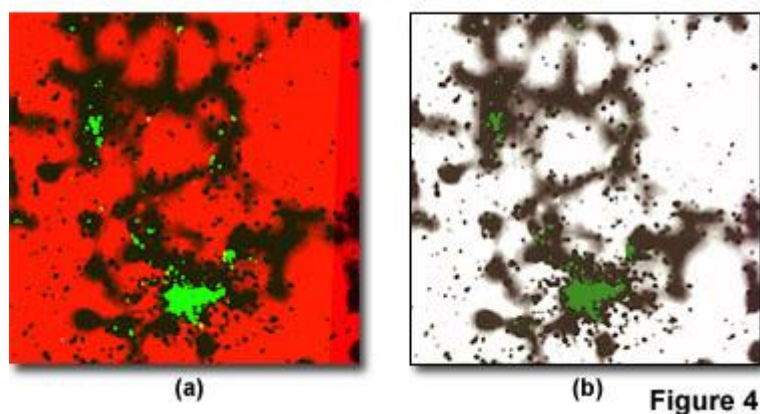


As an example, confocal reflection microscopy offers a significant improvement over conventional brightfield or darkfield microscopy for imaging silver grains in autoradiograms of specimens prepared for *in-situ* hybridization (Figure 3). The out-of-focus signal from the silver grains throughout the emulsion is effectively eliminated from the in-focus image of the silver grains associated with the riboprobe by optical sectioning the emulsion using confocal reflection microscopy.

Illustrated in Figure 3 are several digital images collected from confocal reflection microscopy experiments with silver grains. The specimen is peripheral blood cells from an HIV-infected individual prepared for *in-situ* hybridization and stained with Giemsa. Figure 3(a) illustrates the preparation under standard brightfield illumination, while Figure 3(b) shows the same field in darkfield illumination with a significant amount of out-of-focus debris. The results with confocal reflection microscopy (of the same viewfield) are presented in Figure 3(c). Note that the out-of-focus debris is not imaged in this mode. For comparison purposes, specimens can also be imaged with differential interference contrast, in addition to brightfield and darkfield illumination.

Because the reflected light confocal image and the transmitted (brightfield and darkfield) images are collected simultaneously using the same scanning laser beam (in Figure 3), they are in register with one another and can be digitally merged into a single image. The transmitted light brightfield image records the total cell population either as a grayscale image or a real-color image (provided a real-color transmitted light detector is fitted to the microscope). The darkfield illumination image incorporates a signal from the entire population of silver grains in the complete emulsion, including any contaminating dust particles on the glass surfaces. The confocal reflection microscopy image, in contrast, records only those cells labeled with the probe (Figure 3(c)), and hence is a more accurate measure of the labeled cells than the transmitted light images. Moreover, it is more amenable to quantification of the probe, because the image consists of discrete regions of saturated pixels (signal from the probe) on a black background, and is somewhat reminiscent of a fluorescent image in this respect.

### Merged Images of Silver Grains



The confocal reflection microscopy images are digitally merged with the transmitted light images for display purposes and estimate the number of labeled cells in the total cell population. In most confocal systems, the transmitted light image is collected in one of the channels of the **RGB** image (usually the blue channel), and a reflected light image, or one or more fluorescent images, is collected simultaneously with it, usually into the red and green channels. Displaying the transmitted light image in this manner produces a colored

background, as illustrated in Figure 4(a), instead of the more familiar gradient of gray levels of a typical brightfield or DIC image, or the black background of a darkfield image. A more realistic version of the transmitted light image can be obtained by pasting it onto a different layer from the reflected light image using a digital image editing program such as Adobe PhotoShop (shown in Figure 4(b)).

Confocal reflection microscopy is usually employed in addition to fluorescence to add context to fluorescence images, which can be rather abstract when viewed in isolation (especially confocal fluorescence images, which can consist of a few white pixels on a sea of black). In the examples presented above, the combination of the specific labeling of immunofluorescence and the optical sectioning power of the confocal microscope can actually hamper the interpretation of the images themselves, unless they are digitally merged with a reflected light, transmitted light, or counter-stained fluorescence image.

Although confocal reflection microscopy has limited applications in biomedical imaging, it can sometimes provide additional information from specimens that reflect light or have significant fluctuations of refractive index at certain boundaries. This useful technique, along with transmitted light imaging, may be worth a try when imaging fluorescently labeled specimens with a confocal microscope.

## Confocal Microscopy Image Gallery

The Nikon MicroscopyU Confocal Image Gallery features digital image sequences captured using a Nikon PCM-2000 confocal microscope scanning system coupled to an Eclipse E-600 upright microscope. Successive serial optical sections were recorded along the optical axis of the microscope over a range of specimen planes. These sequences are presented as interactive Java tutorials that allow the visitor to either "play" the series of sections automatically, or to utilize a slider to scroll back and forth through the images.

**Abscission Layer** - Each new leaf forms a specialized layer of cells called an **abscission** that is located between the leaf and the stem and is responsible for the changing colors of leaves in the fall season. The abscission layer is comprised of minute tubules designed to transport water to the leaf and carry carbohydrates back into the tree. In the autumn, the green color, which dominates trees throughout the spring and summer, fades to reveal the color of pigments that have been present in the leaf all along, such as orange and bright yellow.

**Alfalfa Stem** - Alfalfa, or *Medicago sativa*, is a deep-rooted perennial native to the Mediterranean region near Iran but which also grows well in North America and Western Asia. Also called Lucerne, or Purple Medic, it looks very much like clover with a smooth, erect stem growing 2-3 feet tall, grayish-green feathery trifoliate leaves, and egg-shaped leaflets.

**Apple Cedar Rust** - Cedar apple rust (CAR) is a disease affecting apple trees in North America east of the Rocky Mountains. It is caused by the fungus *Gymnosporangium juniperi-virginianae* and can defoliate trees and blemish fruit making them unmarketable.

**Auerbach's Plexus** - The Auerbach's plexus lies between the longitudinal (outer muscle layer) and circular muscular (inner) coats of the duodenum. Peristaltic movements of digesting material originate in the muscles (myogenic) and are initiated by local reflexes.

**Basal Cell Carcinoma** - A common form of skin cancer (90 percent of the cases), basal cell carcinoma may grow slowly at first, but like other malignant cancer cells, can spread to other parts of the body (metastasize). It is estimated that 500,000 new cases of this type of non-melanoma skin cancer occur in the United States each year with about 2,000 deaths annually.

**Basswood (Tilia) Stem** - The American Basswood, *Tilia americana*, is a treasured hardwood tree of the Eastern and Central United States. It has a tall, straight trunk and rounded crown that provides excellent shade during the hot summer months.

**Basswood (Tilia) Root** - The American Basswood is a stately and graceful hardwood tree that grows abundantly in rich moist soil found in the eastern half of North America. The heavily foliated crown produces dark green heart-shaped leaves that reveal lighter colored glistening undersides when blown by a breeze.

**Beach Grass (Marram)** - Marram is the common name for a beach grass that grows on the sandy coasts of Europe, North America, and North Africa and is also known as **psamma** or **sand reed**. These coarse and hardy grasses grow in tufts producing tightly rolled spike-like leaves that are naturally resistant to wind and salt spray.

**Bordered Pits** - Bordered pits are structures found in the conductive tissues of many plants that allow fluids to pass from one cell to another. The tracheids, which transport liquids, are dead cells; their contents decomposed, they are essentially empty. Simple pits are areas of the tracheid cell wall so thin that nutrient rich solutions can pass through them, to be dispersed throughout the plant.

**Cabbage Club Root** - Wilted, yellowing leaves and stunted plants can often signal an infection of club root in cruciferous plants such as cabbage, cauliflower and broccoli, causing significant economic losses to farmers. The most distinctive symptom, however, is the abnormal enlargement, or clubbing, of roots where the disease process is taking place.

**Cerebral Cortex** - The **cerebral cortex** is the part of the brain that sets humans apart from and above all other animals. This sector is primarily responsible for interpreting information sent by the senses such as sight, sound, smell and touch as well as initiating voluntary directed action such as walking or talking.

**Cherry Flower Bud** - Cherry is the name given to several varieties of trees that produce small, almost heart-shaped globular edible fruits that vary in color from deep red to nearly black. The native habitat of the cherry is believed to be woodlands of Europe and Asia.

**Chick Embryo (60 to 70 Hours)** - The chicken is a common domesticated fowl and is commercially valued for meat, eggs, and feathers. Domestic chickens are descended from the wild red jungle fowl that is native to Southeast Asia, which is believed to have been domesticated as far back as 8,000 years ago.

**Chlamydomonas** - *Chlamydomonas* is a large genus of common green algae that are equipped with two relatively long whip-like appendages used for locomotion. Primarily aquatic, algae are found anywhere there is marine and freshwater, moist soil, and even snow.

**Chinese Hamster Ovary Cells** - Chinese hamsters are Old World rodents characterized by soft thick fur, large expandable cheek pouches, and relatively long tails. Because this small breed of hamster has a slender body and a tail that is unusually long, it is thought to resemble a mouse and is often referred to as "mouster".

**Club Mosses** - Allies to the true ferns, the club mosses and spike mosses are ancient plants distributed widely, throughout the tropics and temperate zones. One genus, *Selaginella*, represented by more than 700 species of small and delicate plants, is characterized by having a single, cup-shaped chloroplast per leaf and ligules, small tongue-like structures on the top of each leaf (near its base) that's function has yet to be determined.

**Cork Cells** - Mature cork cells are plant cells that form the protective water-resistant tissue in the outer covering of stems or trunks. Cork cells are genetically programmed not to divide, but instead to remain as they are, and are considered dead cells.

**Corn Grain** - Corn is the common name for the cereal grass widely grown as food for humans and animals. Along with wheat and rice, it is one of the world's chief grain crops and the largest crop grown in the USA. Native to the Americas, corn (*Zea mays*) is the domesticated variety of the Zea grass family, originally was cultivated by Native Americans 8,000 to 10,000 years ago.

**Cup Fungus** - Cup fungi are typically characterized by strikingly colorful cup-shaped mushroom-like structures that are commonly found on rotting wood in forests and in cow pastures. Some of the more brilliant colorations range from bright yellows and greens to pale peach, light orange, and deep scarlet reds.

**Dandelion Root** - Like other flowering plants, the roots of dandelions function to anchor the plant, gather and move water and minerals, store food, and provide a source of cells for growth.

**Dinoflagellates** - Dinoflagellates (Peridinium) are single-celled organisms that propel through watery environments by waving two thread-like structures referred to as **flagella**. These mostly marine creatures are

participants in plankton communities that drift along sea currents and serve as an important source of food for many aquatic animals.

**Dutchman's Pipe Vine Stem** - A native of central and eastern North America, Dutchman's pipe, *Aristolochia durior*, is a climbing vine and part of the birthwort family. The vine is planted often as a screen or cultivated as a porch vine because it is easy and quick to grow. It is distinguished by its large heart-shaped leaves and yellowish or purplish tubular flowers that resemble traditional Meerschaum smoking pipes.

**Elderberry Lenticel** - Elderberry bushes can be found in most forested temperate or subtropical areas around the world. In horticulture, the bushes are often used as garden shrubs and are well known for their fruit, which is used to make wines, syrups, cordial, jellies, pies and also serves as a source of food for wildlife.

**Eyelid (Human)** - The eyelid is engineered to moisten and protect the exposed portion of the eyeball and to shield the visual processing centers from external light sources during sleep. Throughout the waking hours, without requiring conscious effort, eyelids quickly open and shut or "blink" at a rate somewhere between once every two to ten seconds.

**Fava Bean Mitosis** - The fava bean plant (*Vicia faba*) also known as broad bean or horse bean, is a legume belonging to the pea family, Fabaceae. It is cultivated for its seeds, six to eight beans resembling large round limas, packed inside a large, pale-green, velvety pod.

**Fern Anther** - The **anther** is the pollen producing structure of flowering plants that is found in the male reproductive organ known as the **stamen**. Often referred to as the pollen sac, anthers are bi-lobed structures that typically rest atop long slender stalks called **filaments**.

**Fern Indusium** - Fern is a common name for the **cryptogamous** (spore-producing) plants belonging to the division **Filicophyta**, also called **Filicinophyta**. They are primitive vascular plants with true roots, stems, and complex leaves. Most ferns reproduce through the alternation of generations, alternating successive generations of sexual and asexual forms.

**Fern Spores** - Most ferns reproduce through the alternation of generations, alternating successive generations of sexual and asexual forms. The sexual form, called the gametophyte or prothallia, is a tiny kidney-shaped plant and difficult to find in the wild. The asexual form, or sporophyte, is represented by the fern plant as it is commonly known.

**Frog Artery** - The primary function of the heart is to pump oxygen rich blood to organs such as the brain, liver, and kidneys as well as all other tissue. The heart of the frog is different from the hearts of warm-blood animals such as humans.

**Frog Eye (40x Magnification)** - Frogs have eyes that closely coordinate with their long sticky tongues to enable these amphibians to capture fast moving prey with whip-like accuracy. A majority of species possess eyes that bulge from the sides of their heads so that most frogs can see in almost all directions.

**Frog Muscle** - Frogs depend on several types of muscles to carry out their normal daily activities such as pumping blood, breathing, moving about, and retrieving food. The three types of muscle are **striated** (skeletal), **cardiac** (heart), and smooth.

**Frog Stomach** - After outliving dinosaurs, frogs have changed very little from their ancestors who roamed the earth 150 million years ago. These slippery creatures can be found atop freshwater lily pads, among the canopies of tropical rainforests, burrowed deep into the sands of the Australian desert, or even hibernating in Arctic soil.

**Frog Unsegmented Egg** - Unlike their reptile cousins, which are better adapted for reproduction on land with eggs that are protected from desiccation and other harm, frog eggs need a moist environment and often are protected by a gelatinous mass.

**Ginkgo Tree** - The ginkgo tree has changed little in morphology based on 200 million year-old fossils. This beautiful plant is often cultivated as an ornamental tree, particularly in urban areas because it is resistant to smog.

**Grape Black Rot** - Black rot, caused by the fungus *Guignardia bidwellii* is one of the most serious diseases of cultivated grapes in the eastern United States, especially in warm, humid areas. Crop losses can be devastating, ranging from 5 to 80 percent depending on the weather, the variety of grape being grown, and the amount of disease in the vineyard.

**Green Algae** - Members of the Kingdom **Protista**, algae are most common in aquatic habitats, but occur in nearly every environment. They range in size from microscopic to giant kelp that reach 200 feet (60 meters) in length. Algae produce a significant percentage of the Earth's oxygen, are the base of the food chain for nearly all aquatic life, and provide food and industrial products for humans.

**Hamster Cell Nuclei** - Chinese hamster ovary (CHO) cells (sometimes Syrian hamster cells) are very popular for histological, viral, and genetic research, because they are easily cultured as animals or tissues in the laboratory and because hamsters are small, cheap, and reproduce prolifically at an early age.

**Heart Thick Section** - The human heart, typical of mammals, is a four-chambered hollow muscular organ, found between the lungs and enclosed in the pericardium (cardiac) cavity. The average adult heart is about five inches in length and three and a half inches at its broadest part.

**Hollyhock Rust Fungus** - Hollyhocks are prone to rust disease, which generally does not cause death of the plant, but does stunt growth and cause discoloration and premature shedding of leaves.

**Human Bronchogenic Carcinoma** - Bronchogenic carcinoma, or lung cancer, is the leading cause of cancer deaths in the United States and most of the developed world. In the 1990s, more women were dying of lung cancer than of breast cancer, which historically had been the major cancer killer in women.

**Human Cerebellum** - The cerebellum is the portion of the human hindbrain that ensures a movement goes where it is supposed to go, at a proper rate and with a force appropriate to the resistance being overcome.

**Human Choroid Plexus** - The **choroid plexus** is comprised of a network of minute fringed capillaries, which secrete a liquid that is vital to the health of the brain and spinal cord, termed the **cerebrospinal fluid**.

**Human Diaphragm** - The diaphragm, a layer of muscle and fibrous septum, is connected to the spine at the lumbar vertebrae by two crura or pillars. When the diaphragm muscle contracts, it moves downward, making the chest or thoracic cavity longer, while its associated intercostal muscles contract, widening the chest, allowing inspiration. The diaphragm and external intercostal muscles then relax and expiration occurs.

**Human Gallbladder** - Responsible for storing the bile and secreting mucous, the human gallbladder is a pear-shaped muscular sac, lodged under the right lobe of the liver.

**Human Lung** - The respiratory system branches similarly to a tree, with about 17 levels of branching between the trachea and the bronchioles, and results in about 130,000 bronchioles in the average pair of human lungs.

**Human Meissner's Plexus** - The **Meissner's plexus** is an interlacing collection of nerves that connects the outlying smooth muscles to the innermost mucous membranes that line the stomach and intestines.

**Human Neurons** - Nerve cells are one of the fundamental building blocks that separate organic matter (living organism) from inorganic matter (non-living material such as rocks). Individual nerve cells form links that join together to produce a complex and integrated communications network that runs throughout the entire body. These interconnected cells allow the living organism to communicate or interact with its external environment by transmitting information through a coordinated series of electrical and chemical signals.

**Human Post Central Gyrus** - The mystique of the brain intrigues modern biologists and psychologists even as it did the philosophers of ancient times. Brain function is so strongly associated with what it means to be alive and human that the cessation of brain activity is a clinical and legal criterion of death, even when other organs of the body are still functioning.

**Human Submandibular Gland** - The submandibular gland, one of three human saliva glands, produces about two thirds of the average daily output of one liter of saliva. The saliva produced is a viscous solution containing mucin, salts and the enzyme amylase.

**Human Tongue** - The primary function of the tongue in mammals is to provide a mechanism for taste. As a muscle it is also important as a means of creating the negative pressure necessary for infants to suckle, an exclusively mammalian activity.

**Human Trachealis Muscle** - The **trachealis** muscle is a thick band of smooth muscle that bridges the ends of each of the horseshoe-shaped cartilage rings that help to stabilize the entire length of the windpipe.

**Human Uterus** - The human uterus is a specialized organ designed for containing and nourishing a developing embryo from implantation to birth. If fertilization of the egg or ovum occurs, the epithelial lining of the uterus undergoes physiological changes that make it hospitable for the attachment and nurturing of the early embryo.

**Human Vocal Cords** - The term vocal cords can be somewhat misleading because these sound producing structures are not really chords but are folds of expandable tissue that extend across a hollow chamber known as the voice box. When engaged for speaking, the vocal folds can vibrate over 100 vibrations per second -- too fast for the unassisted eye to see.

**Lichen Thallus** - Lichen is an organism that results from intimate cooperation between two distinct life forms, fungi and algae. This tough and hardy partnership can live where nothing else will grow -- even on bare rock.

**Lily Anther Prophase** - The lily, with its definitive reproductive stages, is a favored specimen for illustrating normal cell division. Of special interest are cross sections that present anthers during different stages of development, especially evolution of mature pollen grains from microspore mother cells.

**Lily Anther Sporogenous Tissue** - The **anther** is the pollen producing structure of flowering plants that is found in the male reproductive organ known as the **stamen**. Often referred to as the pollen sac, anthers are bi-lobed structures that typically rest atop long slender stalks called **filaments**.

**Lily Anther Uninucleate Microspores** - The anther has a terminal sac-like architecture that contains spore-producing cells called **microsporocytes**, which undergo meiosis and eventually form grains of pollen.

**Lily Embryos** - Lily is the common name for the family of **Liliaceae** and comprises more than 4000 species of flowering plants. Revered for thousands of years as a symbol of purity, many lilies are cultivated as highly prized ornamental plants including tulips, true lilies, daffodils, hyacinths, and amaryllis.

**Lily Flower Young Bud** - The lily is an herbaceous flowering plant native to the temperate areas of the Northern Hemisphere. The name, lily, is most frequently applied to the 80-100 species belonging to the genus *Lilium* of the family Liliaceae.

**Lumbricus (Earthworm)** - The ***lumbricus terrestris*** is more commonly known as nightcrawler, earthworm, or dew worm. These soil-borne animals generally prefer moist and humid habitats and can be found in orchards, pastures, forests, and grasslands as well as crawling along sidewalks on cloudy days just after a rain.

**Lung Adenocarcinoma** - Lung cancers are divided into small-cell and non-small cell types including adenocarcinoma (cancers of secretory organ linings); each with its own treatment regime.

**Lymph Nodes** - The lymphatic system is comprised of a series of interconnected vessels, ducts, various organs, and structures that constantly circulate a clear and watery fluid that nourishes and protects tissues throughout the body. This precious fluid and its constituents are a major component of the body's immune system and the term **lymph** is derived from the Latin word **lymphā**, meaning water goddess.

**Mammalian Motor Neurons** - Specialized nerves referred to as motor neurons transmit signals that cause skeletal muscle cells to temporarily shorten or contract. The average mass of the human body is comprised of about forty percent skeletal muscle.

**Mammalian Purkinje Fibers** - Purkinje fibers are heart muscle tissues that are specialized to conduct electrical impulses to ventricular cells, which induce the lower chambers of the heart to contract. Enveloped in a small amount of delicate connective tissue, these electroconductive fibers are imbedded in regular cardiac muscle.

**Mammalian Trachea** - The **trachea** or windpipe, is a part of the respiratory system and is comprised of a long slender tube that carries air to and from the lungs. In addition to serving as a passageway for air, this channel humidifies (moistens and warms) air before it reaches delicate lung tissue, and protects the respiratory tract from foreign particles.

**Mammalian Vater-Pacini (Pacini) Corpuscles** - The onion-like Vater-Pacini corpuscles are mechanoreceptors found in the pancreas of cats, but not humans. In humans, the pressure-sensitive, encapsulated nerve fibers are the largest (1 to 4 millimeters in length) lamellated (layered) bodies found in skin, nipples, genitalia, ligaments, and tendons.

**Marchantia Sporophyte** - These mature sporophytes are the asexual reproductive form for the Marchantia order of Bryophytes, moss-like plants of the division **Bryophyta**, also known as liverworts, or "liver plants."

**Medulla Oblongata** - The **medulla oblongata** is a cone-shaped part of the brain that is located on the lowermost portion of the brain stem and gradually transitions into the spinal cord. This specialized area serves as the major pathway for nerve impulses that enter and leave the neural systems confined to the skull.

**Melosira Diatoms** - Diatoms are unicellular phytoplankton that are armored with a protective cell wall composed of silica, and these tiny creatures form the basis of the oceanic food chain.

**Monkey Lip** - Lips form the muscular opening of the mouth and contain numerous tiny capillaries and nerve endings just beneath the thin membrane surface. The center of the lip is comprised of a muscle termed **obicularis oris**, which helps to hold food in the mouth and form facial expression such as smiling and frowning.

**Monocot Root Tip** - **Monocot** plants such as lilies, orchids, palms, irises, and grasses are supplied with an extensive fibrous root system. Although a primary root initially emerges from a seedling, it remains just long enough to establish a foothold and is quickly replaced by the outgrowth of many slender roots.

**Moss Capsule** - Mosses are the most common, diverse, and advanced group of Bryophytes, a division of green, seedless plants that dates back to the Permian period (286 to 245 million years ago).

**Moss Reproductive Tissue** - Mosses are the most common, diverse, and advanced group of Bryophytes, a division of green, seedless plants that dates back to the Permian period (286 to 245 million years ago). In Bryophytes, the antheridium is the female sex organ, which produces eggs.

**Mouse Intestine** - Mouse intestines are very much like those of other vertebrate animals. The large intestine is wider and shorter than the small intestine and its primary function is to absorb water and electrolytes from digestive residues and store fecal matter.

**Mouse Kidney** - Mouse kidneys are located on the dorsal (upper) wall of the abdominal cavity and are securely held in place by fibrous capsules. Like other mammalian kidneys, the outer layer of this rodent's kidney is brownish red and granular in appearance, with a firm consistency.

**Nostoc (Cyanobacteria)** - The **Nostoc** is an aquatic form of bacteria that can be found on moist rock, along the bottom of freshwater lakes and springs, and only rarely in marine habitats. Many of these single-celled organisms form colonies that range from microscopic to macroscopic in size and are often surrounded by a gelatinous sheath.

**Oak Tree Stem** - Oaks, members of the genus **Quercus**, are deciduous, hardwood trees found throughout the world, with about 60 species native to the United States. The lifespan of an oak varies by species (from 50 to more than 200 years) and environmental condition.

**Oleander Leaf** - Oleander, *Nerium oleander*, is an ornamental evergreen that belongs to the dogbane family, **Apocynaceae**. The best-known oleander shrub, called rosebay, is native to the Mediterranean and Middle East regions and is distinguished by dark green leaves that are thick, leathery, and lance-like.

**Onion Root Tip Mitosis** - Onions are among the world's oldest cultivated plants, and their pungent bulbs have probably been used in cooking since humans have been using fire. A member of the lily family, the onion is thought to be a native of Southwestern Asia but is now grown throughout the world.

**Optic Nerve Head** - More commonly known as the **blind spot**, the optic disc does not contain sensitive light receiving cells such as cones and rods and is not capable of detecting a visual image. This region, devoid of photoreceptive cells, is where optic nerve fibers of the retina converge to leave the eyeball -- everyone has one of these blind spots in each eye.

**Ovarian Adenocarcinoma** - Starting in the ovaries as cysts, ovarian cancer may originate from epithelial, germ, or connective tissues, each with its own characteristics and indicated treatment. Adenocarcinomas are cancers of the ovary lining and are epithelial in tissue type.

**Pacinian Corpuscle** - A feature of both human and non-human primates, the Pacinian corpuscle is a mechanoreceptor that responds to pressure or any kind of mechanical stimulus that causes deformation of the corpuscle surrounding the single afferent nerve fiber.

**Peyer's Patches** - **Peyer's patches** are a collection of large oval lymph tissues that are located in the mucus secreting lining of the small intestine. These lymph nodules are especially abundant in the lowest portion of the small intestine that empties into the larger intestinal tract, an area of the digestive system referred to as the **ileum**.

**Pine Blister Rust** - White Pine Blister Rust, a serious disease of pine trees caused by the fungus *Cronartium ribicola*. This fungus also is a disease of the *Ribes* genus (currant and gooseberry bushes), which serves as an alternate host for the fungus.

**Pine Cone** - Pine is the common name for any species belonging to the genus *Pinus*, a member of the family **Pinaceae**, coniferous trees with needle-like leaves. Pinaceae is the largest family of conifers, consisting of about 262 species, and includes fir, larch, spruce, hemlock, cedar and Douglas fir.

**Pine Embryos** - Tiny pine embryos are encased within a seed coat and wait until favorable growing conditions arise before emerging. The most intensely studied pine seeds today belong to the Wollemi pine, a cone-bearing tree whose lineage dates back over 250 million years.

**Pine Tree Roots** - Pine trees are classified as **gymnosperms** and are characterized by a tap root system. When a pine seed germinates, the very first organ to appear is the primary root. As the primary root grows downward to anchor the seedling, it branches secondary roots laterally. Although species of pine trees vary, most have wide spreading but rather shallow root systems that leave them vulnerable to strong gusts of wind.

**Pollen** - Pollen is a seasonal problem for millions of people around the world who suffer from allergic reactions to the antigens embedded on the outer casing of these microscopic grains. Tiny grains of pollen are released into the atmosphere by a wide spectrum of flowers, trees, weeds, grasses and other plants that reproduce seasonally.

**Polypodium Rhizomes** - Mostly **epiphytes** (plants growing above the ground, but supported nonparasitically by another plant or object), polypodium ferns are often found growing from tree trunks and limbs, but sometimes on rocks or even dry ground.

**Pons** - The pons is a broad, horseshoe shaped portion of the brain (often termed the brain stem) located in the upper segment of the region that gradually transitions into the spinal cord.

**Potato Late Blight** - Potato late blight, caused by the fungus *Phytophthora infestans*, is one of the most important potato diseases in the world. It was responsible for the great Irish Potato Famine of the 1840's, leaving over 1 million people dead from famine-related diseases and resulting in the exodus of more than 1.5 million people from Ireland.

**Primate Cornea** - As the first and most powerful lens in the optical system of the primate eye, the cornea with a crystalline lens allows the production of a sharp image at the retinal photoreceptors.

**Primate Iris** - Primates have evolved eyes that are uniquely adapted to their tree dwelling lifestyles and inquisitive nature. The eyes of primates are positioned on the front side of their head so they can peer forward to provide overlapping fields of view or stereoscopic vision. This three-dimensional perspective of the world permits accurate perception of distance, which is very helpful to primates swinging from branch to branch and handling food.

**Primate Meissner's Corpuscles** - Located in the papillae of the dermis (inner layer of primate skin) that project into the hand epidermis (skin outer layer), Meissner's corpuscles are associated with quickly-adapting (**QA**) mechanoreceptor fibers which respond to movements in the range of 2 to 40 millimeters per second, but do not react to constant, steady stimulation. Each Meissner's corpuscle is innervated by two to six nerves.

**Primate Pancreas** - The pancreas is a glandular organ that secretes digestive enzymes into the small intestine by way of the pancreatic duct. Also containing specialized groups of cells called the **islets of Langerhans**, the pancreas produces the hormones -- insulin and glucagon. Secreted directly into the bloodstream, these hormones work together to maintain proper sugar or glucose levels in the blood.

**Primate Skeletal Muscle** - Muscles are tissues composed of bundles of fibers (**fascicles**) having varying lengths and diameters that can shorten, thicken, or lengthen depending on the location and the message sent by the controlling neurons.

**Primate Tongue** - Covered in a mucous membrane, this muscular appendage is comprised of very small nodules termed **papillae** that project along the top surface and provide a rough, unsmooth texture. Tiny bulb-like taste organs, often referred to as **taste buds**, are scattered over the top surface and sides of the tongue.

**Primate Trachea** - The trachea is a thin walled tube that carries air to the lungs and is also commonly known as the windpipe. The tube is lined with a mucous membrane comprised of numerous tiny hairs or cilia that keep dust and other foreign particles from reaching the lungs. Material trapped in the mucous is swept out through the nose or mouth by the upward movement of the cilia.

**Pumpkin Stem** - Botanists are very familiar with the **Cucurbita** stem since it presents a clear demonstration of cell differentiation in the vascular system of a herbaceous plant.

**Rabbit Muscle Fibers** - Rabbit muscle is often used in biomedical research because it is a very good model of human tissue that is readily available at low costs.

**Red Algae - Polysiphonia** are plant-like organisms that are predominantly found in marine environments and are more commonly known as red algae. Although a few species may be found in freshwater, red algae are typically attached to rocks or other plants in tropical and subtropical deep waters or washed along shorelines.

**Retina** - The tiny retina of the eye is packed with more sensory nerve cells than any other organ in the body. When light enters the eye, it passes through the lens and is focused onto the retina. Comprised of light-sensitive nerve tissue located at the rear of the eyeball, the retina sends messages directly to the brain by way of the optic nerve.

**Rhizopus Rot** - Rhizopus rot is a soft rot of harvested or over-ripe stone fruits, such as peaches, nectarines, sweet cherries, and plums. Mold species belonging to the genus **Rhizopus** cause the rot, which initially appears on the fruit as a fuzzy white mass, called the mycelium.

**Sweet Flag Grass** - Sweet flag, **Acorus calamus**, is a grass-like perennial that can grow up to 2 meters or 6.6 feet high. Sweet flag, along with the common cattail, thrives in wet areas like the edges of streams, ponds, and lakes. The thick, erect leaves resemble an iris. The flowers are greenish brown cylinders covered in little rounded spikes, but they rarely flower.

**Sympathetic Ganglion** - Ganglions are nerve tissue masses that are principally comprised of neuron cell bodies that are located outside the central nervous system. This group of nerve cells forms many important

feedback networks by connecting the brain and spinal cord to specialized tissues such as cardiac muscle, smooth muscle, and glands.

**Thymus Gland** - The thymus is a primary lymph organ and a key regulator of the immune system. This small structure is comprised of a mass of glandular tissue that is divided into two soft pinkish-gray lobes and is located in the upper chest above the heart.

**Trichomes** - **Trichomes** are minute highly specialized outgrowths that are found along any surface of a plant and are designed to enhance a plant's chances of survival. These accessory structures occur most often along stems and leaves but can also be found on the surface of petals and also comprise the fragrant and sweet nectararies that draw pollinating creatures.

**Ulothrix** - Ulothrix is a green filamentous freshwater green algae that can reproduce asexually with zoospores that are formed when the environment becomes less favorable.

**Umbilical Cord** - Literally the lifeline between the developing fetus and mother, the umbilical cord is a long, flexible structure consisting of two arteries and one vein surrounded by a gelatinous matrix. The placenta, which connects the mother to the umbilical cord, is an organ that develops in her uterus during pregnancy, which provides nutrients and oxygenated blood for the fetus and eliminates its waste products.

**Wheat Flower** - Wheat is the common name for any of the cereal grasses belonging to the genus *Triticum* and is an important food source for people around the world. Evidence shows that wheat grew as a wild grass in the Middle East nearly 10,000 years ago and was in cultivation by 6,000 BC.

**Wheat Loose Smut** - Loose Smut is a fungal disease that replaces developing kernels of wheat grain with black powder-like masses of spores. This pathogenic fungus, referred to by scientists as *Ustilago tritici*, quietly infects the seeds of cereal crops and stays dormant until spring. Large clouds of black dust arising from combine operations on farms during wheat harvest often reveal smut infestation.

**Wheat Rust** - Wheat rust is a common and serious disease, reducing crop yields both in the United States and in other wheat-growing areas of the world. The disease is caused by a parasitic fungus and can affect both the leaf and stem of wheat plants.

**Wood Cells** - Wood cells, like other plant cells, have cell walls that are absent in animal cells. The three major constituents of a wood cell are cellulose (40 to 50 percent), lignin (23 to 33 percent in softwoods; 16 to 25 percent in hardwoods), and hemicellulose. Many important properties associated with wood are related to the crystalline nature of cellulose in wood cells.

**Zamia Young Ovule** - Although similar in form to palm trees, *Zamia* are dioecious, meaning that the male and female reproductive organs are borne on separate plants. The ovules of the cycads are naked as they are in other ancient seed plants (Gymnosperms) and unlike the flowering plants (Angiosperms) that hold their ovules in ovaries.

**Zea (Corn) Smut** - Smut is a disease of cereals, corn, grasses, onions, and sorghum that can be caused by any of more than 700 species of parasitic fungi. Smuts generally have a negative economic impact on agriculture, because they affect so many food crops. An exception to this is corn smut, which is considered a delicacy in Mexico.

## Laser Scanning Confocal Microscopy

Laser scanning confocal microscopes employ a pair of pinhole apertures to limit the specimen focal plane to a confined volume approximately a micron in size. Relatively thick specimens can be imaged in successive volumes by acquiring a series of sections along the optical (z) axis of the microscope.

This tutorial explores imaging of specimens with a Nikon PCM 2000 laser scanning confocal microscope by creating virtual control systems that simulate how the actual microscope operates. All specimens contained in this tutorial were imaged with the Nikon instrument and are presented as successive z-axis optical sections obtained from the original data.

The tutorial initializes with a randomly selected specimen appearing in the image windows. The left window (entitled **Widefield Image**) reveals how the specimen appears when viewed through widefield illumination in a classical fluorescence microscope, while the right window (entitled **Confocal Image**) presents a thin optical section from the confocal microscope at the same focal plane on the microscope z-axis. Photomultiplier gain is set to approximately 25 percent for both the red and green channels, and the initial scan speed is set to the medium scan rate.

The confocal **Z-Axis Position** and widefield **Focus** sliders are locked together at the same focal plane. They can be uncoupled with the **Focus Lock** checkbox for observation of a single focal plane in one window while the other is translated through successive view fields along the microscope optical axis. Use either the **Z-Axis Position** or **Focus** sliders to scan through successive focal planes, which will produce thin optical sections of the specimen in the confocal image window, and a succession of blurred images in the widefield image window.

To increase the photomultiplier gain in the confocal portion of the tutorial, translate the **PMT Red Gain** and **PMT Green Gain** sliders by moving one or both bars with the mouse cursor. Moving the sliders to the right will increase photomultiplier gain, while moving the sliders to the left decreases the gain. A similar **Brightness** slider for the widefield microscope portion of the applet allows the visitor to change image brightness as seen in a standard fluorescence microscope. The **Scan Line Speed** slider can be employed to adjust the speed of the virtual confocal scanning galvanometer module. As the scan speed is increased to higher values, a corresponding increase in the amount of background noise captured by the photomultipliers is observed in the confocal images. Adjust the scan speed slider to achieve the fastest scan rate with a minimum amount of signal noise.

Pinhole size can be varied using the **Large**, **Medium**, and **Small** radio buttons to toggle between the available **Pinhole Aperture Sizes**. Small pinholes afford the greatest resolution with the confocal microscope, while successively larger pinholes permit more of the fluorescence background noise to appear in the image. After examining a specimen, the **Choose A Specimen** pull-down menu can be accessed to select a new specimen for observation.

In a conventional widefield microscope, thick specimens will produce an image that represents the sum of sharp image details from the in-focus region combined with blurred images from all of the regions that are out of focus. This effect does not significantly deteriorate images at low magnification (10x and below) where the depth of field is large. However, high magnification objectives often feature correspondingly high numerical apertures that produce a limited depth of field, which is defined as the distance between the upper and lower planes of the in-focus region. The area where sharp specimen focus is observed can be a micron or less at the highest numerical apertures. The result is that specimens having a thickness greater than three to five microns will produce images in which most of the light is contributed by regions that are not in exact focus. Contrast will be reduced because of the contribution from a blurred background that is superimposed over a weaker in-focus image.

Several methods have been developed to overcome the poor contrast inherent in imaging thick specimens with a conventional microscope. The easiest solution is to modify the specimen by slicing it into very thin sections, which requires fixation, dehydration, embedding, and staining. This approach is useful for specimens that are obtained from larger sections of tissue, but it will not work for living cells or tissue sections in culture. Another approach is to modify the microscopy techniques utilized in collection of images. Confocal microscopy, multiphoton excitation, and deconvolution techniques enable observation of the details within thick specimens by a process known as **optical sectioning**, without the artifacts that accompany specimen preparation by physical sectioning.

Specimens having a moderate degree of thickness (5 to 15 microns) will produce dramatically improved images with confocal, multiphoton, or deconvolution techniques. The thickest specimens (20 microns and above) will suffer from a tremendous amount of extraneous light originating in out-of-focus regions, and are probably best-imaged using confocal or multiphoton techniques. In order to judge whether a particular specimen should be imaged with conventional, deconvolution, multiphoton excitation, or confocal microscopy, first view the specimen with widefield illumination. Specimens that produce blurred images, but

still contain regions allowing the observer to set focus and see some level of detail, can benefit from either confocal or deconvolution imaging techniques. However, if the view through a conventional microscope is virtually featureless, providing no landmarks for choosing the appropriate area for imaging or for setting focus, then confocal microscopy should be employed for detailed analysis.

Living specimens require special consideration, because they are often sensitive to fluorophores and photobleaching cannot be prevented by addition of suppression reagents. In addition, necessary low concentrations of fluorescent labels usually produce a weak signal having poor contrast. Another concern is that long exposure to intense low-wavelength illumination often limits cell and tissue viability and, consequently, the length of experiments. A good solution may be to employ high quantum efficiency CCD cameras (commonly utilized in widefield microscopy) instead of the photomultiplier and avalanche diode detectors used for confocal and multiphoton methods. In this case, deconvolution techniques can offer the most satisfactory imaging solution.